UNIVERSITY OF CALIFORNIA, SAN DIEGO

Biological Function of the LxCxE-binding Pocket of Retinoblastoma Protein

A dissertation submitted in partial satisfaction of the

requirements for the degree Doctor of Philosophy

in

Biology

by

Jacqueline Bergseid

Committee in charge:

Professor Jean Y.J. Wang, Chair
Professor Randall S. Johnson, Co-Chair
Professor Ju Chen
Professor Cornelis Murre
Professor Geoffrey Wahl

2007

The dissertation of Jacqueline Bergseid is approved, and it

is acceptable in quality and form for publication on

microfilm:

Co-Chair

Chair

University of California, San Diego

2007

DEDICATION

To the people who made this work possible:

my mother, who taught me the value of persistence,

and my husband, whose love carried me through.

TABLE OF CONTENTS

LIST OF FIGURES

Page

Chapter I

Chapter II

Chapter III

Chapter IV

LIST OF TABLES

Page

Chapter II

Chapter III

Chapter IV

ACKNOWLEDGEMENTS

I would like to thank my advisor Jean Y.J. Wang for guiding me through this project.

I would also like to thank Rimma Levenzon and Irina Hunton for their invaluable help with mouse colony maintenance and tissue dissection; Dr. Kenneth Kaushansky, Dr. Amy Geddes, Dr. Ian Hitchcock and Norma Fox for characterization of megakaryocyte progenitors; Dr. Nissi Varki and Dr. Gregory Erickson for histological analysis of tissues; Dr. George Widhopf for characterization of lymphocyte population.

And last, but not least, my heartfelt appreciation goes to the past and present members of the Wang lab, whose humor and camaraderie sustained me through many long days and nights.

VITA

Education

BS, Cell and Developmental Biology, 1996, University of Rochester, Rochester, NY
Graduated *cum laude*
PhD, Biology, 2007
Division of Biological Sciences, University of California, San Diego, La Jolla, CA Thesis advisor: Jean Wang, PhD

Honors

Bausch and Lomb Science Award (1992)
Presidential Academic Fitness Award (1992)
Dean's List, University of Rochester (1992-1996)
McNair Summer Research Fellowship (1995)

Positions

Research Fellow, Department of Neurobiology and Anatomy, School of Medicine and Dentistry, University of Rochester, Rochester, NY **1994**

Cloned rat neuroretinal cells immortalized with viral A12 protein. Cultured cells in depolarized medium for various periods of time and analyzed expression of A12 using heavy metal marked antibodies and Western Blotting.

Research Fellow, Department of Biology, University of Rochester, Rochester, NY **1995-96**

Developed and conducted the introduction of and screen for mutations in βν gene of *Drosophila* integrin using P-element mutagenesis. Set up crosses, screened progeny, collected embryos and stained them for *lac Z* expression using antibodies against β-galactosidase.

Research Assistant, Research and Development, Invitrogen Corporation, Carlsbad, CA **1996-98**

Used standard recombinant DNA techniques to construct 32 vectors, which are currently sold by the company.

Scientist II, Department of Genomics, Genos Biosciences, Inc., La Jolla, CA **1998-99**

Designed, executed and analyzed all aspects of oncology genomics project including exon trapping, cDNA selection, cDNA library screening, identification of new genes, construction of physical and transcriptional maps, sequencing, mutation detection and bioinformational analysis.

Research Technician III, Department of Chemistry, Laboratory of Peter Schultz, PhD, The Scripps Research Institute, La Jolla, CA **1999-2000**

Designed, executed and evaluated experiments to study the effects of small synthetic DNA-binding molecules on transcription of genes in cultured mammalian cells using various promoter constructs fused to luciferase reporter gene. Studied changes in gene expression using Affymetrix DNA chip technology.

Graduate Student with Jean Wang, PhD, Division of Biological Sciences, University of California San Diego, La Jolla, CA **2001-07**

Studied the effect of a point mutation in Retinoblastoma gene (Rb-N750F) by generating a knock-in mouse using gene targeting. Performed extensive physiological and histological analysis in order to describe the resulting phenotype, which included elevated levels of platelets and lymphocytes in the peripheral blood of the mutant animals and female sterility due to anovulation. Performed co-immunoprecipitation experiments using 3T3 cells derived from mutant embryos and wild type control littermates to study biochemical properties of the Rb-N750F.

Publications

Semenova J, and Zusman S. (1996) "Isolation of Mutations in βν Sub-unit of Integrin in *Drosophila Melanogaster*", Proceedings of the Tenth National Conference on Undergraduate Research, vol. III, p.1593-1596.

Chau NB, **Bergseid J**, and Wang JYJ (2006). RB and Cancer. In: Apoptosis and Cancer Therapy, Debatin, K-M. and S. Fulda, ed., Wiley-VCH, Weinheim, Germany, Chapter 21, pp551-567.

Markey MP, **Bergseid J**, Bosco EE, Stengel K, Xu H, Mayhew CN, Jiang Y, Schwemberger SJ, Babcock G, Jegga AG, Reed MF, Aronow BJ, Wang JYJ, Knudsen ES (accepted for publication to Oncogene). Loss of the Retinoblastoma Tumor Suppressor: Differential Action on Transcriptional Programs Related to Cell Cycle Control and Immune Function.

Bergseid J, Jiang Y, Wang JYJ (manuscript in preparation). The LxCxE binding domain of pRb regulates lymphopoiesis, thrombopoiesis and ovulation.

ABSTRACT OF THE DISSERTATION

Biological Function of the LxCxE-binding Domain of Retinoblastoma Protein

by

Jacqueline Bergseid

Doctor of Philosophy in Biology

University of California, San Diego 2007

Professor Jean Y.J. Wang, Chair

Professor Randall S. Johnson, Co-Chair

The product of the retinoblastoma gene (pRb) is a tumor suppressor protein that regulates cellular proliferation, apoptosis and differentiation of numerous tissues in mice. It contains multiple peptide-binding pockets through which it interacts with a host of cellular and viral proteins. The LxCxE-binding pocket of pRb has been highly conserved between pRb proteins from evolutionary distant species; however, the *in vivo* function of this binding pocket is unknown. The crystal structure of pRB bound to LxCxE peptide was used to design a single point mutation, N757F, which specifically inactivates interactions between pRB and LxCxE-containing proteins without affecting the pRB-E2F interaction. The N750F mutation (analogous to N757F in the human RB) was introduced into the mouse *Rb-1* locus by homologous recombination. The $Rb^{N750F/N750F}$ mice do not

exhibit the phenotype of embryonic lethality observed in Rb-null mice. The pRb-N750F protein does not co-immunoprecipitate with E1A, demonstrating disruption of the LxCxE-binding pocket. The $Rb^{+/-}$ mice develop pituitary tumors with 90% penetrance through LOH. By contrast, the pRb-N750F protein retains its pituitary tumor suppression function as evidenced by the lack of pituitary tumors in $Rb^{N750F/N750F}$ and $Rb^{+/N750F}$ mice. This is consistent with the data from tissue culture experiments demonstrating that $Rb^{N750F/N750F}$ fibroblasts do not exhibit any cell cycle defects.

The lack of embryonic lethality in $Rb^{N750F/N750F}$ mice allowed us to study the effect of this mutation on adult tissues. The $Rb^{N750F/N750F}$ mice have elevated levels of platelets and lymphocytes in the peripheral blood. The $Rb^{N750F/N750F}$ females are infertile due to anovulation. These findings demonstrate for the first time that the LxCxE-binding pocket of pRb plays a role in thromobopoiesis, lymphopoiesis and ovulation. The $Rb^{N750F/-}$ mice are born at the frequency of 13% and die by the age of 8 months, indicating that, unlike Rb^{+} allele, the Rb^{N750F} allele is haploinsufficient. The $Rb^{N750F/-}$ females are also infertile due to the lack of FSH and LH function in the ovaries.

CHAPTER I

INTRODUCTION

Retinoblastoma protein (pRB) was first discovered as the product of a gene whose mutation or loss causes cancer of the retina in children. Based on statistical analysis of patient data Alfred Knudson proposed a hypothesis that retinoblastoma was caused by two mutational events(30). He also proposed that in the hereditary form of retinoblastoma, the first mutation is inherited from one of the parents and the second mutation occurs in somatic cells, while in the nonhereditary form, both mutations occur in somatic cells. The presence of a germ line mutation in one allele of the *RB* gene causes a rapid loss of the remaining wild type allele in the retinal cells, leading to the development of bilateral retinoblastoma with multifocal lesions in both eyes before the age of two, with 90% penetrance(34). A spontaneous mutation in one allele of the *RB* gene that occurs in retinal cells increases the probability of another mutational event in the same cells, resulting in a single tumor in one eye which is observed at an older age. In addition to retinoblastoma, $RB^{+/-}$ individuals are at increased risk of developing bladder carcinomas, osteosarcomas and fibrosarcomas, indicating that these tissues also contain cell types that are dependent on the presence of functional pRB for tumor suppression(36).

Analysis of genomic DNA from affected individuals provided an explanation of molecular mechanism for the development of retinoblastoma(6). Comparison of restriction fragment length polymorphism in DNA derived from normal tissues and

tumors revealed that wild type chromosome 13 was invariably lost in tumors. The remaining chromosome 13 contained deletions, rearrangements or translocations. Importantly, none of the seven chromosomes that were also analyzed contained chromosomal mutations, further indicating that gene responsible for the development of retinoblastoma is located on chromosome 13. Subsequent cloning and sequencing of the *RB* gene opened a possibility to study the mechanism of tumorigenesis at the molecular level(21, 25).

Additional evidence that functional pRB is important for tumor suppression came from the findings that several small DNA tumor viruses produce proteins that interact with pRB. Adenovirus E1A (E1A), SV40 T antigen and human papilloma virus (HPV) protein E7 were found to bind directly to pRB and inactivate it(15, 23, 24). Moreover, mutations in viral proteins that abrogated their ability to bind pRB rendered them incapable of transforming cells(8, 24, 39, 41, 46, 48). Together these findings suggested that oncogenic viruses cause cancer by binding to and inactivating endogenous cellular proteins.

Retinoblastoma protein and its functions

Human pRB is 928 amino acids long (Figure 1.1). The protein is divided into four major domains: N, A, B and C. The N-terminus consists of the first 350 amino acids. Its function is very poorly understood, however, it seems to be dispensable for most of pRB functions(26). The A and B domains contain sequences that are essential for most of pRB functions. These domains are also found in two related proteins, p107 and p130. The A/B domain is highly conserved between all three proteins, which together form a family of "pocket" proteins (reviewed in (12, 27)). Two protein-binding

sites are located within the A/B domain: one for E2F transcription factors, and another one for LxCxE-containing proteins(31, 33). The C-terminus contains a docking site for proteins with amino acid sequence PENF.Q, e.g. ABL and BRCA1, a caspase cleavage site, a nuclear localization signal and a CDK binding site(1, 10, 29, 44, 45, 50, 52). The RB protein has a half-life of 8 hours and is synthesized continuously throughout the cell cycle, however, its activity is regulated in a cell cycle-dependent manner by phosphorylation at 16 potential phosphorylation sites scattered along the length of the protein(4, 7, 14, 16, 43, 53).

Over the years, it was shown that the tumor suppressor properties of pRB are derived from its ability to inhibit cell cycle progression by repressing transcriptions of genes necessary for entry into the S phase and DNA replication (reviewed in (13, 18)). During G1, unphosphorylated pRB associates with members of the E2F family of transcription factors(Figure 1.2)(19). At the same time, pRB also binds to various chromatin remodeling proteins. The net result of these interactions is silencing of E2F-regulated promoters by formation of heterochromatin. As cells progress through G1, pRB becomes phosphorylated by Cyclin D1-CDK4/6 complexes and dissociates from E2F, relieving repression of E2F-regulated promoters. This allows for transcription of genes necessary for entry into S phase and DNA replication, e.g. *DHFR*, *thymidine kinase*, *cdc2*, *E2F1* and *cyclins A*, *D* and *E* (reviewed in (13)).

In addition to E2F proteins, numerous other pRB-binding partners have been identified. A recent review article listed 110 pRB binding proteins that have been reported in the literature(38). Most of these proteins require the presence of the A/B pocket in order to interact with pRB. As mentioned earlier, E1A, SV40 T and HPV E7

viral proteins bind to pRB(15, 23, 24). All three proteins contain the LxCxE amino acid sequence, which is required for binding to pRB. Several cellular proteins were also found to bind to pRB via the LxCxE sequence, including HDAC 1 and 2, Cyclin D1, large subunit of Replication Factor C (RF-C), RBP1 and 2, Bog, BRG1 and RNA Pol I transcription factor UBF(3, 5, 17, 20, 22, 35, 40, 47).

The role of pRb in development and tumorigenesis in mice

In order to elucidate the role of pRb in the context of the whole organism, mice with a germ line deletion of *Rb* were created. Unlike humans, mice heterozygous for the mutant *Rb* allele do not develop retinoblastomas. Instead, they succumb to pituitary and thyroid tumors(11, 28, 32). As in human retinoblastoma, murine tumors become homozygous for the Rb deletion by the loss of the remaining wild type *Rb* allele, demonstrating that the mechanism of tumorigenesis is the same in mice and humans, even though different tissues are affected.

The first indication that the scope of pRb function extends beyond suppression of tumorigenesis in a few tissues came from the phenotype of *Rb* knockout mice(11, 28, 32). Homozygous germ line deletions of *Rb* results in embryonic lethality at embryonic day 12.5 (Ed 12.5). *Rb*-null embryos display extensive ectopic S phase entry and elevated levels of apoptosis in the central and peripheral nervous system (CNS and PNS) and in the ocular lens. In fetal liver, the loss of *Rb* leads to decreased cellularization and disruption of erythropoiesis, as evidenced by persistence of nucleated erythrocytes.

In addition to defects in the embryo proper, deletion of *Rb* causes excessive proliferation and incomplete differentiation of trophoblasts, which form the embryonic portion of the placenta(49). These defects result in an increased number of trophoblasts

and decreased blood spaces in the labyrinth layer of the placenta, which leads to a restriction in the exchange of nutrients and oxygen between the mother and the developing embryo.

Rb-null embryos die during development, preventing characterization of pRb function in tissues that form after Ed 12.5 and evaluation of the role of pRb in the maintenance of adult tissues. Moreover, deletion of *Rb* in the whole organism does not allow one to differentiate between the tissues that have intrinsic requirement for pRb and the ones that show defects due to the pathological conditions created by the loss of pRb in other tissues. To overcome these limitations, several tissue-specific knockouts of *Rb* have been created and characterized. Conditional knockout of *Rb* in the epidermis caused hyperplasia, aberrant DNA synthesis and improper differentiation(2). In melanocytes, deletion of *Rb* resulted in hair depigmentation in mice, while in tissue culture, *Rb*-null melanocytes died rapidly by apoptosis(51). In the inner ear, *Rb*-null hair cells continued to undergo mitosis, yet were fully differentiated and functional(42). Conditional inactivation of *Rb* in the liver resulted in BrdU incorporation, increased ploidy and upregulation of E2F target genes in terminally differentiated hepatocytes(37).

Even though numerous tissues were shown to be affected by the loss of both wild type *Rb* alleles, in $Rb^{+/-}$ mice these tissues did not develop tumors. This discrepancy can be explained by two different, although not mutually exclusive, mechanisms. In the first mechanism, the tumors of other tissues do not have enough time to develop, because $Rb^{+/-}$ mice die of pituitary and thyroid tumors before the age of one year. Alternatively, cells in other tissues might not lose the wild type *Rb* allele spontaneously, as occurs in pituitary and thyroid. The data from humans suggest that both mechanisms are at work.

Survivors of childhood retinoblastomas develop bladder carcinomas, osteosarcomas and fibrosarcomas later in life, indicating that these tissues are also susceptible to spontaneous loss of the wild type *RB* allele, but over a longer period of time(36).

In summary, deletion of *Rb* in numerous cell types causes apoptosis, unscheduled cell cycle entry and incomplete differentiation. These findings can be explained by two alternative models of pRB function. In the first model, pRB simply inhibits cellular proliferation (Figure 1.3 A). Disruption of pRB function causes abnormalities in the cell cycle that lead to apoptosis and defective differentiation. In the second model, pRB directly affects apoptosis, differentiation and cell cycle entry through its interactions with different proteins in different cellular contexts (Figure 1.3B).

The role of the LxCxE-binding domain in pRB function

One way to distinguish between two models of pRB function is to create mutations in pRB that would affect only one of its proposed functions. Moreover, such mutations would disrupt the binding of pRB to a subset of its interacting proteins thus providing a molecular basis for various functions of pRB. This approach was made possible by the determination of the crystal structure of pRB bound to HPV E7 peptide containing LxCxE amino acid sequence(33). Guided by the crystal structure, we chose to substitute asparagine (N) 757 of pRB with phenylalanine (F), creating pRB-N757F mutant.

The N757F mutation affected only one protein-binding site and eliminated interactions between pRB and proteins that depend on the LxCxE motif for their binding to pRB(9). pRB-N757F exhibited decreased binding to HPV E7 and HDAC1, but still bound to E2F1. In functional assays, the pRB-N757F mutant, just like the wild type

pRB, was capable of inducing cell cycle arrest in *RB*-null Saos2 cells. However, pRB-N757F was incapable of inducing irreversible growth arrest in differentiated myotubes. Moreover, upon serum induction, pRB-N757F was phosphorylated in response to serum stimulation, while the wild type pRB remained unphosphorylated. In summary, the pRB-N757F mutant was capable of controlling cellular proliferation, but was defective in differentiation. These findings indicate that pRB regulates these processes through two separate mechanisms, arguing for the second model of pRB function (see Figure 1.3B). Additionally, the phenotype of the pRB-N757F mutant demonstrates that different functions of pRB are regulated by different regions of the protein.

In order to further characterize the role of LxCxE-binding pocket, we engineered mice with a germ line mutation in endogenous *Rb* locus, which was functionally equivalent to pRB-N757F substitution in the human protein. By creating Rb^{N750F} mutant mice, we planned to accomplish three goals: (1) to determine whether some of the defects previously observed in Rb-null mice can be also observed in Rb^{N750F} mutants, indicating that these defects are caused by the disruption of interactions between LxCxE-containing proteins and pRb; (2) to test whether the muscle differentiation defect observed in tissue culture experiments with pRB-N757F can be reproduced *in vivo*; and (3) to discover any new tissues that are dependent on pRb for proper function, but have not been discovered previously due to lethality of Rb-null mice.

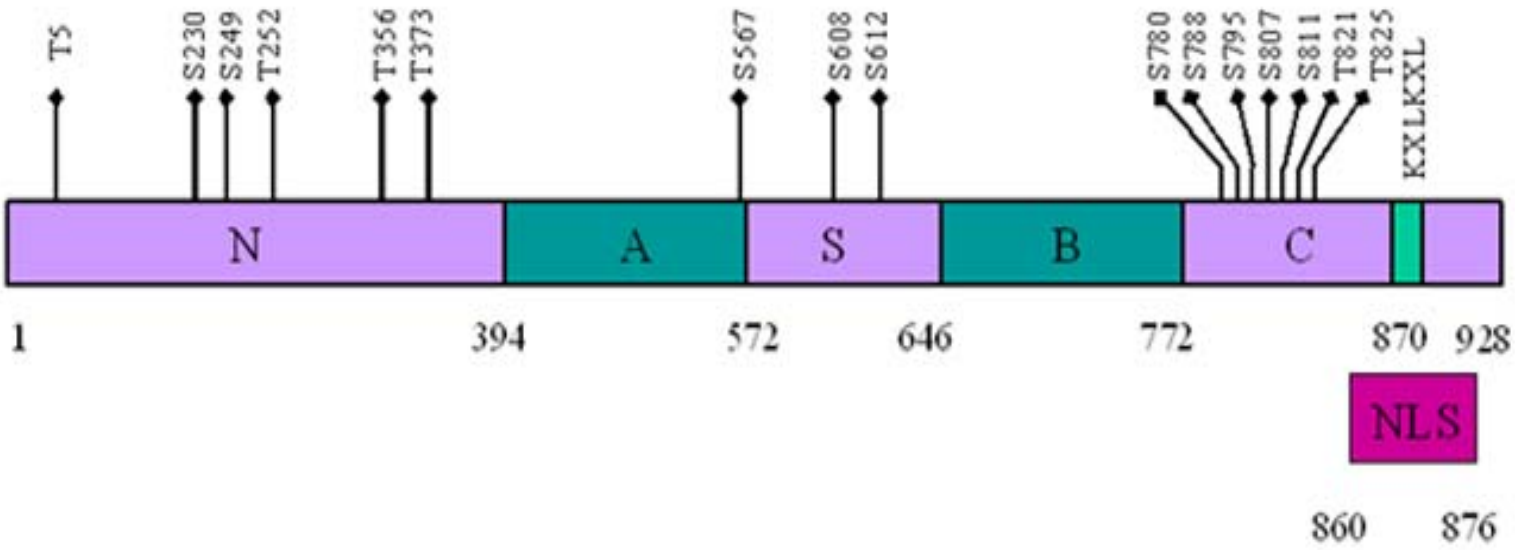

Figure 1.1 Structure of RB protein

pRB is a nuclear protein with 16 potential phosphorylation sites. pRB is divided into four functional domains: N, A, B and C. The A and B domain are separated by a short spacer (S). The function of the N terminus is poorly understood, but it seems to be dispensable for most of pRB functions. The A and B domains are crucial for most of pRB functions and bind numerous proteins, including members of the E2F family of transcription factors and LxCxE-containing proteins. The C terminus is important for regulation of pRB activity. It also contains a docking site for proteins with PENF.Q amino acid sequence, e.g. ABL and BRCA1, a caspase cleavage site, a nuclear localization signal (NLS) and a CDK binding site (KxLKxL).

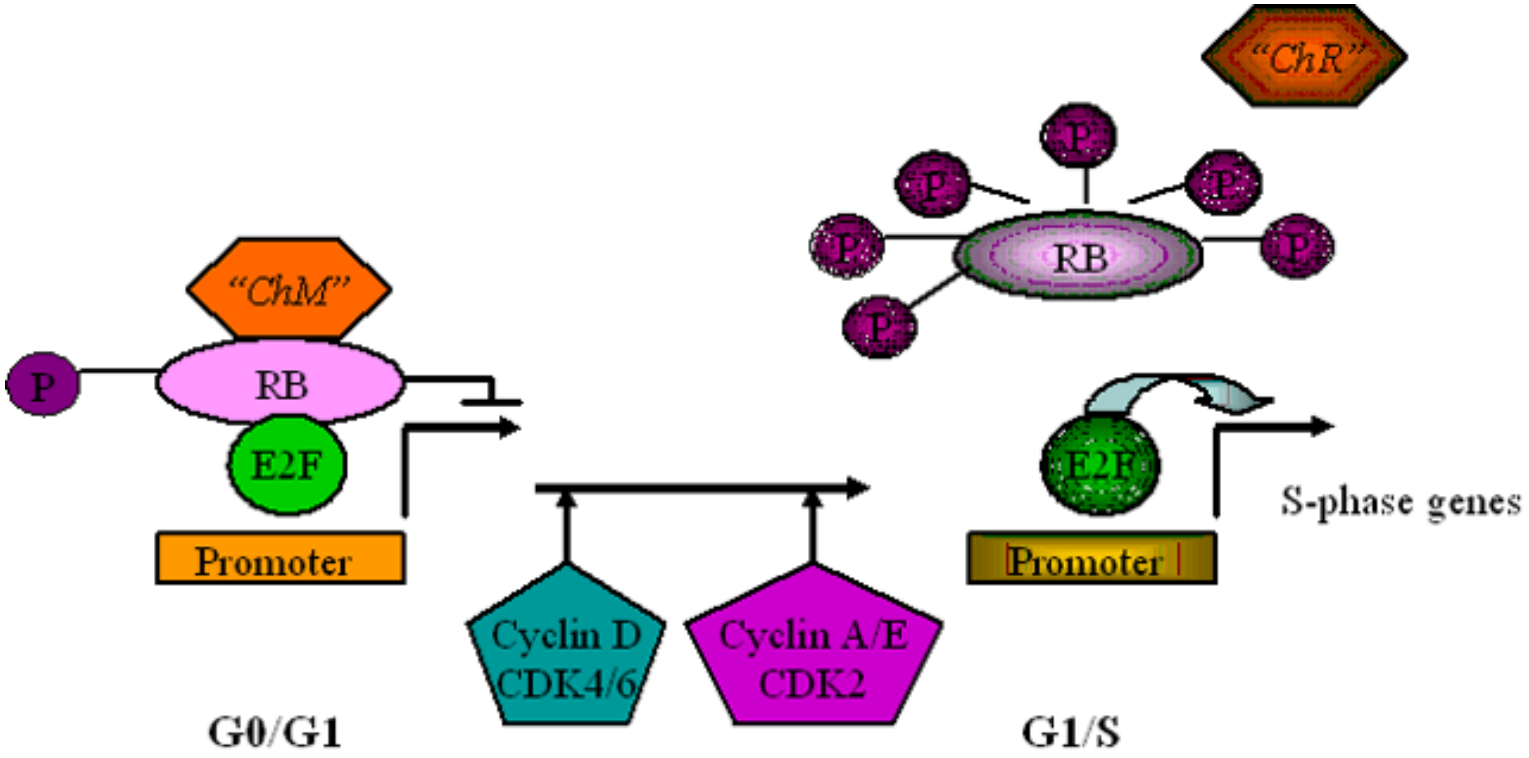

Figure 1.2 RB protein regulates entry into S phase of the cell cycle

In G0/G1 phases of the cell cycle, hypophosphorylated pRB binds to E2F/DP complexes and represses transcription from E2F-regulated promoters by bringing in chromatin modifying enzymes, such as histone deacetylases (HDACs), SWI/SNF, PcG and methylases. In late G1, phosphorylation by Cyclin D/CDK 4/6 and Cyclin A/E/ CDK 2 causes dissociation of pRB from E2F and activation of E2F-regulated promoters. *DHFR*, *thymidine kinase*, *c-myc*, *cdc2*, *E2F-1*, *cyclins A*, *D* and *E* are some of the S-phase genes whose transcription is controlled by E2F.

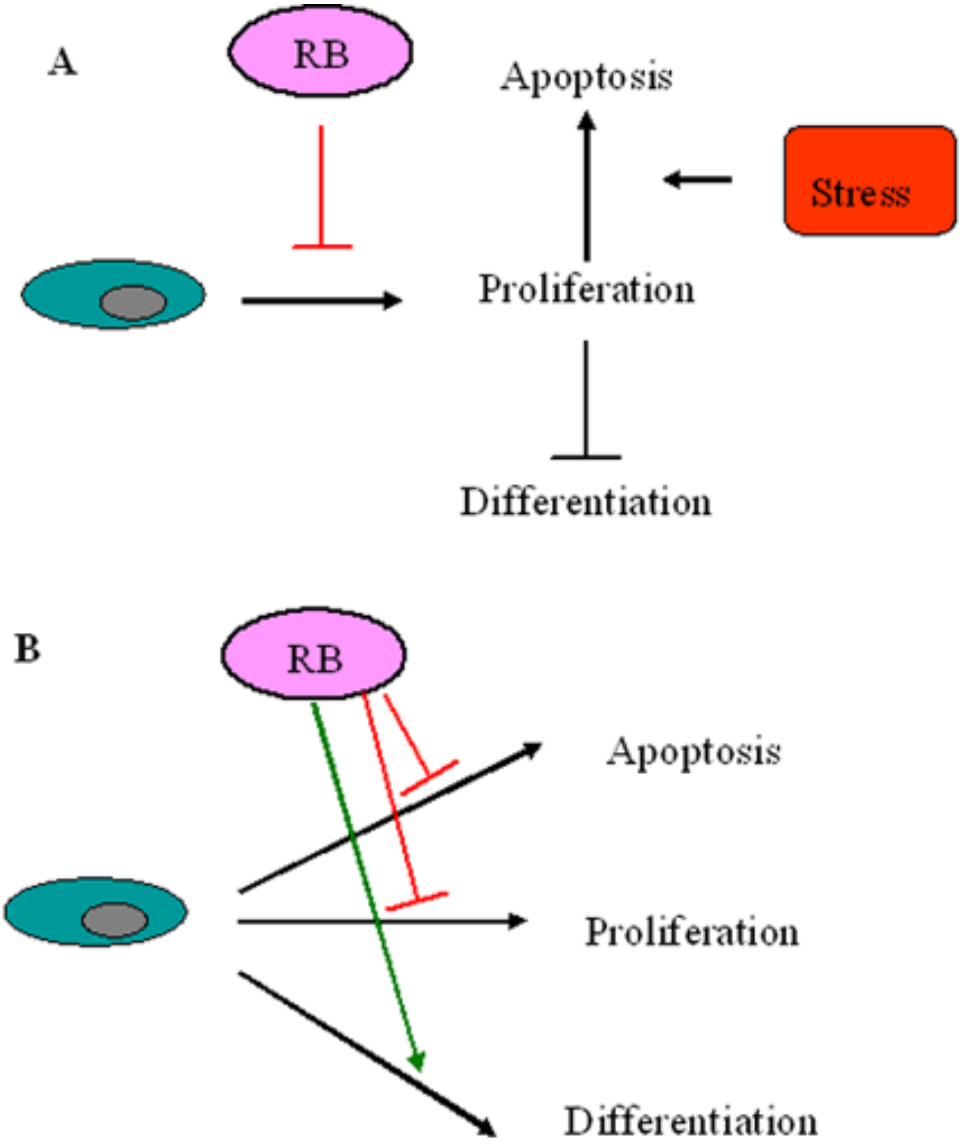

Figure 1.3 Two models of pRB function

A. pRB directly inhibits cellular proliferation. Aberrant apoptosis and incomplete differentiation are secondary consequences of unscheduled cellular proliferation in the absence of pRB. **B.** pRB regulates all three processes directly. This model allows for the possibility of creating mutation in pRB that would compromise regulation of one of the processes without disturbing the regulation of the other two.

REFERENCES

1. **Adams, P. D., X. Li, W. R. Sellers, K. B. Baker, X. Leng, J. W. Harper, Y. Taya, and W. G. Kaelin, Jr.** 1999. Retinoblastoma protein contains a C-terminal motif that targets it for phosphorylation by cyclin-cdk complexes. Mol Cell Biol **19:**1068-80.

2. **Balsitis, S. J., J. Sage, S. Duensing, K. Munger, T. Jacks, and P. F. Lambert.** 2003. Recapitulation of the effects of the human papillomavirus type 16 E7 oncogene on mouse epithelium by somatic Rb deletion and detection of pRb-independent effects of E7 in vivo. Mol Cell Biol **23:**9094-103.

3. **Brehm, A., E. A. Miska, D. J. McCance, J. L. Reid, A. J. Bannister, and T. Kouzarides.** 1998. Retinoblastoma protein recruits histone deacetylase to repress transcription. Nature **391:**597-601.

4. **Buchkovich, K., L. A. Duffy, and E. Harlow.** 1989. The retinoblastoma protein is phosphorylated during specific phases of the cell cycle. Cell **58:**1097-105.

5. **Cavanaugh, A. H., W. M. Hempel, L. J. Taylor, V. Rogalsky, G. Todorov, and L. I. Rothblum.** 1995. Activity of RNA polymerase I transcription factor UBF blocked by Rb gene product.

6. **Cavenee, W. K., T. P. Dryja, R. A. Phillips, W. F. Benedict, R. Godbout, B. L. Gallie, A. L. Murphree, L. C. Strong, and R. L. White.** 1983. Expression of recessive alleles by chromosomal mechanisms in retinoblastoma. Nature **305:**779-84.

7. **Chen, P. L., P. Scully, J. Y. Shew, J. Y. Wang, and W. H. Lee.** 1989. Phosphorylation of the retinoblastoma gene product is modulated during the cell cycle and cellular differentiation. Cell **58:**1193-8.

8. **Chen, S., and E. Paucha.** 1990. Identification of a region of simian virus 40 large T antigen required for cell transformation. J Virol **64:**3350-7.

9. **Chen, T. T., and J. Y. Wang.** 2000. Establishment of irreversible growth arrest in myogenic differentiation requires the RB LXCXE-binding function. Mol Cell Biol **20:**5571-80.

10. **Chen, W. D., G. A. Otterson, S. Lipkowitz, S. N. Khleif, A. B. Coxon, and F. J. Kaye.** 1997. Apoptosis is associated with cleavage of a 5 kDa fragment from RB which mimics dephosphorylation and modulates E2F binding. Oncogene **14:**1243-8.

11. **Clarke, A. R., E. R. Maandag, M. van Roon, N. M. van der Lugt, M. van der Valk, M. L. Hooper, A. Berns, and H. te Riele.** 1992. Requirement for a functional Rb-1 gene in murine development. Nature **359:**328-30.

12. **Classon, M., and N. Dyson.** 2001. p107 and p130: versatile proteins with interesting pockets. Exp Cell Res **264:**135-47.

13. **Cobrinik, D.** 2005. Pocket proteins and cell cycle control. Oncogene **24:**2796-809.

14. **Connell-Crowley, L., J. W. Harper, and D. W. Goodrich.** 1997. Cyclin D1/Cdk4 regulates retinoblastoma protein-mediated cell cycle arrest by site-specific phosphorylation. Mol Biol Cell **8:**287-301.

15. **DeCaprio, J. A., J. W. Ludlow, J. Figge, J. Y. Shew, C. M. Huang, W. H. Lee, E. Marsilio, E. Paucha, and D. M. Livingston.** 1988. SV40 large tumor antigen forms a specific complex with the product of the retinoblastoma susceptibility gene. Cell **54:**275-83.

16. **DeCaprio, J. A., J. W. Ludlow, D. Lynch, Y. Furukawa, J. Griffin, H. Piwnica-Worms, C. M. Huang, and D. M. Livingston.** 1989. The product of the retinoblastoma susceptibility gene has properties of a cell cycle regulatory element. Cell **58:**1085-95.

17. **Defeo-Jones, D., P. S. Huang, R. E. Jones, K. M. Haskell, G. A. Vuocolo, M. G. Hanobik, H. E. Huber, and A. Oliff.** 1991. Cloning of cDNAs for cellular proteins that bind to the retinoblastoma gene product. Nature **352:**251-4.

18. **DiCiommo, D., B. L. Gallie, and R. Bremner.** 2000. Retinoblastoma: the disease, gene and protein provide critical leads to understand cancer. Semin Cancer Biol **10:**255-69.

19. **Dimova, D. K., and N. J. Dyson.** 2005. The E2F transcriptional network: old acquaintances with new faces. Oncogene **24:**2810-26.

20. **Dowdy, S. F., P. W. Hinds, K. Louie, S. I. Reed, A. Arnold, and R. A. Weinberg.** 1993. Physical interaction of the retinoblastoma protein with human D cyclins. Cell **73:**499-511.

21. **Dryja, T. P., J. M. Rapaport, J. M. Joyce, and R. A. Petersen.** 1986. Molecular detection of deletions involving band q14 of chromosome 13 in retinoblastomas. Proc Natl Acad Sci U S A **83:**7391-4.

22. **Dunaief, J. L., B. E. Strober, S. Guha, P. A. Khavari, K. Alin, J. Luban, M. Begemann, G. R. Crabtree, and S. P. Goff.** 1994. The retinoblastoma protein and BRG1 form a complex and cooperate to induce cell cycle arrest. Cell **79:**119-30.

23. **Dyson, N., P. M. Howley, K. Munger, and E. Harlow.** 1989. The human papilloma virus-16 E7 oncoprotein is able to bind to the retinoblastoma gene product. Science **243:**934-7.

24. **Egan, C., S. T. Bayley, and P. E. Branton.** 1989. Binding of the Rb1 protein to E1A products is required for adenovirus transformation. Oncogene **4:**383-8.

25. **Friend, S. H., R. Bernards, S. Rogelj, R. A. Weinberg, J. M. Rapaport, D. M. Albert, and T. P. Dryja.** 1986. A human DNA segment with properties of the gene that predisposes to retinoblastoma and osteosarcoma. Nature **323:**643-6.

26. **Goodrich, D. W.** 2003. How the other half lives, the amino-terminal domain of the retinoblastoma tumor suppressor protein. J Cell Physiol **197:**169-80.

27. **Grana, X., J. Garriga, and X. Mayol.** 1998. Role of the retinoblastoma protein family, pRB, p107 and p130 in the negative control of cell growth. Oncogene **17:**3365-83.

28. **Jacks, T., A. Fazeli, E. M. Schmitt, R. T. Bronson, M. A. Goodell, and R. A. Weinberg.** 1992. Effects of an Rb mutation in the mouse. Nature **359:**295-300.

29. **Janicke, R. U., P. A. Walker, X. Y. Lin, and A. G. Porter.** 1996. Specific cleavage of the retinoblastoma protein by an ICE-like protease in apoptosis. Embo J **15:**6969-78.

30. **Knudson, A. G., Jr.** 1971. Mutation and cancer: statistical study of retinoblastoma. Proc Natl Acad Sci U S A **68:**820-3.

31. **Lee, C., J. H. Chang, H. S. Lee, and Y. Cho.** 2002. Structural basis for the recognition of the E2F transactivation domain by the retinoblastoma tumor suppressor. Genes Dev **16:**3199-212.

32. **Lee, E. Y., C. Y. Chang, N. Hu, Y. C. Wang, C. C. Lai, K. Herrup, W. H. Lee, and A. Bradley.** 1992. Mice deficient for Rb are nonviable and show defects in neurogenesis and haematopoiesis. Nature **359:**288-94.

33. **Lee, J. O., A. A. Russo, and N. P. Pavletich.** 1998. Structure of the retinoblastoma tumour-suppressor pocket domain bound to a peptide from HPV E7. Nature **391:**859-65.

34. **Lohmann, D. R., and B. L. Gallie.** 2004. Retinoblastoma: revisiting the model prototype of inherited cancer. Am J Med Genet C Semin Med Genet **129:**23-8.

35. **Magnaghi-Jaulin, L., R. Groisman, I. Naguibneva, P. Robin, S. Lorain, J. P. Le Villain, F. Troalen, D. Trouche, and A. Harel-Bellan.** 1998. Retinoblastoma protein represses transcription by recruiting a histone deacetylase. Nature **391:**601-5.

36. **Matsunaga, E.** 1980. Hereditary retinoblastoma: host resistance and second primary tumors. J Natl Cancer Inst **65:**47-51.

37. **Mayhew, C. N., E. E. Bosco, S. R. Fox, T. Okaya, P. Tarapore, S. J. Schwemberger, G. F. Babcock, A. B. Lentsch, K. Fukasawa, and E. S. Knudsen.** 2005. Liver-specific pRB loss results in ectopic cell cycle entry and aberrant ploidy. Cancer Res **65:**4568-77.

38. **Morris, E. J., and N. J. Dyson.** 2001. Retinoblastoma protein partners. Adv Cancer Res **82:**1-54.

39. **Munger, K., B. A. Werness, N. Dyson, W. C. Phelps, E. Harlow, and P. M. Howley.** 1989. Complex formation of human papillomavirus E7 proteins with the retinoblastoma tumor suppressor gene product. Embo J **8:**4099-105.

40. **Pennaneach, V., I. Salles-Passador, A. Munshi, H. Brickner, K. Regazzoni, F. Dick, N. Dyson, T. T. Chen, J. Y. Wang, R. Fotedar, and A. Fotedar.** 2001. The large subunit of replication factor C promotes cell survival after DNA damage in an LxCxE motif- and Rb-dependent manner. Mol Cell **7:**715-27.

41. **Phelps, W. C., K. Munger, C. L. Yee, J. A. Barnes, and P. M. Howley.** 1992. Structure-function analysis of the human papillomavirus type 16 E7 oncoprotein. J Virol **66:**2418-27.

42. **Sage, C., M. Huang, K. Karimi, G. Gutierrez, M. A. Vollrath, D. S. Zhang, J. Garcia-Anoveros, P. W. Hinds, J. T. Corwin, D. P. Corey, and Z. Y. Chen.** 2005. Proliferation of functional hair cells in vivo in the absence of the retinoblastoma protein. Science **307:**1114-8.

43. **Takaki, T., K. Fukasawa, I. Suzuki-Takahashi, K. Semba, M. Kitagawa, Y. Taya, and H. Hirai.** 2005. Preferences for phosphorylation sites in the retinoblastoma protein of D-type cyclin-dependent kinases, Cdk4 and Cdk6, in vitro. J Biochem (Tokyo) **137:**381-6.

44. **Tan, X., S. J. Martin, D. R. Green, and J. Y. Wang.** 1997. Degradation of retinoblastoma protein in tumor necrosis factor- and CD95-induced cell death. J Biol Chem **272:**9613-6.

45. **Welch, P. J., and J. Y. Wang.** 1993. A C-terminal protein-binding domain in the retinoblastoma protein regulates nuclear c-Abl tyrosine kinase in the cell cycle. Cell **75:**779-90.

46. **Whyte, P., N. M. Williamson, and E. Harlow.** 1989. Cellular targets for transformation by the adenovirus E1A proteins. Cell **56:**67-75.

47. **Woitach, J. T., M. Zhang, C. H. Niu, and S. S. Thorgeirsson.** 1998. A retinoblastoma-binding protein that affects cell-cycle control and confers transforming ability. Nat Genet **19:**371-4.

48. **Wolf, D. A., H. Hermeking, T. Albert, T. Herzinger, P. Kind, and D. Eick.** 1995. A complex between E2F and the pRb-related protein p130 is specifically targeted by the simian virus 40 large T antigen during cell transformation. Oncogene **10:**2067-78.

49. **Wu, L., A. de Bruin, H. I. Saavedra, M. Starovic, A. Trimboli, Y. Yang, J. Opavska, P. Wilson, J. C. Thompson, M. C. Ostrowski, T. J. Rosol, L. A. Woollett, M. Weinstein, J. C. Cross, M. L. Robinson, and G. Leone.** 2003. Extra-embryonic function of Rb is essential for embryonic development and viability. Nature **421:**942-7.

50. **Yarden, R. I., and L. C. Brody.** 1999. BRCA1 interacts with components of the histone deacetylase complex. Proc Natl Acad Sci U S A **96:**4983-8.

51. **Yu, B. D., M. Becker-Hapak, E. L. Snyder, M. Vooijs, C. Denicourt, and S. F. Dowdy.** 2003. Distinct and nonoverlapping roles for pRB and cyclin D:cyclin-dependent kinases 4/6 activity in melanocyte survival. Proc Natl Acad Sci U S A **100:**14881-6.

52. **Zacksenhaus, E., Z. Jiang, D. Chung, J. D. Marth, R. A. Phillips, and B. L. Gallie.** 1996. pRb controls proliferation, differentiation, and death of skeletal muscle cells and other lineages during embryogenesis. Genes Dev **10:**3051-64.

53. **Zarkowska, T., and S. Mittnacht.** 1997. Differential phosphorylation of the retinoblastoma protein by G1/S cyclin-dependent kinases. J Biol Chem **272:**12738-46.

CHAPTER II

GENERATION OF Rb^{N750} MICE

INTRODUCTION

Numerous insights into the functions of genes have been gained by mutating them and analyzing the consequences of specific mutations for a living system. The majority of such studies are performed by mutating cDNA that encodes a gene of interest and introducing it into tissue culture cells, which are then subjected to various treatments. The response to treatments is compared between cells that received the wild type copy of a gene and the ones that received a mutant copy. Such experiments provide a direct way of testing the effects of a given mutation on the function of a gene, thanks to the simplicity of the experimental system and the tightly controlled conditions under which experiments are performed. However, the biological relevance of results obtained from such studies is often limited by several factors. First, cultured cells have adapted to survive under conditions that differ dramatically from the conditions encountered inside a living organism. For example, the oxygen concentration encountered by the cells inside tissues is 3%, which is much lower than the 20% atmospheric concentration of oxygen that cell lines are exposed to. Second, many commonly used cell lines have been maintained in culture for many years and might have accumulated numerous mutations that an experimenter has no way of detecting, but which, nonetheless, might influence the function of a gene under study. Third, cultured cells are typically grown in relative isolation, without the presence of other cell types or extracellular matrix that would normally be found in a tissue. Fourth, complex processes such as development,

differentiation, homeostasis, tumorigenesis or aging cannot be faithfully recreated in a cell culture setting. All these limitation can be overcome by studying the function of a mutant protein in the context of a whole organism.

Gene targeting technology in mice enables researchers to introduce a desired mutation directly into the genomic locus that encodes the gene of interest. In such "knockin" mice expression of a mutant protein is under the control of endogenous regulatory elements(6, 10, 17). Knockin mice provide an ideal system for studying the function of a mutant protein under physiological conditions in every mouse tissue that expresses this protein. Moreover, knockin mice allow one to determine what role, if any, a protein of interest plays in various complex processes such as development or tumorigenesis and how an engineered mutation affects this role.

Generation of knockin mice involves three major steps: (1) cloning of a targeting construct that contains the desired mutation, (2) isolation of embryonic stem (ES) cell clones that incorporated the targeting construct by homologous recombination and (3) injection of cells from these clones into blastocysts to obtain mice derived from mutant ES cells.

The targeting construct is made by subcloning a segment of genomic DNA that encodes a part of the gene to be mutated into a vector that enables propagation of this DNA segment in *E. coli*. The genomic DNA is then altered to produce a desired mutation. Furthermore, two additional alterations are necessary to generate the final targeting construct: an insertion of an antibiotic resistance gene and creation of a new restriction site. These two alterations are crucial for the ability to isolate ES cells that have incorporated the targeting construct by homologous recombination. The presence of

an antibiotic resistance gene ensures that only ES cells with a stable integration of the targeting construct in their genomic DNA survive selection. The overwhelming majority of these cells, however, would contain the targeting construct that integrated randomly throughout the genome(14). A new restriction site is used to screen for those few clones in which the targeting construct inserted the mutated sequence into the genomic locus of the gene of interest by homologous recombination.

Mouse ES cells are remarkable in the sense that they can be propagated and manipulated in culture, and yet, once inserted back into embryos, are able to contribute to numerous tissues, including the germ line, ultimately giving rise to a whole animal. This quality of ES cells is exploited when genetically altered ES cells are injected into the host embryos at the blastocyst stage. The resulting embryos are then transferred into a foster mother where they complete their prenatal development. The extent to which ES cells contribute to the tissues of a host embryo is evaluated by observing the coat color of the pups. Since ES cells are derived from mice with agouti coat color and host embryos are obtained from mice with black coat color, the mice that incorporated injected ES cells would have patches of brown-colored fur or be completely brown if ES cells gave rise to the majority of tissues in that mouse. Such chimeric mice are then bred in order to transmit the engineered mutation through the germ line ultimately giving rise to animal homozygous for the new mutation.

MATERIALS AND METHODS

Targeting Construct

Fragments of genomic DNA containing the *Rb* coding region were subcloned into pBluescript II SK+ (Stratagene, 212205). Mutagenesis was performed using QuikChange Multi Site-Directed Mutagenesi Kit (Stratagene, 200514). The targeting construct was assembled using standard cloning techniques with restriction enzymes as well as recombineering, as described in details in the RESULTS section.

The following primers were used to generate homology regions for recombineering. Homology region 2 (HR 2), amplified using 3'HA/URT/SacII,F (5'-CTGTCCGCGGCCAGCTGTGCAGAAACTTCA-3') and 3' HA/UTR/NotI, R (5'-GCGGCCGCGGCTCTGAACAACTAGTTT-3'). Homology region 3 (HR 3), amplified using Ex23/NotI,F (5'-GCGGCCGCCTACCTTGTCACCAATACC-3') and In23/BamHI,F (5'-GGATCCGACATTCAACAGCCTATCCC-3'). Homology region 4 (HR 4), amplified using In23/EcoRI,F (5'-GAATCCGGGATAGGCTGTTGAATGTC-3')and In23/SalI,R (5'-GTCGACGCCTGTT CTACTTAGCAA G-3').

Embryonic Stem Cell Culture

TC1 mouse embryonic stem (ES) cells derived from 129 Sv/Ev/Tac strain were cultured using protocol supplied by Phil Leder (Department of Genetics, Harvard Medical School, Boston, MA). Cells were maintained in high glucose DMEM with GlutaMAX^{TM} (Invitrogen 10566-016) supplemented with 16% FBS (Hyclone SH30070.03), vitamins (Invitrogen 11120-052), penicillin/streptomycin (Invitrogen 15070-063), 100 μM non-essential amino acids (Invitrogen 11140-050), 100 μM

betamercaptoethanlol (β-ME, Sigma M3148) and 1000 units/ml of leukemia inhibitory factor (LIF, Chemicon ESG1106).

The targeting construct (10 μg) was linearized using NotI. DNA was purified by phenol/chlorophorm extraction and electroporated into $20x10^6$ cells at passage 14 (BioRad Gene Pulser, 250 V, 500 μF). In parallel, the same construct was also submitted to the UCSD Transgenic Mouse Core facility where it was electroporated into R1 line of mouse ESC.

After electroporation, cells were plated onto 6 cm dishes containing a feeder layer of irradiated *Rag1*$^{-/-}$ mouse embryonic fibroblasts (MEFs). *Rag1*$^{-/-}$ MEFs are resistant to G418 because they have *Neo* gene inserted into the *Rag1* locus. Cells were allowed to recover for two days in non-selecting media. G418 selection (200 μg/ml) was introduced at day three and maintained for a total of 10 days with media being changed every day for the first three days and then every other day. Surviving clones were expanded in non-selecting media for another two days. Individual colonies were isolated by picking them off the plate with a Pipetteman, trypsinized and plated into duplicate 96-well plates. After three days of expansion, one plate was frozen at -80^{o}C to serve as a master stock of ES cells, while the other plate was used as a source of DNA for screening.

ES cells from three clones found to contain homologous integration of the targeting construct were defrosted, plated at low density and sub-cloned. Twelve individual colonies were isolated from each primary clone by the same method and screened again for homologous recombination of the targeting construct.

Southern Blotting

ES cells from each clone were lysed by incubation in 50 µl of lysis buffer (10 mM Tris-HCl pH 7.5, 10 mM EDTA, 10 mM NaCl, 0.5% Sarcosyl w/v, 1 mg/ml proteinase K) at 60^{o}C for 3 hours. Genomic DNA was precipitated using 150 µl of 150 mM NaCl in 100% ethanol, washed with 70% ethanol and re-suspended in 50 µl of TE (10 mM Tris-HCl pH 7.4, 0.1 mM EDTA) at 37^{o}C overnight. DNA was then digested with XbaI at 37^{o}C overnight, loaded onto a 0.7% TBE gel and electrophoresed at 45V overnight. The next morning gel was incubated successively in depurination solution (0.25 M HCl), denaturation solution (1.5 M NaCl; 0.5 M NaOH) and neutralization solution (1.5 M NaCl; 0.5 M Trizma base, pH 7.5). All incubations were performed with gentle rocking at room temperature for 30 min. After each step, the gel was rinsed with ddH_2O before the next solution was added. DNA was transferred onto Hybond nylon membrane (Amersham RPN303N) in 20X SSC (3M NaCl, 0.3M Na_3citrate.2H_2O, pH 7.0) overnight. DNA was cross-linked to the membrane by baking in the vacuum oven at 80^{o}C for 2 hours.

Southern blots were screened using a probe that contained sequences from exon 19 and intron 19, which lay outside the targeting construct. The probe was generated by amplifying a region of genomic DNA (SP500,F 5'-TAAGTAGCTAACTCCTGGAA-3' and SP500,R 5'-GTGATATGCTTAGTGTCAC-3'). The probe was labeled with dCTP[ά-^{32}P] using RediPrime II kit (Amersham RPN1633) according to the manufacturer's instructions.

The membranes were incubated with the denatured probe in UltraHyb buffer (Ambion, 8670) at 42^{o}C overnight. Unbound probe was washed away by rinsing the

membranes in 2X SSC/0.5% SDS at 42°C for 30 min twice. The membranes were exposed to autoradiography film at -80°C for seven days.

PCR

ES clones were screened using PCR (KOD Hot Start Polymerase, Novagen 71086-3) with primer SS4636,F (5'-CCATCTCTCCAGCCCCTTCATTT-3') located just outside the 5' terminus of the targeting construct and primer SSneo,R (5'-CGCCTTCTTGACGAGTTCTTCTG-3') located within the Neo cassette. PCR conditions were as follows: 94°C for 2 minutes; 94°C for 30 seconds, 60°C for 30 seconds, 68°C for 4 minutes times 35 cycles; 68°C for 10 minutes.

RT-PCR

Expression of the Rb^{N750F} allele was confirmed by sequencing the product of RT-PCR reaction. Total RNA was purified from ES cells using TRIzol^{R} (Invitrogen) and used as a template in RT-PCR reaction (SuperScript One-Step, Invitrogen 10928-034). A region of mRNA encoding Exons 21 through 24 was amplified using primer Ex21,F (5'-CAAGGTGAAGAACATCGACC-3') and primer Ex23,R (5'-ATGATTCACCA ATTGAGACC-3'). The resulting 400 bp product was purified and sequenced with internal primer Ex22,R (5'-ATCTCGGAGTCATTTTTGTGGG-3').

Isolation of Mouse Tail DNA

Tail tips (0.5 cm) were digested in 500 µl of lysis buffer (10 mM Tris-HCl pH 7.5, 400 mM NaCl, 2 mM EDTA, 0.5% SDS, 100 µg/ml Proteinase K) at 55ºC overnight. After the tissue was completely digested, 161 µl of saturated NaCl solution was added and tubes were incubated on ice for 30 minutes. Proteins and SDS were precipitated by centrifugation at 4ºC for 10 minutes. Supernatant was transferred into a new tube. DNA

was precipitated by adding 1 ml of cold 100% ethanol and centrifugation at 4ºC for 20 minutes. Supernatant was discarded and DNA pellet was washed with 70% ethanol twice. After the second wash, tubes were air-dried at room temperature for 20 minutes to allow the remaining ethanol to evaporate. DNA pellet was re-suspended in 200 µl of TE (10 mM Tris-HCl, pH 8; 1 mM EDTA).

Genotyping PCR

Presence of the *Rb-N750F*^{Neo} allele was detected using primer Rb7321,F (5'-AGTATGCCTCCACCAGGGTATGTT-3'), primer Rb7516,R (5'-CCAGGATCCGTAA GGGTGAACTA-3') and primer SSneo,R (5'-CGCCTTCTTGACGAGTTCTTCTG-3'). PCR conditions were as follows: 94^{o}C for 2 minutes; 94^{o}C for 30 seconds, 65^{o}C for 45 seconds, 72^{o}C for 45 seconds times 35 cycles; 72^{o}C for 10 minutes.

Presence of the Prm-Cre gene was detected using primers Cre-1 (5'-CTGCATTACCGGTCGATGCA-3') and Cre-2 (5'-ACGTCCACCGGCATCAACGT-3'). PCR conditions were as follows: 94^{o}C for 2 minutes; 94^{o}C for 30 seconds, 65^{o}C for 30 seconds, 72^{o}C for 30 seconds times 35 cycles; 72^{o}C for 10 minutes.

Excision of the Neo cassette was detected using primers Rb7321,F (5'-AGTATGCCTCCACCAGGGTATGTT-3') and Rb7825,R (5'-CACACATTCAC TAAATGCAC-3'). PCR conditions were as follows: 94^{o}C for 2 minutes; 94^{o}C for 30 seconds, 65^{o}C for 45 seconds, 72^{o}C for 45 seconds times 35 cycles; 72^{o}C for 10 minutes.

RESULTS

Generation of the Targeting Construct by Recombineering

A 6.4 kb fragment of mouse genomic DNA spanning exon 21 through 24 of *Rb* gene was sub-cloned into pBSK+ vector using Eco RI and Sac I restriction enzymes (Figure 2.1, construct A). The AAC codon of asparagine 750 was substituted with the TTC codon for phenylalanine. A new Xba I restriction site was created in intron 21 by site-directed mutagenesis (Figure 2.1, construct B). Both mutated regions and all exons were sequenced to ensure that no other changes were inadvertently introduced during cloning and mutagenesis.

Construct B was further modified by extending the 3' homology arm to include exons 25 through 27 and 3' untranslated region (UTR). This additional fragment was cloned using recombineering(5). Initially, a 300 bp fragment at the 3' terminal end of the 3' UTR was amplified to generate homology region (HR) 2. It was then cloned into construct B using Sac I restriction enzymes (Figure 2.2). Homology region 1 (HR1) was created by the virtue of a 300 bp overlap between the 3' end of construct A and 5' end of the extension fragment. The resulting plasmid was linearized and electroporated into DY380 competent cells together with a fragment of mouse genomic DNA containing intron 24 through the 3'UTR of the *Rb* coding region.

The DY380 *E. coli* strain carries three bacteriophage λ genes integrated into the bacterial chromosome as a defective prophage. Two of these genes are required for homologous recombination: *exo* encodes a 5'-3' exonuclease (Exo) that acts on the 5' end of the linear double-stranded DNA (dsDNA) fragment to produce 3' single-stranded DNA (ssDNA) overhangs; *bet* encodes a pairing protein (Beta) that binds to the 3'

ssDNA overhangs generated by Exo and promotes annealing of this ssDNA to a homologous sequence present on another fragment of DNA(9, 12). The third gene *gam* encodes a protein that inhibits the RecBCD exonuclease activity of *E.coli*, which would otherwise destroy linear dsDNA. The bacteriophage genes are expressed from the strong λ P_L promoter, which is under the control of the temperature-sensitive λ *cI857* repressor. Expression of *exo*, *bet* and *gam* is induced by incubating DY380 bacterial cultures at 42ºC for 15 minutes. Since both construct B and the 3' extension fragment are linear, neither can be propagated in *E. coli*. When DNA sequences that comprise HR1 and HR2 in construct B recombine with DNA in HR1 and HR2 in the 3' extension fragment, a circular plasmid is generated. This plasmid now has the ability to replicate.

The products of recombineering were selected by plating DY380 cultures on agar plates containing 100 μg/ml of ampicillin. Surviving colonies were screened for the presence of 3' extension by restriction analysis using Sac I.

Recombineering was also used to insert a selection cassette (the neomycin resistance gene driven by a hybrid PGK-EM7 promoter and flanked by loxP sites) into intron 23 of the extended construct. Briefly, 300 bp fragments of intron 23 adjacent to the insertion site were amplified by PCR to create homology region 3 (HR 3) and homology region 4 (HR 4). HR 3 and HR 4 were cloned 5' and 3' of the loxP sites of the Neo cassette. The targeting construct was linearized using Sal I and electroporated into DY380 *E. coli* together with the Neo cassette flanked by sequences from intron 23 (Figure 2.3). To screen for recombineering products, the culture was plated on agar plates containing 50 μg/ml of kanamycin. Clones that incorporated the Neo cassette were

resistant to kanamycin due to the expression of the *Neo* gene driven by the EM7 promoter. Surviving clones were screened using Xba I.

Gene Targeting

A total of 525 individual TC1 clones were picked. Additionally, 400 R1 clones were received from the UCSD Transgenic Mouse Core facility. All clones were screened by PCR and Southern blotting for homologous recombination of the targeting construct using primers and probe shown in Figure 2.4 A. Two clones appeared to be positive by PCR as determined by the presence of the expected 3.5 kb band (Figure 2.4 B), while seven clones were positive by Southern blotting (including the two that were identified by PCR) as evident by the appearance of an additional band at 7 kb (Figure 2.4 C). Therefore, the targeting frequency of Rb^{N750F} construct was 0.77%. Expression of the Rb^{N750F} allele was confirmed by sequencing the product of RT-PCR reaction (Figure 2.4 D and E).

Generation and Breeding of Rb^{N750F} mice

Blastocyst injection procedure was performed by the UCSD Transgenic Mouse Core. ES cells from two clones were injected into C57/BL6 blastocysts. Injection of ES cells from clone 5F11 (TC1) produced 14 pups, 6 of which were chimeras, while ES cells from clone 9A5 (R1) produced 18 pups, 10 of which were chimeras (Table 2.1).

Table 2.1 Results of blastocyst injections

Clone	# of progeny		# of chimeras	
	Males	Females	Males	Females
5F11	13	1	6	0
9A5	9	9	7	3

All resulting male chimeras were crossed to C57/BL6 females to test for the ability of $Rb^{N750F(Neo)}$ ES cells to contribute to the germ line of these males (Figure 2.5). The percentage of agouti-colored progeny born to each chimera ranged from 10% to 100%. Overall, the frequency of germ line transmission was 56% for chimeras derived from clone 5F11 and 43% for chimeras derived from clone 9A5.

Agouti progeny were genotyped for the presence of the $Rb^{N750F(Neo)}$allele (Figure 2.6A). Fifty percent of agouti progeny derived from 5F11 clone and 35 % of agouti progeny derived from 9A5 clone inherited the mutant allele. In order to remove the Neo cassette from intron 23, mice carrying $Rb^{N750F(Neo)}$allele were crossed to 129 Sv/Ev/Tac mice that contained a random integration of the *Cre* recombinase gene driven by the protamine promoter (PrmCre)(8). Males that carried $Rb^{N750F(Neo)}$ and PrmCre expressed Cre recombinase during spermatogenesis, which led to excision of the Neo cassette in the sperm DNA. These males were crossed to 129 Sv/Ev/Tac females to generate mice with the Rb^{N750F} allele and no Neo cassette. Excision of the Neo cassette was confirmed by PCR (Figure 2.6B). $Rb^{+/N750F}$ mice were intercrossed to generate homozygous $Rb^{N750F/N750F}$ mice of mixed 129/BL6 background.

Chimeric males that showed germ line transmission of the $Rb^{N750F(Neo)}$allele were also crossed to 129 Sv/Ev/Tac females to generate mice of pure background. All progeny born to these males were genotyped for the presence of $Rb^{N750F(Neo)}$ allele. The Neo cassette was removed as described above. The resulting $Rb^{+/N750F}$ mice were intercrossed to generate $Rb^{N750F/N750F}$ mice of pure 129 Sv/Ev/Tac background.

Genotyping of the progeny born to $Rb^{+/N750F}$ mice revealed that $Rb^{N750F/N750F}$ mutants are viable and are born at a slightly lower-than-expected Mendelian ratio (21%).

Table 2.2 Mendelian distribution of *Rb*^{N750F} allele.

Genotype	*Rb*$^{+/+}$	*Rb* $^{+/N750F}$	*Rb* $^{N750F/N750F}$
# of males	59	115	44
# of females	72	117	55
Total #	131	232	99
Percentage	28	50	21

DISCUSSION

Gene targeting technology in mice is a well established technique that has been used successfully for almost 20 years to generate mutations in numerous genes. However, the targeting frequency varies widely from 1% to 78% because each time a different genomic location is being altered (1, 2, 4, 7, 13, 15, 16). Two factors have been shown to affect targeting frequency: the source of genomic DNA used to make the targeting construct and the length of the homology arms on each side of the mutation within a targeting construct. Experiments with genomic DNA and ES cells derived from different strains of mice demonstrated that the highest frequency was achieved when both the DNA and the cells came from same strain of mice(13). Analysis of targeting frequencies obtained with targeting constructs of various lengths led to the recommendations that the optimal length of the homology arms to be 0.5-2 kb for the short arm and 3-5 kb for the long arm(3). Both of these findings were taken into consideration when the *Rb*^{N750F} targeting construct was generated: the genomic DNA came from the same 129 Sv/Ev/Tac strain of mice that TC1 cells were derived from and the homology arms were 2.4 kb and 10.2 kb for the short and long arms, respectively. However, the overall targeting frequency was still only 0.77%. Moreover, the targeting frequency was equally low in TC1 cells (4/525) and R1 cells (3/400). Since genomic

DNA used to generate the Rb^{N750F} targeting construct was derived from the same strain of mice that TC1 cells were derived from, one would expect the targeting frequency to be higher in TC1 cells than in R1 cells, which are derived from a different strain of mice(11). Therefore, the low efficiency of homologous recombination of the Rb^{N750F} targeting construct is probably due to an intrinsically low propensity for recombination in that area of the genome.

PCR screen missed most of the clones with targeted integration (5 out of 7). This was probably due to the fact that 3.5 kb of genomic DNA was amplified using crudely purified template. Typically, it is recommended that the length of the short homology arm should not exceed 2 kb if PCR is used to screen for homologous recombination events. For constructs with long homology arms, Southern blotting provides a more reliable method of screening.

Targeted ES cells efficiently contributed to the germ line with 13 out of 14 chimeric males producing litters that contained agouti pups. This indicated that ES cells were cultured under conditions that preserved their ability to produce healthy sperm. Additionally, the $Rb^{N750F/Neo}$ allele was transmitted through the germ line to 42% of agouti progeny, indicating that neither the mutation itself nor the presence of the Neo cassette were lethal. Excision of the Neo cassette was efficient, with 25 % of the progeny inheriting Rb^{N750F} allele.

Mice heterozygous and homozygous for Rb^{N750F} allele were born at the expected Mendelian ratio indicating that this mutation, unlike homozygous knockout of *Rb*, does not cause embryonic lethality. Therefore, the developmental defects observed in *Rb*-null mice are not caused by the inability of pRb to bind LxCxE-containing proteins. Because

$Rb^{N750F/N750F}$ mice are viable, we will be able to study the effects of this mutation in all tissues, and identify new organs and new processes that require the presence of a functional pRb but that have not been identified previously due to embryonic lethality of *Rb*-null mice.

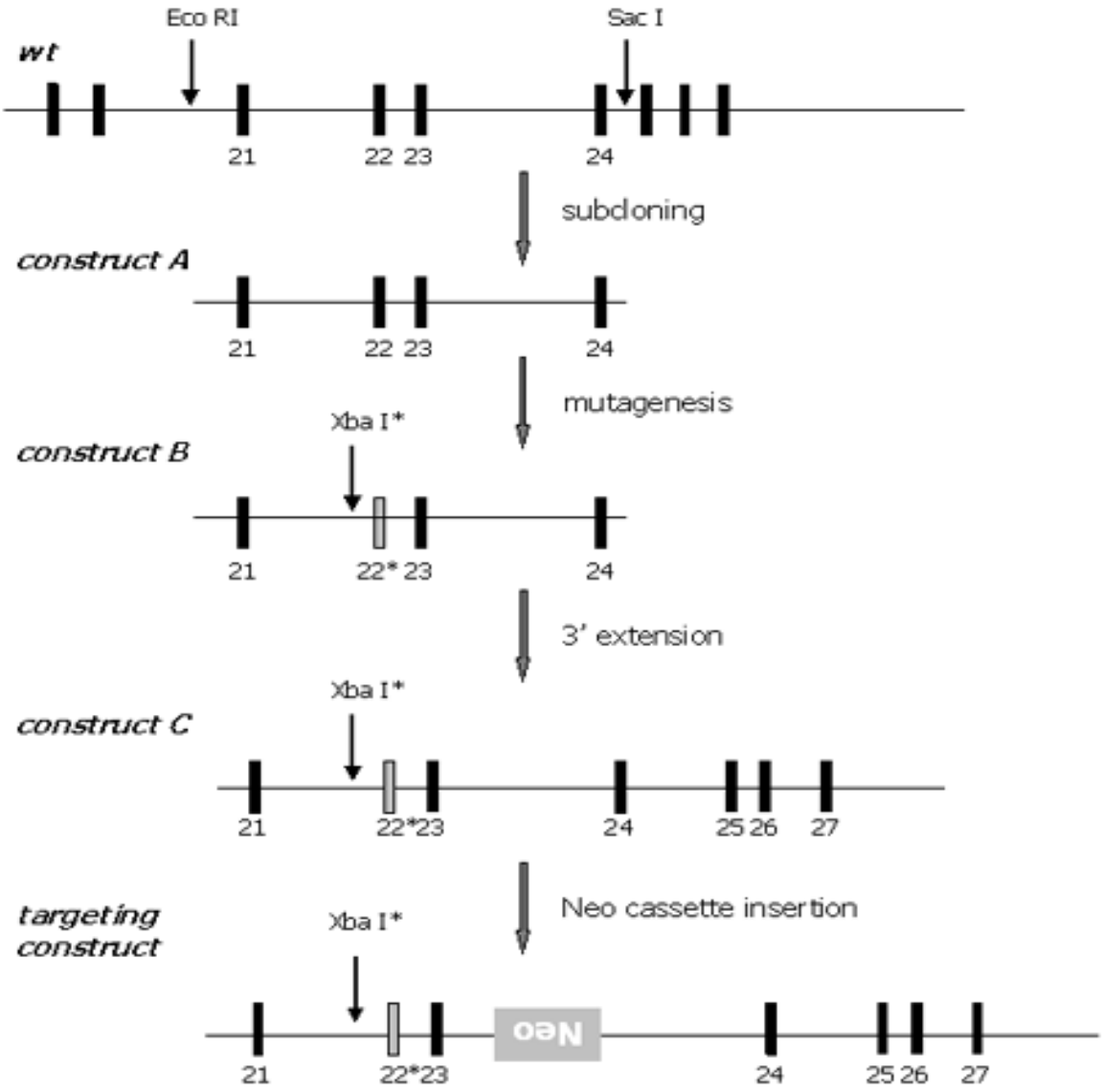

Figure 2.1 Cloning strategy for generating the targeting construct.

A 6.4 kb fragment of genomic DNA encoding *Rb* was subcloned from BAC to create construct A. The AAC codon for asparagine (N) 750 in exon 22 was mutated to the TTC codon for phenylalanine (F) and a new Xba I site was created in intron 21 (construct B). The 3' arm of construct B was extended to include exons 25 through 27 and 3' URT (construct C). The Neo cassette was inserted into intron 23 to generate the final targeting construct.

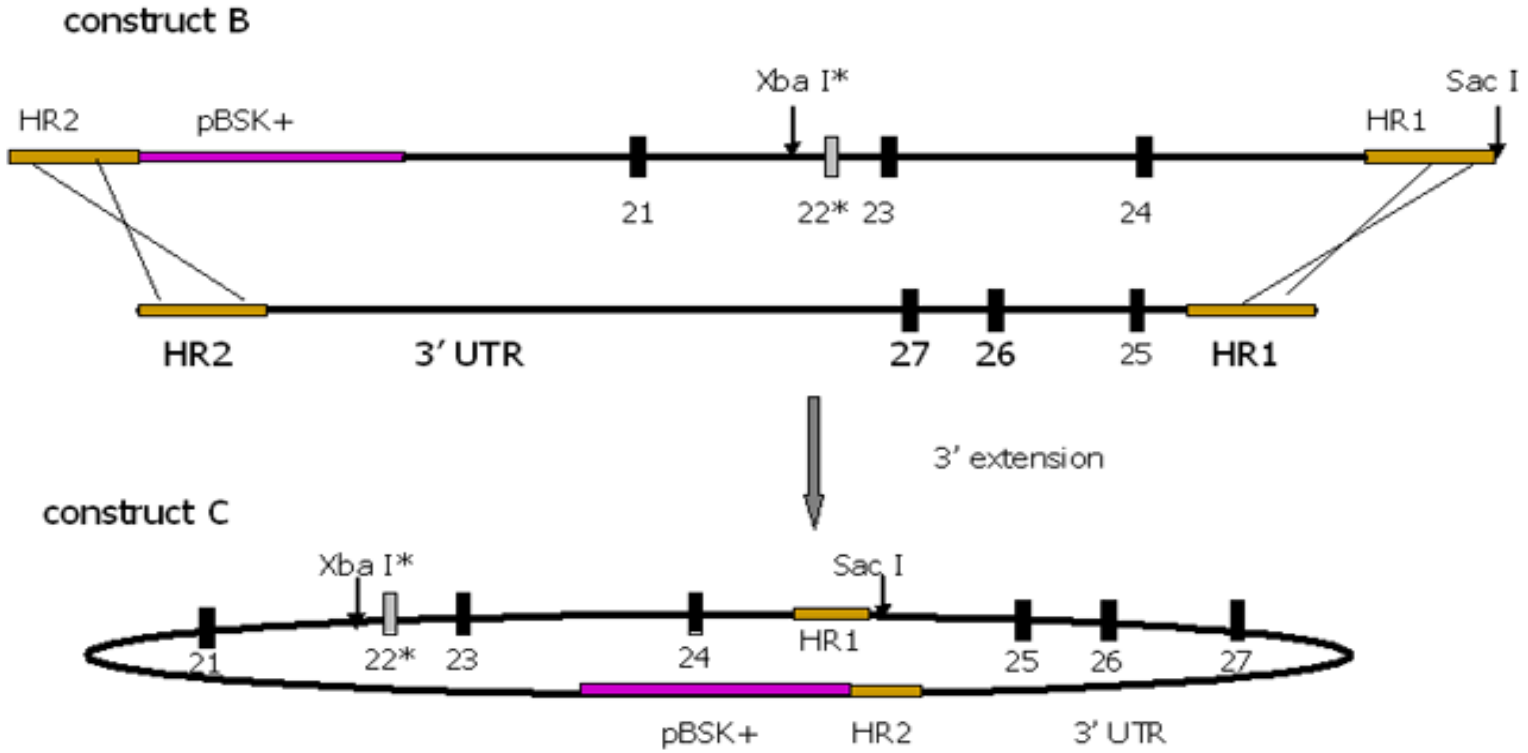

Figure 2.2 Addition of the 3' extension using recombineering.

Construct B contains homology regions 1 and 2 (HR1 and HR1) that correspond to the terminal 300 bp of the 5' and 3' ends of the 3' extension fragment. When linearized construct B and 3' extension fragment are electroporated together into DY380 bacteria, recombination occurs within homology regions producing construct C.

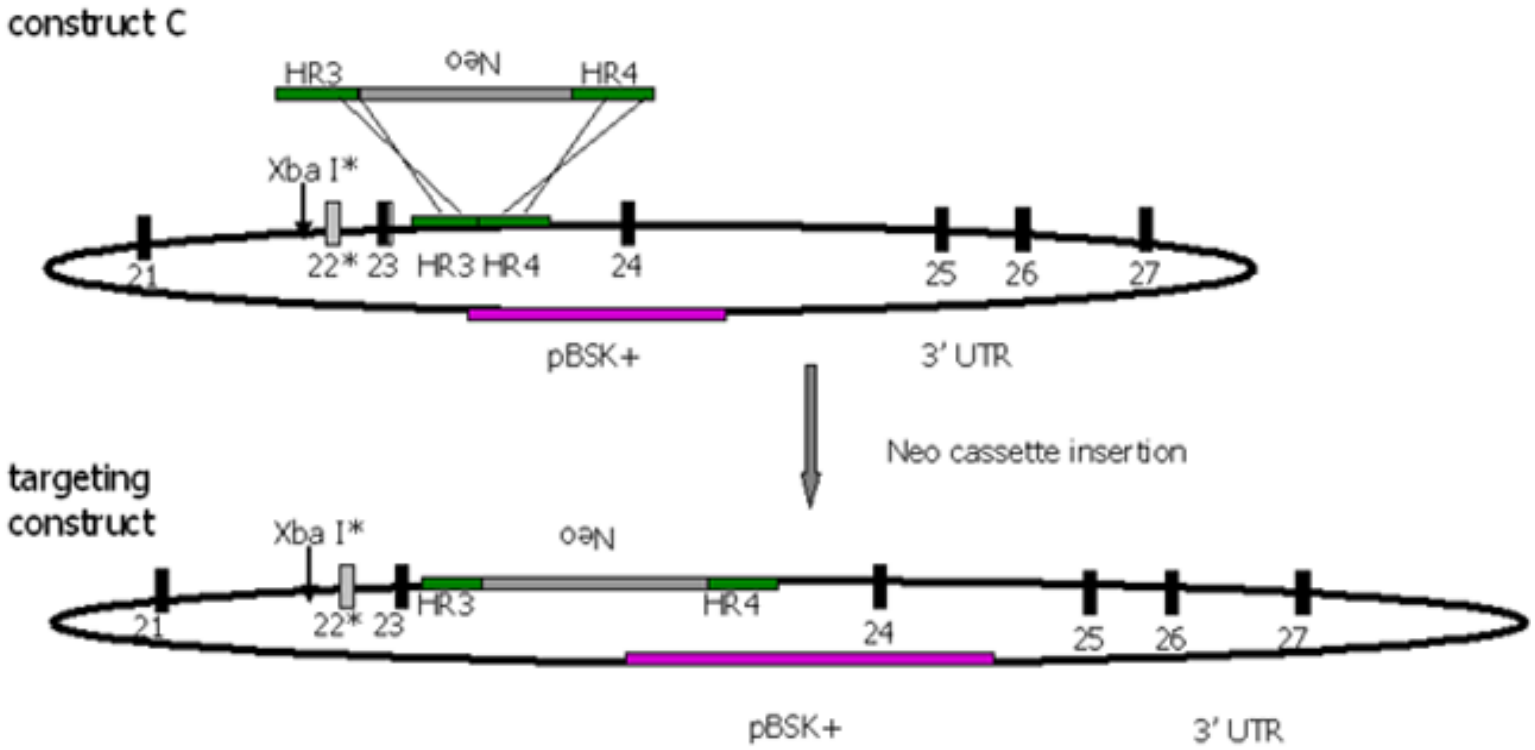

Figure 2.3 Insertion of the Neo cassette using recombineering.

The Neo cassette flanked by homology regions 3 and 4 (HR3 and HR4) and construct C were cotransformed into DY380 bacteria. Recombination within HR3 and HR4 resulted in insertion of the Neo cassette into intron 23, producing the final targeting construct.

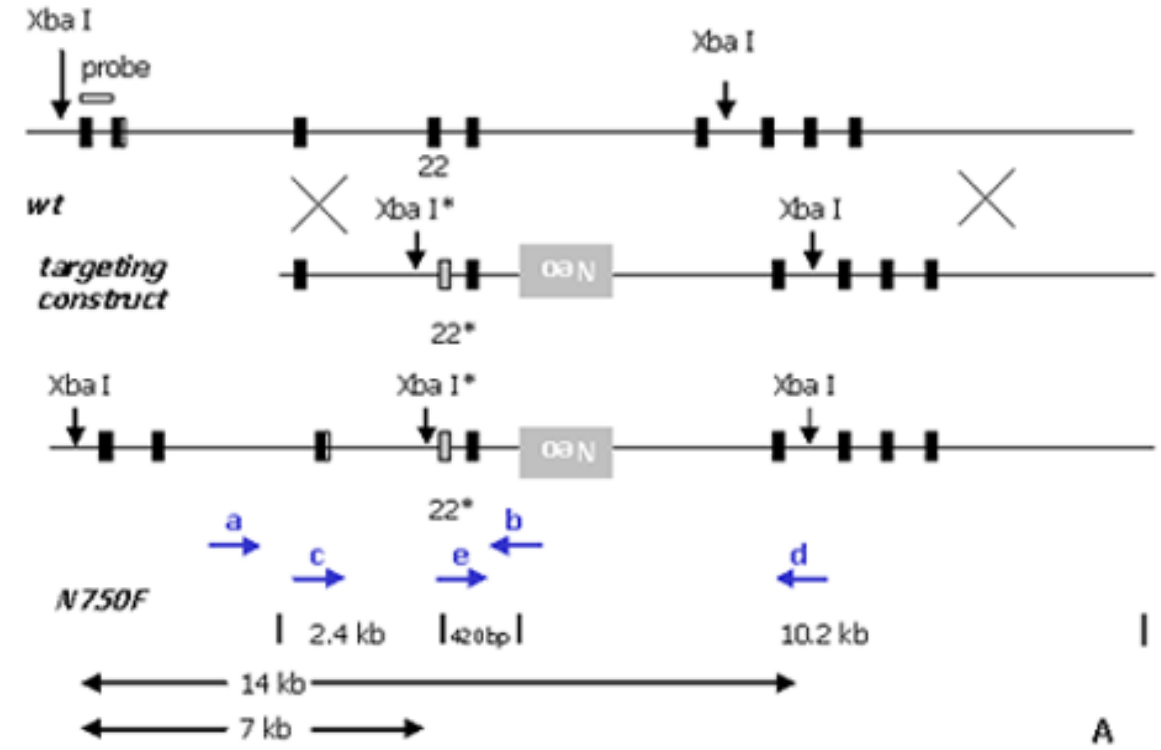

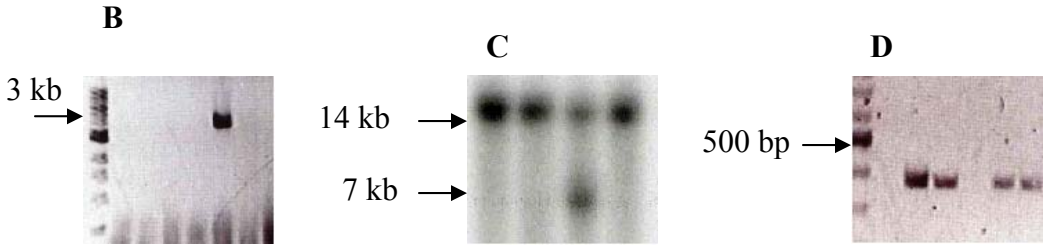

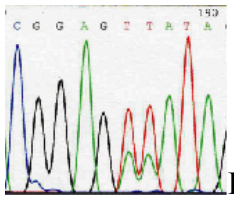

E

Figure 2.4 Generation of *Rb*$^{+/N750F}$ ES cells

A. Targeting strategy and screening scheme for Southern blotting. A probe located in Exon 19 was used to detect homologous recombination between targeting construct and genomic DNA in *Rb* locus. The locations of primers used in PCR screening, RT-PCR and sequencing are also shown. **B.** PCR of genomic DNA: a 3.5 kb band generated by primers ***a*** (SS4636,F) and ***b*** (SSneo,R) is present only in clones that contain *Rb*$^{N750F\ Neo}$ allele. **C.** Southern blot of genomic DNA digested with Xba I. The upper 14 kb band corresponds to the wild type allele while the lower 7 kb band corresponds to *Rb*$^{N750F\ Neo}$ allele. **D.** RT-PCR of total RNA isolated from sub-clones: a 400 bp product was generated using primers ***c*** (Ex21,F) and ***d*** (Ex23,R). **E.** The resulting product was sequenced with internal primer ***e*** (Ex22,R).

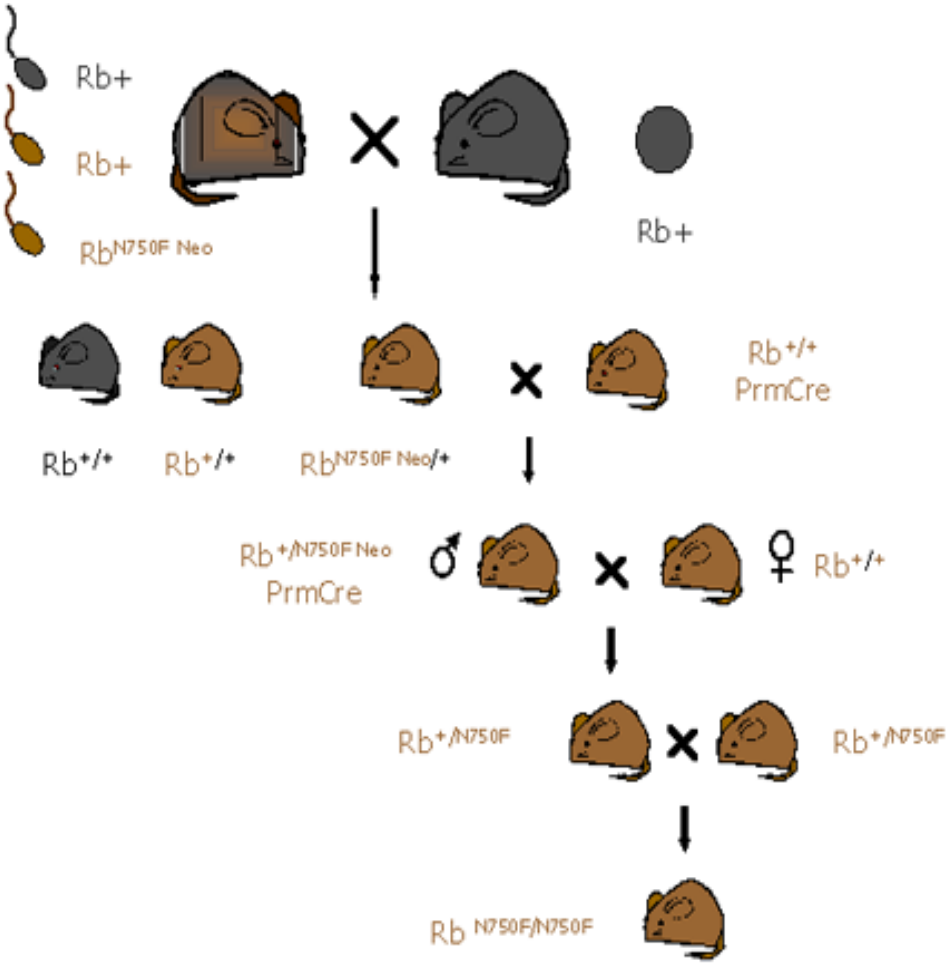

Figure 2.5 Testing for germ line transmission and breeding of *Rb*$^{N750F/N750F}$ mice.

Male chimeras were crossed to C57/BL6 females. Presence of agouti progeny in the resulting litters indicated that ES cells were contributing to germ line of these chimeras. Agouti progeny that were heterozygous for *Rb*$^{N750F\ Neo}$ allele were crossed to PrmCre mice that express Cre recombinase under the control of a protamine promoter, which is active during spermatogenesis. Males that inherited both *Rb*$^{N750F\ Neo}$ allele and PrmCre were crossed to wild type females to generate mice that carried *Rb*^{N750F} allele without the Neo cassette. The resulting *Rb*$^{+/N750F}$ mice were interbred to produce homozygous mutant mice.

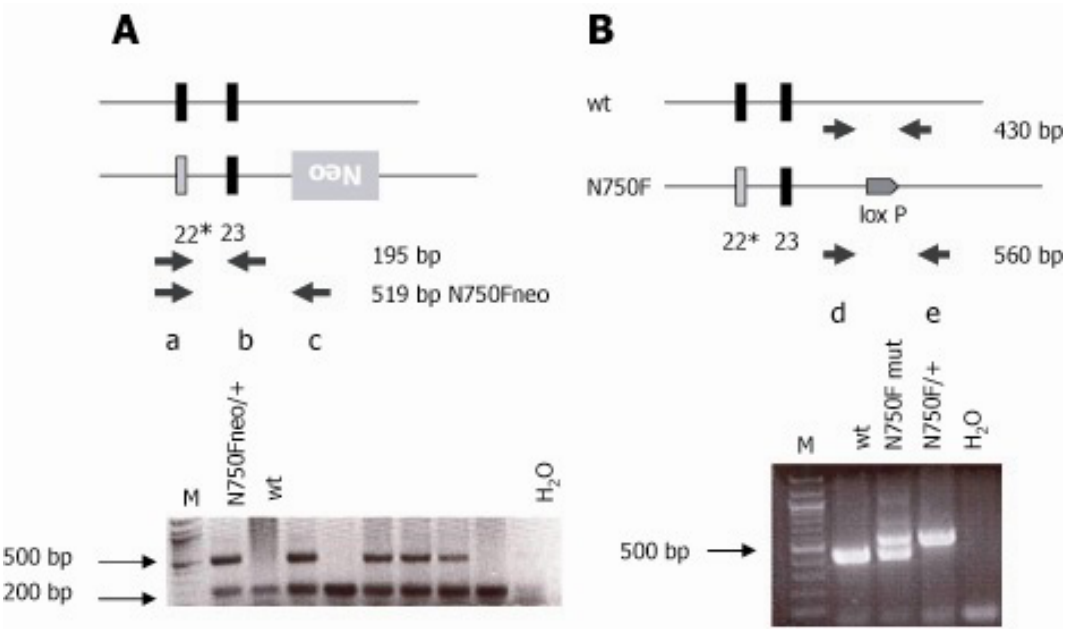

Figure 2.6 Genotyping PCR for transmission of *Rb*^{N750F} allele and Neo cassette excision.

A. Germ line transmission of *Rb*$^{N750F\ Neo}$ allele was detected by the presence of 519 bp band generated by primers ***a*** (Rb7321,F) and ***c*** (SSneo,R). The 195 bp band generated by primers ***a*** and ***b*** (Rb7516,R) served as a control for PCR reaction. **B.** Neo cassette excision was indicated by a 130-bp increase in the size of PCR product generated by primers ***d*** (Rb7321,F) and ***e*** (Rb7825,R).

REFERENCES

1. **Adair, G. M., R. S. Nairn, J. H. Wilson, M. M. Seidman, K. A. Brotherman, C. MacKinnon, and J. B. Scheerer.** 1989. Targeted homologous recombination at the endogenous adenine phosphoribosyltransferase locus in Chinese hamster cells. Proc Natl Acad Sci U S A **86:**4574-8.

2. **Camerini-Otero, R. D., and R. Kucherlapati.** 1990. Right on target. Applications of Homologous Recombination to Human Disease sponsored by the National Institutes of Health (NIGMS, NIDDK, and NICHD) Bethesda, MD, USA, November 6-8, 1989.

3. **Hasty, P., J. Rivera-Perez, and A. Bradley.** 1991. The length of homology required for gene targeting in embryonic stem cells. Mol Cell Biol **11:**5586-91.

4. **Koller, B. H., and O. Smithies.** 1989. Inactivating the beta 2-microglobulin locus in mouse embryonic stem cells by homologous recombination. Proc Natl Acad Sci U S A **86:**8932-5.

5. **Liu, P., N. A. Jenkins, and N. G. Copeland.** 2003. A highly efficient recombineering-based method for generating conditional knockout mutations. Genome Res **13:**476-84.

6. **Mansour, S. L.** 1990. Gene targeting in murine embryonic stem cells: introduction of specific alterations into the mammalian genome. Genet Anal Tech Appl **7:**219-27.

7. **Mansour, S. L., K. R. Thomas, and M. R. Capecchi.** 1988. Disruption of the proto-oncogene int-2 in mouse embryo-derived stem cells: a general strategy for targeting mutations to non-selectable genes. Nature **336:**348-52.

8. **O'Gorman, S., N. A. Dagenais, M. Qian, and Y. Marchuk.** 1997. Protamine-Cre recombinase transgenes efficiently recombine target sequences in the male germ line of mice, but not in embryonic stem cells. Proc Natl Acad Sci U S A **94:**14602-7.

9. **Poteete, A. R.** 2001. What makes the bacteriophage lambda Red system useful for genetic engineering: molecular mechanism and biological function. FEMS Microbiol Lett **201:**9-14.

10. **Robertson, E. J.** 1991. Using embryonic stem cells to introduce mutations into the mouse germ line. Biol Reprod **44:**238-45.

11. **Simpson, E. M., C. C. Linder, E. E. Sargent, M. T. Davisson, L. E. Mobraaten, and J. J. Sharp.** 1997. Genetic variation among 129 substrains and its importance for targeted mutagenesis in mice. Nat Genet **16:**19-27.

12. **Stahl, F. W.** 1998. Recombination in phage lambda: one geneticist's historical perspective. Gene **223:**95-102.

13. **te Riele, H., E. R. Maandag, and A. Berns.** 1992. Highly efficient gene targeting in embryonic stem cells through homologous recombination with isogenic DNA constructs. Proc Natl Acad Sci U S A **89:**5128-32.

14. **Thomas, K. R., and M. R. Capecchi.** 1987. Site-directed mutagenesis by gene targeting in mouse embryo-derived stem cells. Cell **51:**503-12.

15. **Thomas, K. R., K. R. Folger, and M. R. Capecchi.** 1986. High frequency targeting of genes to specific sites in the mammalian genome. Cell **44:**419-28.

16. **Zijlstra, M., E. Li, F. Sajjadi, S. Subramani, and R. Jaenisch.** 1989. Germ-line transmission of a disrupted beta 2-microglobulin gene produced by homologous recombination in embryonic stem cells. Nature **342:**435-8.

17. **Zimmer, A.** 1992. Manipulating the genome by homologous recombination in embryonic stem cells. Annu Rev Neurosci **15:**115-37.

CHAPTER III

PHENOTYPE OF *Rb*$^{N750F/N750F}$ MEFs AND 3T3s

INTRODUCTION

Primary mouse embryonic fibroblasts (MEFs) and immortalized cell lines derived from them (3T3) have been widely used to study the effect of *Rb* loss on various cellular functions. Because pRb was known to be phosphorylated by several Cyclin/CDK complexes, *Rb*-null MEFs were closely examined for any alterations in the cell cycle. Surprisingly, only mild perturbations of this process were detected: a slight decrease in the length of G1 and a slight increase in the length of S phase(8). The loss of pRb resulted in elevated levels of expression of Cyclin E, Cyclin D1 and Cyclin A. Later experiments demonstrated that the combined loss of all members of the pocket family proteins – pRb, p107 and p130 – was necessary to achieve profound cell cycle defects, as well as spontaneous immortalization and insensitivity to contact inhibition(20). Despite very mild cell cycle defects, the gene expression profile of *Rb*-null MEFs was significantly different from that of wild type controls. Specifically, a number of genes involved in cell cycle regulation, DNA replication and mitosis were upregulated in *Rb*$^{-/-}$ MEFs(2, 12). Further analysis revealed that many of those upregulated genes were under the control of the E2F family of transcription factors(12). These findings provided additional support for the importance of interactions between pRb and E2F proteins for cell cycle regulation and tumorigenesis.

In addition to positive regulators of transcription, pRb also interacts with several transcriptional repressors and chromatin remodeling proteins, many of which contain the LxCxE amino acid motif(5, 9, 10, 13, 15, 21). This peptide sequence was initially identified in viral oncoproteins SV40 T antigen, HPV E7 and E1A, and was found to be crucial for their ability to bind to pRb(4, 6, 7). The crystal structure of pRB bound to the LxCxE containing peptide of HPV E7 protein made it possible to rationally design mutations in pRB that would affect only a subset of its binding partners(11). An asparagine-to-phenylalanine substitution of amino acid 757 was designed to disrupt the binding of pRB to LxCxE-containing proteins(3). Initial experiments with pRB-N757F mutant showed that it was indeed unable to bind to LxCxE-containing proteins (HPV E7, E1A and HDAC1). However, it could still bind to E2F1 and induce cell cycle arrest in Saos2 cells, indicating that pRB-N757F retained the ability to regulate cell cycle progression.

Myogenic differentiation experiments with *Rb*-null cells demonstrated the crucial role of pRb in this process(18). *Rb*-null MEFs induced to differentiate into myotubes exhibited morphological changes and expressed early markers of myogenic lineage. However, *Rb*-null MEFs displayed low expression of late differentiation markers, e.g. myosin heavy chain (MyHC), and were unable to permanently exit the cell cycle, indicating that the process of myogenic differentiation was incomplete. Experiments with pRB-N757F mutant demonstrated that cells expressing this protein were capable of initiating myogenic differentiation, but were unable to establish irreversible growth arrest in myotubes(3). This finding indicates that the LxCxE-binding domain of pRB plays a crucial role in this process.

In order to further characterize the effect of specifically disrupting the interactions between pRb and LxCxE-containing proteins, we studied cells from $Rb^{N750F/N750F}$ mice. These mice were created by gene targeting and carry an asparagine-to-phenylalanine substitution at position 750, which is equivalent to the N757F substitution in the human protein (see Chapter II). In $Rb^{N750F/N750F}$ cells the mutant protein is expressed from the genomic locus under the control of the endogenous regulatory elements and at the physiological level. Therefore, this system provides a well-controlled environment in which to study the role of the LxCxE-binding domain in the function of pRb.

MATERIALS AND METHODS

Cell culture

To generate MEFs, pregnant females (gestational day 10-13) were sacrificed by CO_2 asphyxiation. Embryos were removed and rinsed in PBS. The heads were cut off and used as a source of genomic DNA for genotyping. The trunks were minced, trypsinized and aspirated several times to achieve single cell suspensions. Cells were cultured in growth media consisting of DMEM (Mediatec 45000-312) supplemented with 10% FBS (Hyclone SH30088.03), 100 I.U./ml of penicillin and 100 μg/ml of streptomycin (Mediatec 30-002-CI) and 56μM β-mercaptoethanol (Sigma M3148).

To derive 3T3 cells, $1x10^6$ of MEFs were plated into five 6-cm dishes at 200,000 cells per dish and passaged every three days until the number of cells was doubling at every passage.

For myogenic differentiation experiments, cells were cultured in differentiation media: DMEM (Mediatec 45000-312) supplemented with 2% horse serum (Invitrogen

16050-130), 100 I.U./ml of penicillin and 100 μg/ml of streptomycin (Mediatec 30-002-CI). Early passage (3-6) MEFs were used in all experiments. All comparisons were made between cells at identical passage number obtained from littermate controls.

For contact inhibition experiments, MEFs were plated at 300,000 cells per 6 cm dish. Media was changed every day. Cells were trypsinized and counted on days 2, 4, 6, 8 and 10.

Genotyping

Heads obtained from the embryos were digested in lysis buffer (10 mM Tris-HCl, pH 7.5; 400 mM NaCl, 2 mM EDTA, 0.5% SDS, 100 μg/ml Proteinase K) at 55ºC overnight. After the tissue was completely digested, saturated NaCl solution was added in the amount equal to 1/3 volume of the lysis buffer, and tubes were incubated on ice for 30 minutes. Proteins and SDS were precipitated by centrifugation at 4ºC for 10 minutes. Supernatant was transferred into a new tube. DNA was precipitated by adding 2 volumes of cold 100% ethanol and centrifugation at 4ºC for 20 minutes. Supernatant was discarded and the DNA pellet was washed with 70% ethanol twice. After the second wash, tubes were air-dried at room temperature for 20 minutes to allow the remaining ethanol to evaporate. DNA pellets were resuspended in 200 μl of TE (10 mM Tris-HCl, pH 8; 1 mM EDTA).

Plasmids

pMSCVpuro vector was purchased from Clontech (K-1062-1). E1A was cloned XhoI and EcoRI into pMSCVpuro. pBabepuro vector was described by Morgenstern et. al(14). MyoD was cloned into pBabepuro using BamHI and EcoRI restriction sites.

Generation of stable cell lines

BOSC 23 ecotropic retrovirus packaging cell line was used to produce retrovirus(19). Cells were transfected with pMSCVpuro or pMSCVpuro-E1A using Lipofectamine 2000^{TM} (Invitrogen 11668-019) according to the manufacturer's protocol, and incubated at 37ºC, 5% CO_2 for 12 hours. Media was changed and cells were incubated for an additional 48 hours. Virus-containing media was harvested, filtered and added to plates that contained MEFs or 3T3 cells at 50% confluence. The next day, media was changed and puromycin selection was introduced (4 μg/ml for MEFs and 2 μg/ml for 3T3). Selection was removed after three days and surviving clones were expanded. Expression of E1A was verified by immunoblotting.

Myogenic differentiation

3T3 or MEFs were plated onto glass cover slips at 50% confluence and infected with retroviral MyoD. Twenty four hours after infection, puromycin selection was introduced and maintained for 3 days in order to enrich for infected cells. After puromycin selection was removed, cells were grown to full confluence and switched to differentiation media for 3 days. To determine the ability of myotubes to incorporate BrdU, cells were placed back in growth media and labeled with BrdU (10 μM) for 24 hours.

Immunofluorescence

Cover slips with attached cells were washed with PBS once. Cells were fixed in 3.7% formaldehyde for 20 minutes and permeabilized with 0.3% Triton-X for 15 minutes. To prevent non-specific binding of antibodies, cells were incubated in PBS with 10% normal goat serum for 1 hour. Primary antibody staining was carried out at room

temperature for 2 hours. Cover slips were rinsed in PBS three times for 5 minutes to wash out unbound antibody. Secondary antibody staining was carried out at room temperature for 2 hours followed by three 5-minute rinses in PBS. Cells were stain with Hoechst solution and mounted onto glass slides using Gel/Mount (Biomeda, M01). Cells were counted on a Zeiss Axioskop. Myosin heavy chain (MyHC) was detected using monoclonal anti-myosin antibody (Sigma, clone MY-32) at 1:200 dilution. BrdU was detected using rat anti-BrdU antibody (Accurate Chemical and Scientific, OTB0030) at 1:500 dilution.

Immunoprecipitations and Western analysis

Cells pellets were resuspended in TT lysis buffer (25 mM Tris-HCl, pH 7.5; 250 mM KCl, 0.5% NP-40, 0.1% Triton X, 5 mM EDTA, 25 mM NaF, 14 mM betamercaptoethanol, protease inhibitors (Sigma, P8340)) and incubated with rotation at 4ºC for 20 minutes. Lysates were sonicated to break up DNA and centrifuged at 4ºC for 20 minutes. Protein concentration was determined using Protein Assay reagent (BioRad 500-0006).

For immunoprecipitations, primary antibody was added to cell lysate and the total volume was brought up to 1 ml with TT lysis buffer. Tubes were incubated with rotation at 4ºC for 2 hours. 20 µl of Protein A (Amersham, 17-0469-01) and 20 µl Protein G (Amersham, 17-0618-04) linked to Sepharose beads were added to each tube and incubated with rotation at 4ºC for another 2 hours. Protein complexes bound to beads were precipitated by centrifugation and washed with 1 ml of TT lysis buffer three times. Proteins were eluted by boiling in 3X SDS Sample Buffer (200 mM Tris-HCl pH 6.8, 30

mM EDTA, 6% SDS, 30% glycerol, 0.1% Bromophenol Blue) for 5 minutes and loaded onto polyacrylamide gels for electrophoresis.

The following antibodies were used: monoclonal anti-E1A (Santa Cruz sc-25), polyclonal anti-E1A (Santa Cruz sc-430), monoclonal anti-Rb (Pharmingen 554136), polyclonal anti-Rb 851(23), polyclonal anti-p107 (Santa Cruz sc-318), polyclonal anti-p130 (Santa Cruz sc-317), monoclonal anti-tubulin (Sigma, clone B-5-1-2).

FACS

Early passage MEFs were collected by trypsinization, rinsed in cold PBS and fixed in 70% ethanol at -20ºC overnight. The next day cells were washed in cold IFA buffer (1X HEPES, 4% FBS) and precipitated by centrifugation. Cell pellet was resuspended in 1M HCl with 0.7% Triton X, incubated at room temperature for 10 minutes, washed with 4 ml of IFA buffer and precipitated again. Cell pellets were rinsed again with 4 ml of IFA buffer twice and resuspended in 0.5 ml of water with 16 µl of 1M HCl. Cell suspension was incubated at 97-100ºC for 10 minutes and transferred on ice for additional 10 minutes. Cells were rinsed in 1.5 ml of IFA buffer with 0.5% Tween 20 and precipitated by centrifugation. Cells were labeled with anti-BrdU antibody conjugated to FITC (2µl in 50 µl of IFA buffer) in the dark for 30 minutes. Labeling solution was washed out with 1 ml of IFA buffer with 0.5% Tween 20. Cells were labeled with propidium iodide and treated with RNase A solution (125 µg/ml of propidium iodide and 25 µg/ml of RNase A). FACS analysis was performed on FACSCalibur (BD Biosciences).

Microarray analysis of gene expression

Total RNA was extracted from 10^5 to 10^6 cells using RNeasy kit (Qiagen 74104) following manufacturer's protocol. Reverse transcription to cDNA was carried out using Low RNA Input Linear Amplification kit (Agilent Technologies 5184-3523). The resulting cDNA was labeled either with cy5 or cy3 dCTP (Perkin Elmer). Efficiency of fluorescent dye labeling was determined by Nanodrop (Nanodrop, Wilmington, DE). 750 ng cDNA was put on each Whole Genome Mouse Array chip (Agilent G4122A) and processed according to the manufacturer's instructions. The array was scanned with Agilent Scanner. The raw data were generated by Agilent Feature Extraction 8.0(FE) software.

RESULTS

N750F mutation disrupts binding of pRb to Adenovirus E1A protein

To confirm the inability of pRb-N750F to bind LxCxE-containing proteins, we tested the interactions between this mutant and adenovirus E1A protein. E1A was introduced by retroviral infection into 3T3 cells derived from either wild type or $Rb^{N750F/N750F}$ embryos. Expression of pRb and E1A in 3T3 cells was confirmed by Western blotting (Figure 3.1 A). E1A was expressed at similar levels in $Rb^{+/+}$ and $Rb^{N750F/N750F}$ 3T3 cells. As expected, polyclonal anti-E1A antibody efficiently precipitated wild type pRb, but not from mutant pRb (Figure 3.1 B). The reciprocal co-immunoprecipitation with anti-Rb antibody demonstrated binding of pRb to E1A in wild type but not mutant 3T3 cells (Figure 3.1 C). These experiments confirm that

substitution of asparagine 750 with phenylalanine in murine pRb effectively destroyed its ability to bind LxCxE-containing proteins.

Terminally differentiated *Rb*$^{N750F/N750F}$ myotubes are resistant to re-stimulation with serum

Myogenic differentiation can be modeled in tissue culture cells by expression of myogenic transcription factor MyoD combined with culturing in low-serum media at high density. Under these conditions cells differentiate into myotubes and withdraw permanently from the cell cycle. Subsequent re-stimulation with serum does not result in DNA synthesis. The role of pRb in terminal differentiation of myotubes has been well-established. Rb-/- myotubes have been shown to express early markers of myogenic differentiation, however, the expression of late markers was dramatically reduced, as compared to the wild type myotubes(18). Moreover, Rb-/- myotubes were not able to withdraw permanently from the cell cycle and continued to replicate DNA, as evidenced by BrdU incorporation, even while being cultured in low-serum media.

Myogenic differentiation experiments conducted using *Rb*-null MEFs reconstituted with human pRB demonstrated that differentiated myotubes expressing pRB-N757F mutant were able to incorporate BrdU following re-stimulation with serum, while myotubes expressing wild type pRB maintained post-mitotic state(3). In order to test whether these findings can be reproduced with endogenous murine pRb-N750F, we subjected *Rb*$^{N750F/N750F}$ and control wild type MEFs to myogenic differentiation. We found that both mutant and wild type MEFs were capable of differentiating into myotubes, as confirmed by expression of late muscle differentiation marker MyHC (Figure 3.2). Once differentiated, neither *Rb*$^{N750F/N750F}$ nor wild type myotubes

incorporated BrdU, indicating that these cells permanently withdrew from the cell cycle. Therefore, unlike human pRB-N757F, murine pRb-N750F was capable of maintaining permanent growth arrest in differentiated myotubes.

Accelerated immortalization rate of $Rb^{N750F/N750F}$ MEFs

During the process of 3T3 derivation, we noticed that $Rb^{N750F/N750F}$ MEFs immortalized at an earlier passage than wild type MEFs, although this phenotype was not 100% penetrant (Figure 3.3). In order to determine the cause of accelerated immortalization, we performed cell cycle analysis of asynchronously growing early passage MEFs. Because pRb is an important regulator of the cell cycle progression, we attempted to determine whether this process was perturbed in $Rb^{N750F/N750F}$ cells. No differences were detected in the length of G1, S and G2/M phases in wild type, $Rb^{N750F/+}$ and $Rb^{N750F/N750F}$ MEFs (Figure 3.4 A-C). We also found that $Rb^{N750F/+}$ and $Rb^{N750F/N750F}$ MEFs were still sensitive to contact inhibition (Figure 3.4 D). Therefore, we discovered that the LxCxE-binding domain of pRb contributes to immortalization process of MEFs in tissue culture; however, it does not significantly alter cell cycle progression or causes the loss of sensitivity to contact inhibition.

The LxCxE-binding domain of pRb does not regulate genes whose expression is altered in Rb-null MEFs

Associations between pRb, members of the E2f family of transcription factors and several transcriptional repressors point to a role for pRb in regulation of gene expression. Several studies examined the effect of pRb loss on gene expression profiles in MEFs(2, 12). They reported that Rb-/- MEFs exhibit increased expression levels of genes involved in cell proliferation, DNA metabolism and transcription, some of which are

under the transcriptional control of E2f family transcription factors(2). Interestingly, there was also a decrease in the expression level of genes that are associated with immune response and response to pathogen or injury(12). Specifically, the downregulated genes encoded chemokines, complement factors, cell surface antigens and receptors.

We tested whether $Rb^{N750F/N750F}$ MEFs would exhibit deregulation of gene expression in a pattern similar to those reported in *Rb*-null MEFs. We discovered that there was no overlap between the genes deregulated by the complete loss of pRb and the loss of the LxCxE-binding function of pRb, indicating that the LxCxE-binding domain does not control expression of genes involved in cell proliferation, DNA metabolism, and transcription. This finding was consistent with our observation that the cell cycle of $Rb^{N750F/N750F}$ MEFs was unperturbed. Moreover, since pRb-N750F was still capable of binding to members of the E2f family transcription factors, we would not expect to see any deregulation of E2f-controlled genes.

pRb-N750F protein compromises the ability of E1A to deregulate gene expression

Infection of wild type MEFs with a virus expressing adenovirus E1A protein induces changes in gene expression similar to the ones associated with the loss of pRb. Specifically, several cell cycle genes are upregulated in both E1A-infected and *Rb*-null MEFs. However, these genes are expressed normally in $Rb^{N750F/N750F}$ MEFs (Figure 3.5). These findings imply that E1A and pRb-N750F affect gene expression by a different mechanism, i.e. E1A deregulates genes expression by dissociating pRb from E2f, not by displacing some LxCxE-containing proteins from pRb. Because E1A cannot bind to the

pRb-N750F mutant, we explored the ability of E1A to deregulate gene expression in $Rb^{N750F/N750F}$ MEFs. Interestingly, only 7 genes (Mcm3, Fen1, Rfc5, Msh2, Hmgn2 and Hat1) were still upregulated, implying that E1A can control expression of these genes through a mechanism that does not involve binding to pRb through the LxCxE motif. However, upregulation of other cell cycle genes was absolutely dependent on E1A-pRb interactions.

The LxCxE-binding domain of pRb regulates expression of numerous homeobox genes in primary MEFs

The gene expression pattern of $Rb^{N750F/N750F}$ MEFs was distinctly different from that of wild type controls. Surprisingly, a large group of homeobox genes, as well as several other transcription factors involved in pattern formation during embryogenesis were deregulated (Table 3.1).

Table 3.1 Deregulation of pattern-formation genes in $Rb^{N750F/N750F}$ MEFs

Upregulated in $Rb^{N750F/N750F}$				Downregulated in $Rb^{N750F/N750F}$	
Gene name	Fold change	Gene name	Fold change	Gene name	Fold change
Hox b2	10.5	Emx2	3.8	Hox a10	3.1
Hox b3	1.6	Fox g1	14.1	Hox a13	1.7
Hox b4	1.9	Hmga1	3	Hox d13	16
Hox b5	3.6	Ihx 8	2.3	Fox c1	2
Hox b6	3	Irx 1	2.3	Fox d1	18.9
Hox b7	6.7	Irx 2	2	Fox f2	5.3
Hox c6	10	Sox 11	2.2	Fox o1	2
Hox c8	2.5	Twist 2	3.3	Fox p1	1.8
Hox c10	3.4	Vax 2	5.2	Bmp 4	4.6
Hox d8	2	Zfhx 4	2.5	Sox 6	1.9

Therefore, we report for the first time that LxCxE-binding domain of pRb regulates gene expression of numerous genes, including homeodomain and several other transcription factors that regulate pattern formation during embryogenesis.

DISCUSSION

We utilized the crystal structure of pRB A/B pocket bound to HPV E7 LxCxE-containing peptide to engineer a mutation in pRB that would eliminate the interactions between these two proteins. We characterized pRB-N757F mutant by examining its biochemical properties and discovered that it was indeed unable to bind adenovirus E1A, HPV E7 and HDAC1 proteins(3). However, it was still able to bind E2F1, demonstrating a specific disruption of the LxCxE-binding domain of pRB. We also discovered that the pRB-N757F mutant was capable of regulating cell cycle progression in Saos2 cells, but was unable to establish irreversible growth arrest in myotubes.

Based on these results, we proceeded to create mice with a targeted mutation in pRb protein that was equivalent to pRB-N757F mutation. Cells from $Rb^{N750F/N750F}$ embryos were used to study the role of LxCxE-binding domain of pRb in various biological processes.

Initially, we performed biochemical characterization of the pRb-N750F protein. Just like its human homologue, pRb-N750F was unable to bind adenoviral E1A protein, confirming the disruption of the LxCxE-binding domain. This finding demonstrates that any phenotypes observed in $Rb^{N750F/N750F}$ cells, as well as in mice, are the result of a disruption of interactions between pRb and LxCxE-containing proteins.

The LxCxE-binding domain of pRb is dispensible for myogenic differentiation

Differentiation of $Rb^{N750F/N750F}$ MEFs into myotubes resulted in expression of MyHC, the appearance of myotube morphology and permanent withdrawal from the cell cycle. We could not see the defect in establishment of irreversible growth arrest previously observed with pRB-N757F mutant. The most likely explanation for this discrepancy is the fact that the human pRB is only 90% identical to the murine pRb, and, therefore, might not be able to substitute for it completely in the myogenic differentiation assays. Alternatively, the molecular mechanisms of establishing permanent growth arrest during muscle differentiation might be fundamentally different in humans and mice. In human myotubes, the LxCxE-binding domain of pRB might be crucial for this process, and, therefore, disruption of interactions between pRB and an LxCxE-containing protein would render differentiated human myotubes incapable of permanently withdrawing from the cell cycle. In mice, however, the interactions between pRb and an LxCxE-containing protein might be dispensable for the establishment of irreversible growth arrest in differentiated myotubes, so inactivation of the LxCxE-binding domain would not compromise this process.

The LxCxE-binding domain of pRb contributes to immortalization of MEFs

During 3T3 derivation we observed that $Rb^{N750F/N750F}$ MEFs immortalized at earlier passages than their wild type littermate controls, however, the processes of cell cycle regulation and contact inhibition in mutant MEFs were still intact. These findings were in agreement with the mouse data showing that $Rb^{N750F/N750F}$ mutants did not develop neoplasms (see Chapter II).

Several reports have demonstrated that pRb is involved in silencing E2F target genes during cellular senescence and terminal differentiation. Specifically, pRb was found to associate with *Cyclin A* and *PCNA* promoters in senescent, but not quiescent human fibroblasts(16). Upon infection, *ras* oncogene induces senescence in human fibroblasts, as evidenced by the formation of senescence-associated heterochromatic foci in the nucleus and downregulation of S-phase genes. Inactivation of pRb by E1A prevents formation of senescence-associated heterochromatic foci and leads to re-expression of *Cyclin A*, *PCNA*, and *MCM3*, indicating that pRb is necessary for establishment of senescent phenotype in human fibroblasts.

Differentiation represents another form of senescence that is characterized by permanent withdrawal from the cell cycle. In differentiated myotubes, promoters of several S-phase genes (*B-Myb*, *Cyclin E*, *Cyclin D1* and *DHFR*) have been shown to contain histone H3 methylated at lysine 9 (H3K9Me), which is associated with gene silencing and heterochromatin(1). Methylation of these promoters is dependent on Suv39h, as depletion of Suv39h by siRNA severely reduced the amount of H3K9Me found at these promoters. Additionally, depletion of Suv39h in myoblasts blocked their differentiation into myotubes, as determined by decreased levels of expression of muscle-specific differentiation markers: myogenin, myosin heavy chain and muscle creatine kinase. These data demonstrate the importance of Suv39h pathway for establishing irreversible growth arrest during differentiation.

Interestingly, pRb has been shown to associate with Suv39h methylase activity(17). The binding of pRb to Suv39h is indirect and involves another protein HP1, which uses LxCxE motif to bind to pRb. Together, pRb, Suv39h and HP1 were shown to

methylate histone H3 on Lysine 9 on the *Cyclin E* promoter. Therefore, increased rates of immortalization of $Rb^{N750F/N750F}$ MEFs might be explained by the inability of the pRb-N750F to bind to HP1, which in turn could lead to the inability to silence S-phase genes and inability to establish cellular senescence.

Regulation of gene expression by the LxCxE-binding domain of pRb

Analysis of gene expression in $Rb^{-/-}$ MEFs revealed elevated levels of expression of a large number of genes associated with cell cycle progression and DNA synthesis, confirming the importance of pRb in regulating S-phase entry. However, expression of these genes was not affected in $Rb^{N750F/N750F}$ MEFs, consistent with the observation that the cell cycle of $Rb^{N750F/N750F}$ MEFs was unperturbed. Expression of adenoviral E1A mimicked the loss of pRb by upregulating the expression of genes associated with cell cycle progression and DNA synthesis. However, the level of expression did not increase for some of these genes when $Rb^{N750F/N750F}$ MEFs were infected with E1A, indicating that upregulation of these genes was dependent on the ability of E1A to bind pRb.

We also discovered that in $Rb^{N750F/N750F}$ MEFs expression of a large set of homeobox genes, as well as several other transcription factors involved in pattern formation during embryogenesis, is deregulated. Previous studies with *Rb*-null MEFs did not detect deregulated expression of these genes. This might be due to the fact that in the complete absence of pRb, either p107 or p130, which also have the ability to bind LxCxE-containing proteins, have substituted for this function of pRb. However, N750F mutation did not trigger this compensatory mechanism because the Rb protein, although a mutant one, was still present in $Rb^{N750F/N750F}$ MEFs.

These findings are somewhat surprising, considering that no homeotic transformations were observed in $Rb^{N750F/N750F}$ mice (see Chapter IV). It is possible that the LxCxE-binding domain of pRb is crucial for regulating expression of homeobox genes in MEFs but not in cell types that normally express them in the developing embryo. This hypothesis is supported by the fact that genes associated with immune response and response to pathogen or injury are down-regulated in *Rb*-null MEFs(12). However, mice with tissue-specific knockout of pRb in hematopoietic stem cells do not exhibit any immunological defects(22).

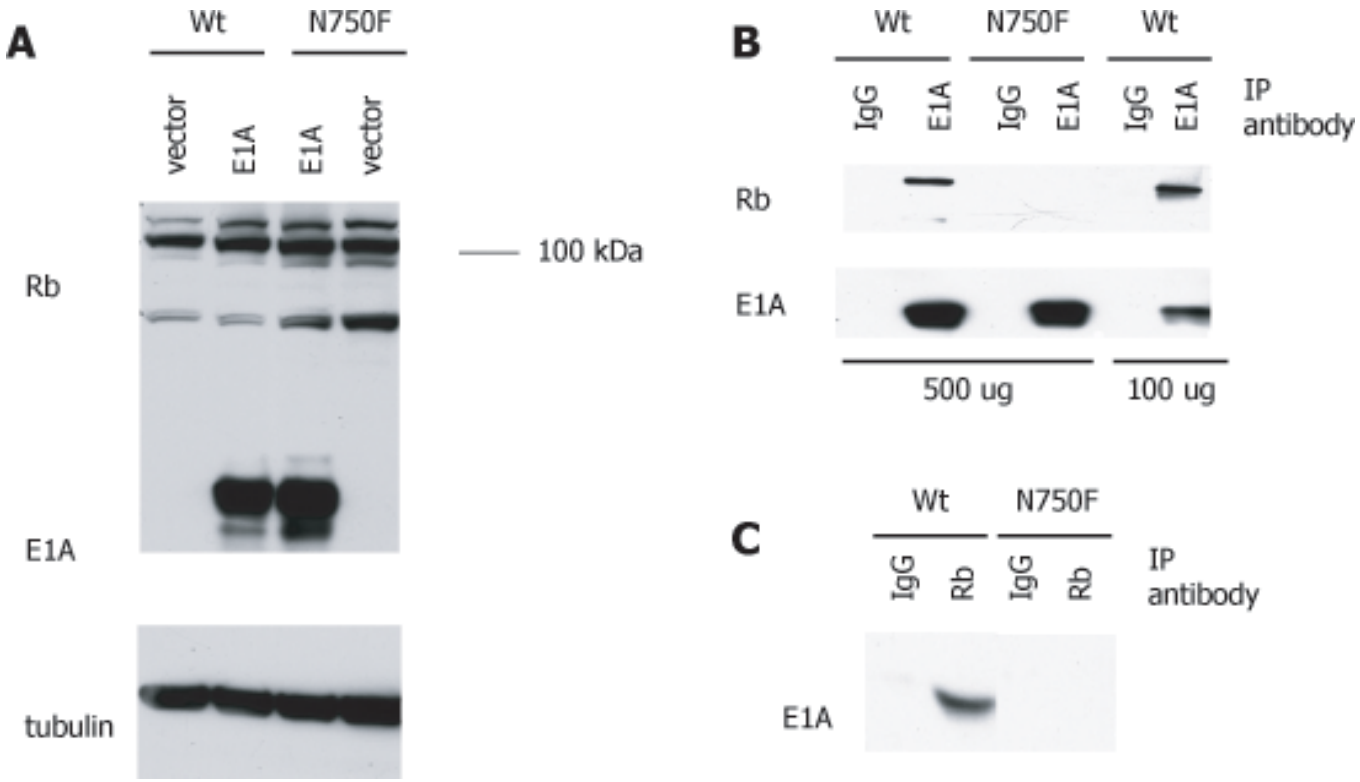

Figure 3.1 pRb-N750F does not bind to Adenovirus E1A

A. Wild type and $Rb^{N750F/N750F}$ 3T3 cells were infected with either pMSCVpuro or pMSCVpuro-E1A. Expression of pRb and E1A was confirmed by Western blotting. **B.** Co-immunoprecipitation using polyclonal anti-E1A antibody brings down wild type pRb but not pRb-N750F mutant. The efficiency of immunoprecipitation is assessed by probing bound proteins with monoclonal anti-E1A antibody. **C.** Co-immunoprecipitation using polyclonal anti-Rb antibody brings down E1A from wild type but not $Rb^{N750F/N750F}$ mutant cells.

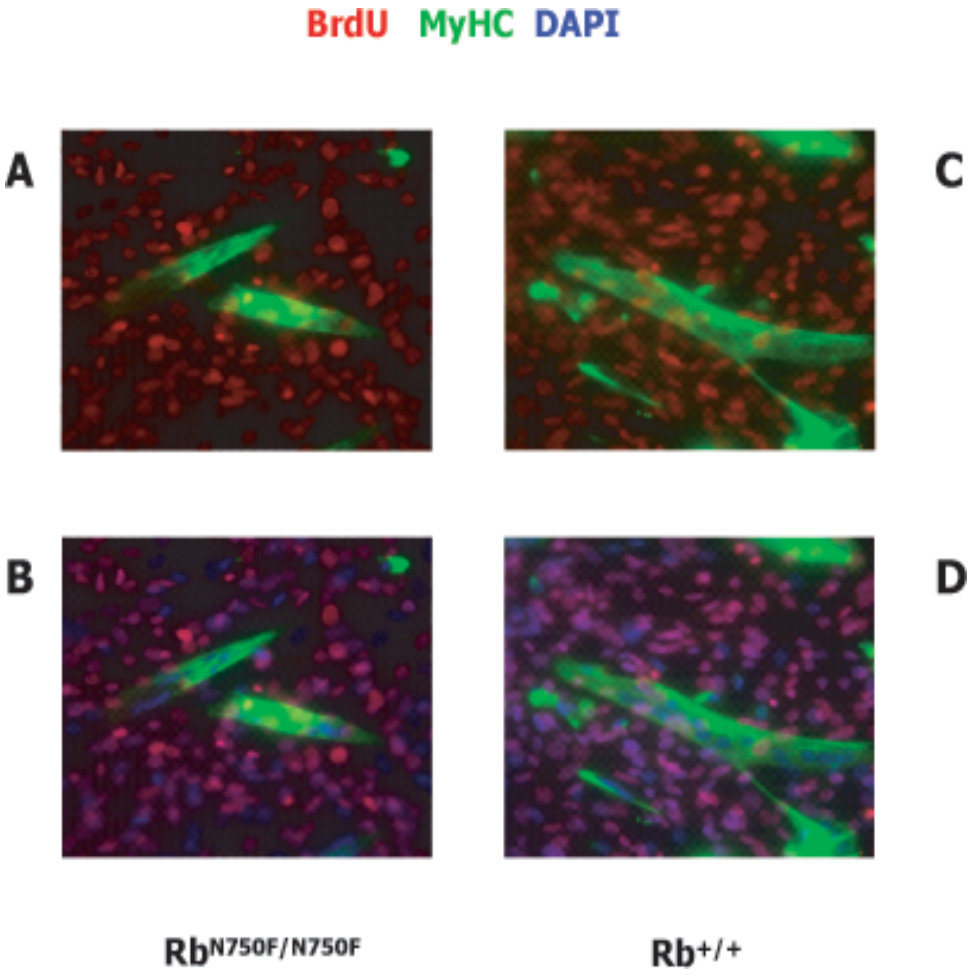

Figure 3.2 Terminally differentiated *Rb*$^{N750F/N750F}$ myotubes are resistant to re-stimulation with serum

MEFs were converted to myotubes by culturing in low serum and expression of MyoD. After 3 days of differentiation, cells were placed into high serum media containing BrdU for 24 hours. Cells were stained for BrdU incorporation and expression of muscle differentiation marker myosin heavy chain (MyHC).
A and **B**. *Rb*$^{N750F/N750F}$ **C** and **D**. *Rb*$^{+/+}$ Magnification is 40X.

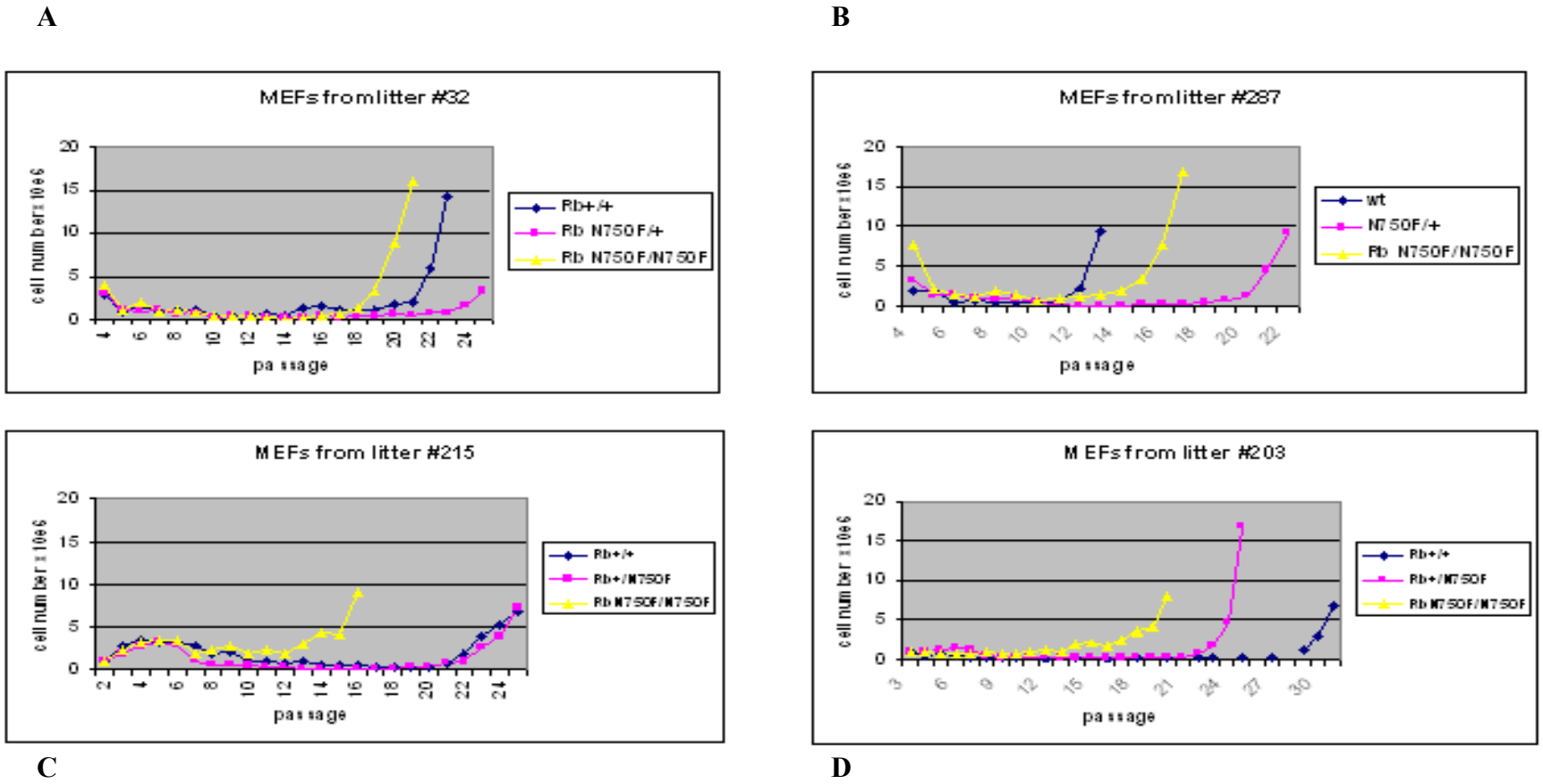

Figure 3.3 Accelerated immortalization of *Rb*$^{N750F/N750F}$ MEFs

Early passage MEFs were subjected to the 3T3 passaging protocol until the number of cells was doubling every three days. Four sets of MEFs from separate litters were used (**A-D**).

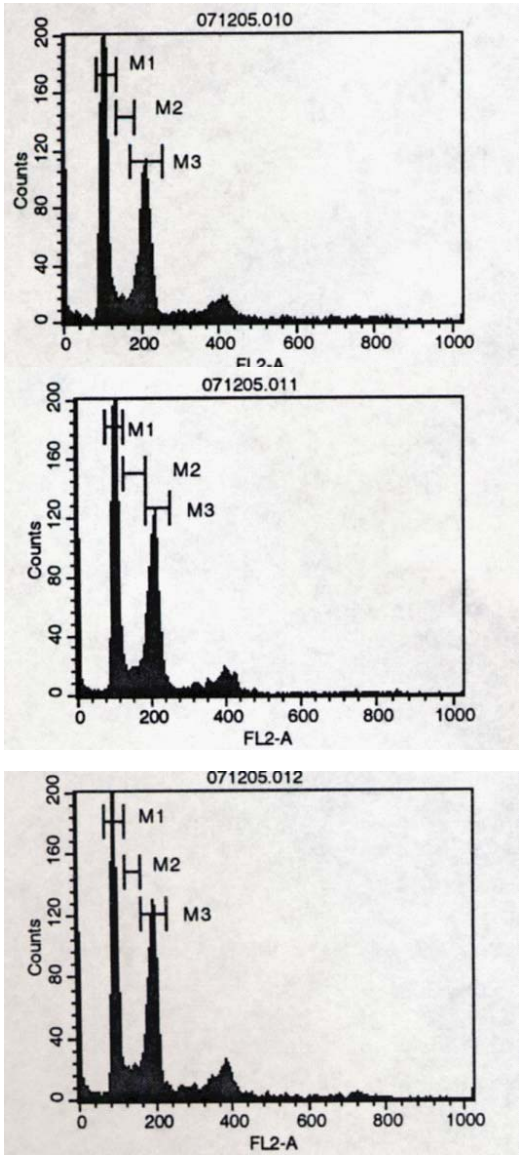

	$Rb^{+/+}$	$Rb^{N750F/+}$	$Rb^{N750F/N750F}$
% in G1	38	40	35
% in S	6	9	7
% in G2/M	33	32	34

D

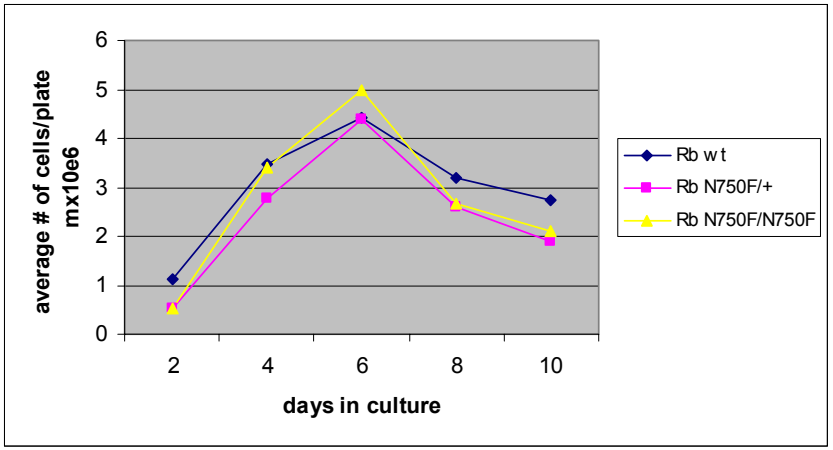

Figure 3.4 ***$Rb^{N750F/N750F}$*** **MEFs exhibit normal cell cycle progression and respond to contact inhibition**

Asynchronously growing wild type (**A**), $Rb^{N750F/+}$ (**B**) and $Rb^{N750F/N750F}$ (**C**) MEFs display similar cell cycle kinetics and respond to contact inhibition (**D**).

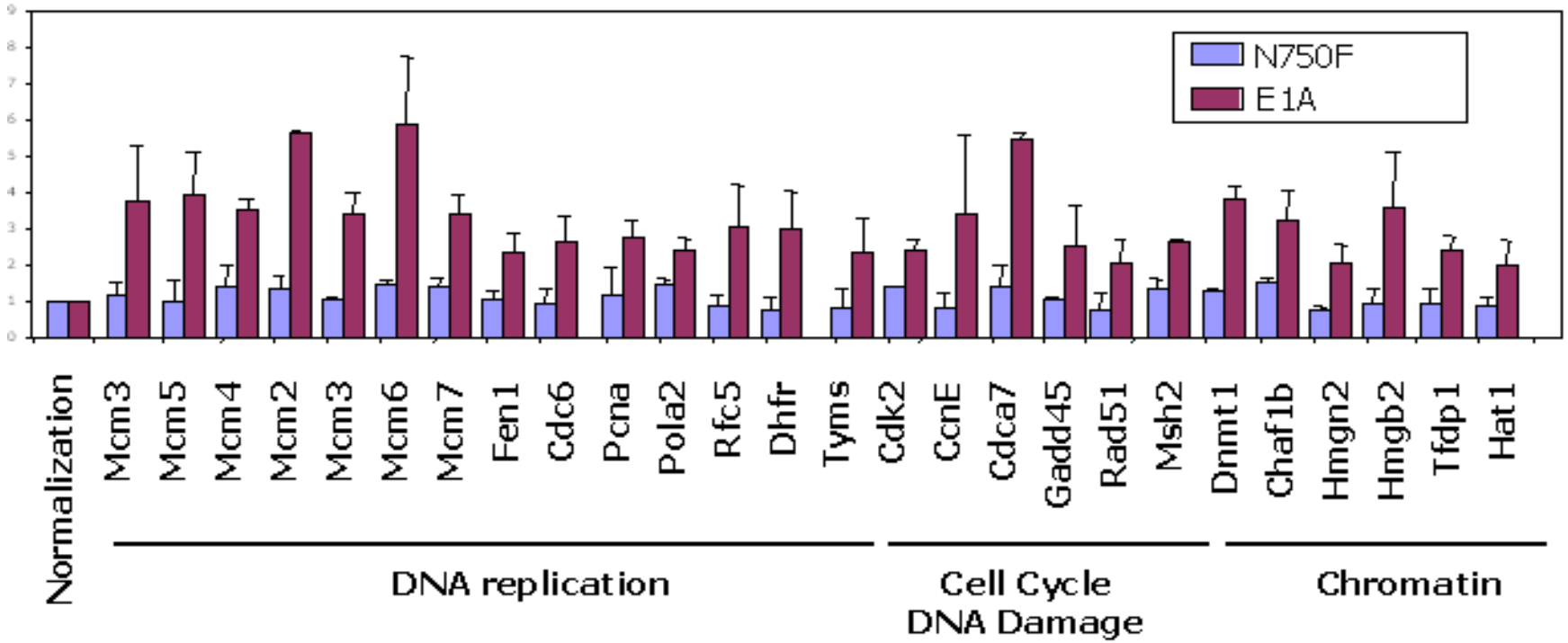

Figure 3.5 ***Rb*$^{N750F/N750F}$ MEFs do not exhibit upregulation of cell cycle genes whose expression is increased by infection with Adenovirus E1A protein**

Gene expression analysis was performed with RNA isolated from asynchronously growing wild type MEFs infected with Adenovirus E1A protein and *Rb*$^{N750F/N750F}$ MEFs.

REFERENCES

1. **Ait-Si-Ali, S., V. Guasconi, L. Fritsch, H. Yahi, R. Sekhri, I. Naguibneva, P. Robin, F. Cabon, A. Polesskaya, and A. Harel-Bellan.** 2004. A Suv39h-dependent mechanism for silencing S-phase genes in differentiating but not in cycling cells.

2. **Black, E. P., E. Huang, H. Dressman, R. Rempel, N. Laakso, S. L. Asa, S. Ishida, M. West, and J. R. Nevins.** 2003. Distinct gene expression phenotypes of cells lacking Rb and Rb family members. Cancer Res **63:**3716-23.

3. **Chen, T. T., and J. Y. Wang.** 2000. Establishment of irreversible growth arrest in myogenic differentiation requires the RB LXCXE-binding function. Mol Cell Biol **20:**5571-80.

4. **DeCaprio, J. A., J. W. Ludlow, J. Figge, J. Y. Shew, C. M. Huang, W. H. Lee, E. Marsilio, E. Paucha, and D. M. Livingston.** 1988. SV40 large tumor antigen forms a specific complex with the product of the retinoblastoma susceptibility gene. Cell **54:**275-83.

5. **Dunaief, J. L., B. E. Strober, S. Guha, P. A. Khavari, K. Alin, J. Luban, M. Begemann, G. R. Crabtree, and S. P. Goff.** 1994. The retinoblastoma protein and BRG1 form a complex and cooperate to induce cell cycle arrest. Cell **79:**119-30.

6. **Dyson, N., P. M. Howley, K. Munger, and E. Harlow.** 1989. The human papilloma virus-16 E7 oncoprotein is able to bind to the retinoblastoma gene product. Science **243:**934-7.

7. **Egan, C., S. T. Bayley, and P. E. Branton.** 1989. Binding of the Rb1 protein to E1A products is required for adenovirus transformation. Oncogene **4:**383-8.

8. **Herrera, R. E., V. P. Sah, B. O. Williams, T. P. Makela, R. A. Weinberg, and T. Jacks.** 1996. Altered cell cycle kinetics, gene expression, and G1 restriction point regulation in Rb-deficient fibroblasts. Mol Cell Biol **16:**2402-7.

9. **Lai, A., J. M. Lee, W. M. Yang, J. A. DeCaprio, W. G. Kaelin, Jr., E. Seto, and P. E. Branton.** 1999. RBP1 recruits both histone deacetylase-dependent and

-independent repression activities to retinoblastoma family proteins. Mol Cell Biol **19:**6632-41.

10. **Lavender, P., L. Vandel, A. J. Bannister, and T. Kouzarides.** 1997. The HMG-box transcription factor HBP1 is targeted by the pocket proteins and E1A. Oncogene **14:**2721-8.

11. **Lee, J. O., A. A. Russo, and N. P. Pavletich.** 1998. Structure of the retinoblastoma tumour-suppressor pocket domain bound to a peptide from HPV E7. Nature **391:**859-65.

12. **Markey, M. P., J. Bergseid, E. E. Bosco, K. Stengel, H. Xu, C. N. Mayhew, Y. Jiang, S. J. Schwemberger, G. F. Babcock, A. G. Jegga, M. F. Reed, B. J. Aronow, and J. Y. Wang.** Loss of the Retinoblastoma tumor suppressor: differential action on transcriptional program related to cell cycle control and immune function. manuscript in preparation.

13. **Meloni, A. R., E. J. Smith, and J. R. Nevins.** 1999. A mechanism for Rb/p130-mediated transcription repression involving recruitment of the CtBP corepressor. Proc Natl Acad Sci U S A **96:**9574-9.

14. **Morgenstern, J. P., and H. Land.** 1990. Advanced mammalian gene transfer: high titre retroviral vectors with multiple drug selection markers and a complementary helper-free packaging cell line. Nucleic Acids Res **18:**3587-96.

15. **Murphy, D. J., S. Hardy, and D. A. Engel.** 1999. Human SWI-SNF component BRG1 represses transcription of the c-fos gene. Mol Cell Biol **19:**2724-33.

16. **Narita, M., S. Nunez, E. Heard, M. Narita, A. W. Lin, S. A. Hearn, D. L. Spector, G. J. Hannon, and S. W. Lowe.** 2003. Rb-mediated heterochromatin formation and silencing of E2F target genes during cellular senescence. Cell **113:**703-16.

17. **Nielsen, S. J., R. Schneider, U. M. Bauer, A. J. Bannister, A. Morrison, D. O'Carroll, R. Firestein, M. Cleary, T. Jenuwein, R. E. Herrera, and T. Kouzarides.** 2001. Rb targets histone H3 methylation and HP1 to promoters. Nature **412:**561-5.

18. **Novitch, B. G., G. J. Mulligan, T. Jacks, and A. B. Lassar.** 1996. Skeletal muscle cells lacking the retinoblastoma protein display defects in muscle gene expression and accumulate in S and G2 phases of the cell cycle. J Cell Biol **135:**441-56.

19. **Pear, W. S., G. P. Nolan, M. L. Scott, and D. Baltimore.** 1993. Production of high-titer helper-free retroviruses by transient transfection. Proc Natl Acad Sci U S A **90:**8392-6.

20. **Sage, J., G. J. Mulligan, L. D. Attardi, A. Miller, S. Chen, B. Williams, E. Theodorou, and T. Jacks.** 2000. Targeted disruption of the three Rb-related genes leads to loss of G(1) control and immortalization. Genes Dev **14:**3037-50.

21. **Tevosian, S. G., H. H. Shih, K. G. Mendelson, K. A. Sheppard, K. E. Paulson, and A. S. Yee.** 1997. HBP1: a HMG box transcriptional repressor that is targeted by the retinoblastoma family. Genes Dev **11:**383-96.

22. **Walkley, C. R., and S. H. Orkin.** 2006. Rb is dispensable for self-renewal and multilineage differentiation of adult hematopoietic stem cells. Proc Natl Acad Sci U S A **103:**9057-62.

23. **Welch, P. J., and J. Y. Wang.** 1993. A C-terminal protein-binding domain in the retinoblastoma protein regulates nuclear c-Abl tyrosine kinase in the cell cycle. Cell **75:**779-90.

CHAPTER IV

PHENOTYPE OF $Rb^{+/N750F}$, $Rb^{N750F/N750F}$ and $Rb^{-/N750F}$ MICE

INTRODUCTION

Gene targeting in mice has revealed important roles for pRb in differentiation, survival and tumorigenesis of various tissues. Unlike humans, mice heterozygous for the wild type *Rb* allele do not develop retinoblastomas. Instead, they succumb to pituitary and thyroid tumors(7, 17, 19). Homozygous germ line deletion of *Rb* results in embryonic lethality at embryonic day 12.5 (Ed 12.5)(7, 17, 19). *Rb*-null embryos display extensive ectopic S phase entry and elevated levels of apoptosis in the central and peripheral nervous system (CNS and PNS) and in the ocular lens. In fetal liver, the loss of *Rb* leads to decreased cellularization and disruption of erythropoiesis as evidenced by persistence of nucleated erythrocytes.

In addition to defects in the embryo proper, deletion of *Rb* causes excessive proliferation and incomplete differentiation of trophoblasts, which form the embryonic portion of the placenta(38). These defects result in an increased number of trophoblasts and decreased blood spaces in the labyrinth layer of the placenta, which lead to a restriction in the exchange of nutrients and oxygen between the mother and the developing embryo.

Rb-null embryos die during development, preventing characterization of pRb function in tissues that form after Ed 12.5 or evaluation of the role of pRb in the maintenance of adult tissues. Moreover, deletion of *Rb* in the whole organism does not allow one to differentiate between the tissues that have an intrinsic requirement for pRb and the ones that show defects

due to the pathological conditions created by the loss of pRb in other tissues. To overcome these limitations, several tissue-specific knockouts of *Rb* have been created and characterized.

The functional requirement for pRb in the CNS was assessed by a tissue-specific knockout of *Rb* in the telencephalon (a region of the neural tube that gives rise to cerebral hemispheres). Mice with telencephalon-specific deletion of *Rb* survived until birth, but died shortly thereafter(12). Examination of the brain tissue obtained from these mice revealed that neurons were still undergoing ectopic proliferation at a level comparable to that seen in the *Rb*-null embryos. Surprisingly, no aberrant apoptosis of the neurons was observed in the *Rb*-null telencephalon. These findings indicated that ectopic proliferation of the neurons in the CNS initially observed in *Rb*-null embryos was caused by the absence of pRb in the neurons. However, apoptosis of the neurons was a physiological consequence of *Rb* disruption in other embryonic tissues.

Ectopic proliferation of the neurons and the absence of apoptosis were also observed in the CNS of mice with tissue-specific knockout of *Rb* limited to the CNS, PNS and ocular lens(23). In the latter two tissues, these knockout mice recapitulated the same defects observed in the PNS and ocular lens of *Rb*-null embryos, indicating that apoptosis and ectopic proliferation were caused by the loss of pRb from these tissues.

A defect in erythrocyte enucleation in *Rb*-null embryos prompted further investigation of the pRb function in erythropoiesis. Analysis of erythroid progenitors isolated from fetal livers (the site of hematopoiesis in the embryo) revealed that the loss of pRb from these cells resulted in mitotic arrest, failure to upregulate the differentiation marker

TER119 and inability to enucleate(33). The requirement of pRb for erythrocyte enucleation was shown to be cell-autonomous, because in tissue culture *Rb*-null erythrocytes did not enucleate even in the presence of wild type erythrocytes(6). Furthermore, pRb was shown to be crucial for stress-induced erythropoiesis(33). When bone marrow of lethally irradiated mice was transplanted with fetal liver cells obtained from *Rb*-null embryos, the mice did not survive beyond 5 months postirradiation, while mice that received wild type transplants lived past 12 months postirradiation. These results demonstrated the essential function of pRb in differentiation of hematopoietic stem cells (HSC) from the fetal liver. In contrast, pRb was shown to be dispensable for self-renewal and differentiation of adult HSC(35). No defects were detected in the peripheral blood and bone marrow of mice with HSC-specific knockout of *Rb*, indicating different requirements for pRb in the process of hematopoiesis in two different organs.

The loss of *Rb* in skeletal muscles causes postnatal lethality due to defects in muscle differentiation and reduction in muscle fiber(41). The timing of *Rb* expression was found to be crucial for muscle differentiation. When *Rb* was removed during the early stages of muscle differentiation using Cre recombinase driven by the promoter of myogenic transcription factor Myf5, the resulting mice displayed a severe reduction in muscle mass, and died right after birth due to the inability to breathe(16). However, when *Rb* was removed during the late stages of muscle differentiation using Cre recombinase driven by muscle creatine kinase (MCK) promoter, no defects in muscles were observed; the mice were healthy and viable.

The presence of placental defects in *Rb*-null embryos raised a possibility that some of the phenotypes observed in these embryos were cause by malfunctioning of the placenta. To address this possibility, *Rb*-null embryos with wild type placenta were created. These embryos survived until birth and did not display some of the defects originally observed in the *Rb* knockout(9, 38). Specifically, in the CNS, apoptosis was suppressed, but ectopic cell cycle entry was still detected, in agreement with earlier observations(12, 23). However, apoptosis and ectopic cell cycle entry were not suppressed in the lens, confirming the previously reported cell-autonomous requirement of pRb in this tissue(23). The normal architecture of the fetal liver was also restored by the wild type placenta, but nucleated erythrocytes were still present in increased numbers. The muscle differentiation defects were not rescued by the wild type placenta, and mutant pups died soon after birth.

In addition to CNS, PNS, ocular lens, liver and muscle, several other tissues were shown to require pRb for proper differentiation and function. Conditional knockout of *Rb* in the epidermis caused hyperplasia, aberrant DNA synthesis and improper differentiation(2). In melanocytes, deletion of *Rb* resulted in hair depigmentation in mice, while in tissue culture, *Rb*-null melanocytes died rapidly by apoptosis(40). In the inner ear, *Rb*-null hair cells continued to undergo mitosis, yet were fully differentiated and functional(31). Conditional inactivation of *Rb* in the liver resulted in BrdU incorporation, increased ploidy and upregulation of E2F target genes in terminally differentiated hepatocytes(25).

Even though numerous tissues were shown to be affected by the loss of both wild type *Rb* alleles, $Rb^{+/-}$ mice did not develop tumors in these tissues. This discrepancy can be explained by two different, although not mutually exclusive, mechanisms. In the first

mechanism, the tumors of other tissues do not have enough time to develop, because $Rb^{+/-}$ mice die of pituitary and thyroid tumors before the age of one year. Alternatively, cells in other tissues might not lose the wild type *Rb* allele spontaneously, as occurs in pituitary and thyroid. The data from humans suggest that both mechanisms exist. Survivors of childhood retinoblastomas develop bladder carcinomas, osteosarcomas and fibrosarcomas later in life, indicating that these tissues, just like the retina, are also susceptible to spontaneous loss of the wild type *RB* allele, but over a longer period of time(24).

In summary, deletion of *Rb* disrupts proliferation and differentiation of numerous cell types. Additionally, the loss of pRb in one tissue can create a pathological condition that will affect other tissues, for example, hypoxia that results from defective differentiation of erythrocytes causes apoptosis in the neurons of the CNS(23).

Elucidation of molecular mechanisms that bring about defects associated with the loss of pRb has been severely hampered by the presence of several protein-binding sites within pRb, and a large number of proteins that reportedly interact with pRb. We attempted to reduce this complexity by making a specific mutation in the *Rb* gene and studying the properties of the resulting protein. The N750F mutation in pRb affects only one protein-binding site and eliminates interactions between pRb and a subset of proteins that use LxCxE motif to bind to pRb(5). By creating Rb^{N750F} mutant mice, we planned to accomplish three goals: (1) to determine whether some of the defects previously observed in Rb-null mice can be also observed in Rb^{N750F} mutants, indicating that these defects are caused by the disruption of interactions between LxCxE-containing proteins and pRb; (2) to test whether the muscle differentiation defect observed in tissue culture experiments with pRB-N757F can

be reproduced *in vivo*; and (3) to discover any new tissues that are dependent on pRb for proper function, but have not been discovered previously due to lethality of Rb-null mice.

MATERIALS AND METHODS

Histology

Mice were sacrificed by CO_2 asphyxiation. All tissues were collected immediately and fixed in 10% buffered formalin at room temperature for at least 24 hours. Samples that contained bones were fixed in decalcifying solution (Cal-Ex II, Fisher, CS511-1D) for three days. Preparation of paraffin blocks, tissue sectioning and hematoxylin-eosin staining were carried out by the UCSD Histology Core facility.

Isolation of Mouse Tail DNA

Tail tips (0.5 cm) were digested in 500 µl of lysis buffer (10 mM Tris-HCl, pH 7.5; 400 mM NaCl, 2 mM EDTA, 0.5% SDS, 100 µg/ml Proteinase K) at 55ºC overnight. After the tissue was completely digested, 161 µl of saturated NaCl solution was added and tubes were incubated on ice for 30 minutes. Proteins and SDS were precipitated by centrifugation at 4ºC for 10 minutes. Supernatant was transferred into a new tube. DNA was precipitated by the addition of 1 ml of cold 100% ethanol and centrifugation at 4ºC for 20 minutes. Supernatant was discarded and DNA pellet was washed twice with 70% ethanol. After the second wash, tubes were air-dried at room temperature for 20 minutes to allow the remaining ethanol to evaporate. The DNA pellet was resuspended in 200 µl of TE (10 mM Tris-HCl, pH 8; 1 mM EDTA).

Genotyping PCR

The Rb^{N750F} allele was detected using Rb7321,F (5'-AGTATGCCTCCACCAGGGTATGTT-3') and Rb7825,R (5'-CACACATTCACTAA ATGCAC-3') primers. PCR conditions were as follows: 94°C for 2 minutes; 94°C for 30 seconds, 65°C for 45 seconds, 72°C for 45 seconds times 35 cycles; 72°C for 10 minutes.

Blood collection and analysis

Blood was drawn from the tail vein of anesthetized mice and analyzed within four hours of collection. Approximately 100 µl of blood was placed into EDTA-containing polypropylene microtubes (Becton Dickinson, #365973) and mixed immediately to ensure proper anticoagulation. Samples were analyzed in duplicates for complete blood cell counts with leukocyte differential and platelet counts on a Hemavet 850FS MultiSpecies Hematology System (Drew Scientific), according to the manufacturer's operating instructions.

Bone marrow collection

Mice were sacrificed by CO_2 asphyxiation. Both femurs were dissected out and flushed with 5 ml of IMDM media (Invitrogen 12440-053). Cells were pelleted by centrifugation and resuspended in 500 µl of PBS with 0.5% FBS (Hyclone SH30088.03). Cold lysis buffer (Stem Cell Technologies 07850) was added to a final volume of 5 ml and cells were incubated on ice for 15 minutes. This treatment resulted in preferential lysis of erythrocytes. The remaining intact cells were pelleted again by centrifugation and washed three times in PBS with 0.5% FBS before being used for various assays.

Colony-forming cell assays

Freshly isolated bone marrow cells ($60x10^3$) were plated in IMDM with methylcellulose (gelling agent), Stem Cell Factor (SCF), IL-3, IL-6 and Erythropoietin (MethoCult™ kit, Stem Cell Technologies, 03434) according to the protocol supplied by the manufacturer. Cells were incubated at 37ºC with 0.5% CO_2 for 12 days. Colonies were identified and counted under an inverted Nikon Eclipse microscope at 40X.

Megakaryocytic progenitor colony assay

Freshly isolated bone marrow cells ($2x10^5$) were plated in IMDM with collagen, IL-3 (5ng/ml) and Thrombopoietin (5ng/ml) (MegaCult™-C kit, Stem Cell Technologies, 04972) according to the protocol supplied by the manufacturer. Cells were grown in chamber slides (provided with the MegaCult™-C kit) at 37ºC with 0.5% CO_2 for 8 days. Slides were dehydrated and stained for acetylcholinesterase activity to detect megakaryocyte progenitors using the reagents and protocol supplied with MegaCult™-C kit.

FACS

For megakaryocyte analysis, bone marrow cells were labeled with anti-CD41-phycoerythrin antibody conjugate (BD Biosciences) in the dark for 45 minutes. After the incubation, cells were washed with PBS, resuspended in 500 µl of PBS with 2% paraformaldehyde and analyzed on a FACSCalibur (BD Biosciences). For each sample, 50,000 events were counted.

For lymphocyte analysis, blood was collected from periorbital space of anesthetized mice into tubes containing heparin solution (100 U/ml). 25 µl of whole blood with heparin

were diluted with 25 µl of FACS buffer (FB) (RPMI 1640 without phenol red, 3% fetal calf serum (FCS) and 0.05% sodium azide). Then, 50 µl of FB containing antibodies was added to each sample. Lymphocytes in the blood sample were stained with anti-B220 (BD Pharmingen 555274) and anti-CD3 (BD Pharmingen 555274) antibodies at the final concentration of 10 µg/ml and 0.33 µg/ml, respectively. After a 20 minute incubation on ice, cells were washed twice with 100 µl of FB, spun down and re-suspended in 100 ul of Solution A fixative (Caltag GAS-004). Red blood cells were lysed by incubation with shaking at room temperature for 20 minutes. The remaining cells were washed three times with 100 µl of FB and re-suspended in 200 µl of FB for analysis on FACSCalibur (BD Biosciences). Data were analyzed using FlowJo software (Tree Star, San Carlos, CA). Viable lymphocytes were defined by light scatter characteristics.

RESULTS

Rb$^{N750F/N750F}$ mice are viable

Rb knockout mice die during prenatal development with numerous neurological and hematological defects(7, 17, 19). To determine the viability of *Rb*$^{N750F/N750F}$ mutants, heterozygous *Rb*$^{+/N750F}$ mice were intercrossed and their progeny were genotyped at the age of three weeks. We found that *Rb*$^{N750F/N750F}$ mutant mice represented 21% of the total progeny (Table 4.1). Therefore, the loss of interactions between pRb and LxCxE- containing proteins does not cause the developmental defects that lead to death of *Rb*-null embryos.

Table 4.1 Mendelian distribution of *Rb*^{N750F} allele

Genotype	*Rb*$^{+/+}$	*Rb* $^{+/N750F}$	*Rb* $^{N750F/N750F}$
# of males	59	115	44
# of females	72	117	55
Total # of mice	131	232	99
Percentage	28	50	21

Rb$^{N750F/N750F}$ mice do not develop pituitary tumors

Rb$^{+/-}$ mice have been shown to develop pituitary tumors as early as 6 months, with no mice surviving longer than one year of age(17). To determine tumor susceptibility, *Rb*$^{+/N750F}$ mice were followed for up to 20 months, but none of the 30 animals developed pituitary tumors (Table 4.2). Similarly, all 24 *Rb* $^{N750F/N750F}$ mice, as well as 19 control animals sacrificed at the age of 11-15 months were free of pituitary or any other tumors. These results demonstrate that the LxCxE-binding pocket of pRb does not contribute to pituitary tumorigenesis.

Table 4.2 Tumor-free survival of *Rb*$^{+/N750F}$ and *Rb* $^{N750F/N750F}$ mice

Genotype	Age, months	n	% tumor-free
Rb$^{+/+}$	11-15	19	100
Rb $^{+/N750F}$	20	30	100
Rb $^{N750F/N750F}$	11-15	24	100
Rb$^{+/-}$ (37)	11	25	0

The muscle tissue in *Rb*$^{N750F/N750F}$ mice develops normally

Loss of *Rb* in skeletal muscles causes postnatal lethality due to defects in differentiation and a dramatic reduction in muscle mass(16, 41). Histological examination of the residual *Rb*-null muscle fibers found them to be short and irregular in shape. Tissue culture experiments with pRB-N757F demonstrated that this mutant was capable of

supporting myogenic differentiation; however, it was defective in establishing irreversible growth arrest in terminally differentiated myotubes(5). Prompted by these findings, we conducted a thorough examination of muscle tissue from $Rb^{N750F/N750F}$ mutant mice. However, we were unable to detect any abnormalities in the overall architecture of muscle fibers in skeletal (Figure 4.1 A and B) as well as cardiac (Figure 4.1 C and D) muscle. Therefore, we concluded that the LxCxE-binding pocket of pRb does not play a role in muscle differentiation *in vivo*.

Erythrocytes of $Rb^{N750F/N750F}$ mice differentiate and function normally

The cell-autonomous function of pRb in erythrocyte differentiation has been well documented. Rb-null embryos have reduced red blood cell count and display severe defects in erythrocyte maturation, characterized by increased numbers of nucleated red blood cells in the liver and in peripheral circulation(7, 17, 19). During stress-induced erythropoiesis, pRb regulates erythroblast expansion and promotes enucleation (33). Moreover, under these conditions, the absence of pRb leads to a dramatic reduction in hematocrit and hemoglobin.

We performed complete blood cell counts on samples obtained from $Rb^{N750F/N750F}$ mutant and wild type littermate control mice in order to determine whether the loss of the LxCxE-binding pocket of pRb would reproduce any of the erythtroid defects observed in Rb-/- embryos (Table 4.3 and Table 4.4). We found a slight decrease (5.9%) in red blood cell counts in $Rb^{N750F/N750F}$ mutant mice of 129 Sv/Ev/Tac background, but the hematocrit was unchanged (Table 4.4). No abnormalities were found after examining blood smears from the mutant mice. Therefore, the LxCxE-binding pocket of pRb does not contribute to the development of erythroid defects observed in Rb-null mice.

Table 4.3 Complete blood cell count (129/B6 mixed background)
Abbreviations: WBC, white blood cells; RBC, red blood cells; HGB, hemoglobin; HCT, hematocrit; MCV, mean corpuscular (cell) volume; MCH, mean corpuscular (cell) hemoglobin; MCHC, mean corpuscular (cell) hemoglobin concentration; RDW red (cell) distribution width; PLT, platelets; MPV, mean platelet volume.

N750F knock in SUMMARY	**Wild Type**		**N750F/N750F**		**N750F v. Wild Type**		
129/B6 44-50 weeks	Mean	S.D.	Mean	S.D.	**% change in N750F**		**t test p value (if <0.1)**
Hematology	n = 12		n = 15				
WBC (K/µL)	6.6	3.11	9.38	3.56	**42.1**	**% increase**	**0.043**
Neutrophils (%)	35.1	8.78	33.39	13.07			
Neutrophils (K/µL)	2.28	1.23	3.23	2.15			
Lymphocytes (%)	58.97	9.16	61.4	15.47			
Lymphocytes (K/µL)	3.97	2.15	5.64	2.64	**42.1**	**% increase**	**0.089**
Monocytes (%)	5.37	1.31	4.31	0.92	**19.8**	**% decrease**	**0.021**
Monocytes (K/µL)	0.32	0.1	0.4	0.16			
Eosinophils (%)	0.41	0.28	0.83	2.14			
Eosinophils (K/µL)	0.02	0.02	0.1	0.3			
Basophils (%)	0.15	0.14	0.08	0.06			
Basophils (K/µL)	0.01	0.01	0.01	0.01			
RBC (M/µL)	10.07	1.75	9.32	1.5			
HGB (g/dL)	14.1	1.9	13.9	1.6			
HCT (%)	51.4	7.2	51	5.5			
MCV (fL)	51.9	6.7	55.6	6.5			
MCH (pg)	14.2	1.3	15.1	1.3	**6.1**	**% increase**	**0.086**
MCHC (g/dL)	27.5	1.7	27.2	1.9			
RDW (%)	20.9	3	21.6	1.4			
PLT (K/µL)	683	140	921	163	**34.9**	**% increase**	**<0.001**
MPV (fL)	5.5	0.38	5.49	0.38			

Table 4.4 Complete blood cell count (129 Sv/Ev/Tac pure background)

Abbreviations: WBC, white blood cells; RBC, red blood cells; HGB, hemoglobin; HCT, hematocrit; MCV, mean corpuscular (cell) volume; MCH, mean corpuscular (cell) hemoglobin; MCHC, mean corpuscular (cell) hemoglobin concentration; RDW red (cell) distribution width; MPV, mean platelet volume.

N750F knock in SUMMARY	**Wild Type**		**N750F/N750F**		**N750F v. Wild Type**		
129 pure 16-24 weeks	Mean	S.D.	Mean	S.D.	**% change in N750F**		**t test p value (if <0.1)**
Hematology	n = 17		n = 17				
WBC (K/µL)	6.73	1.66	10.3	3.77	**53.1**	**% increase**	**0.001**
Neutrophils (%)	32.98	9.98	26.64	7.77	**19.2**	**% decrease**	**0.047**
Neutrophils (K/µL)	2.24	0.94	2.72	1.34			
Lymphocytes (%)	61.41	9.99	68.41	7.72	**11.4**	**% increase**	**0.029**
Lymphocytes (K/µL)	4.11	1.23	7.09	2.85	**72.3**	**% increase**	**<0.001**
Monocytes (%)	5.12	1	4.61	1.01			
Monocytes (K/µL)	0.34	0.08	0.45	0.1	**32.9**	**% increase**	**0.001**
Eosinophils (%)	0.26	0.33	0.23	0.42			
Eosinophils (K/µL)	0.02	0.02	0.03	0.07			
Basophils (%)	0.11	0.11	0.09	0.15			
Basophils (K/µL)	0.01	0.01	0.01	0.03			
RBC (M/µL)	9.64	0.63	9.07	0.62	**5.9**	**% decrease**	**0.012**
HGB (g/dL)	14.7	0.7	14.3	0.8			
HCT (%)	57.7	3	57	3.5			
MCV (fL)	59.9	2.2	63	3.3	**5.1**	**% increase**	**0.003**
MCH (pg)	15.2	0.6	15.8	0.8	**3.5**	**% increase**	**0.034**
MCHC (g/dL)	25.5	0.5	25.1	0			
RDW (%)	19.5	0.6	20.6	1	**5.3**	**% increase**	**0.001**
PLT (K/µL)	537	69	663	71	**23.4**	**% increase**	**<0.001**
MPV (fL)	5.4	0.18	5.37	0.18			

Accelerated platelet formation leads to megakaryocyte depletion from the bone marrow of *Rb*$^{N750F/N750F}$ mice

While performing complete blood cell counts, we noticed an increase in the number of platelets in the peripheral blood of $Rb^{N750F/N750F}$ mice in both 126/BL6 mixed and 129 Sv/Ev/Tac pure backgrounds (Tables 4.3 and 4.4). We analyzed the differences further and found that they were statistically significant (Figure 4.2 A and B). Moreover, the difference was much more pronounced in females than in males (Figure 4.2: compare females in C and D with males in E and F). These results indicate that the LxCxE-binding domain of pRb regulates platelet number in a sex-dependent manner, which is a novel function of this domain.

In order to determine the source of increased platelets, we assessed the number of various types of progenitor cells that ultimately give rise to platelets. Hematopoietic stem cells undergo several successive rounds of differentiation in the bone marrow, ultimately giving rise to megakaryocytes whose cytoplasm then fragments to produce platelets (Figure 4.3). We hypothesized that the increase in platelet number may result from overproduction of one or more types of the progenitor cells (yellow boxes in Figure 4.3). We isolated cells from the bone marrow of $Rb^{N750F/N750F}$ mutant mice (n=5) and wild type control littermates (n=5) and cultured them in semi-solid medium supplemented with growth factors that promote proliferation of three types of hematopoietic progenitors: BFU-E (blood forming units - erythroid), CFU-GM (colony-forming units – granulocyte, macrophages) and CFU-GEMM (colony-forming units – granulocyte, erythrocyte, monocyte, megakaryocyte). CFU-GM and CFU-GEMM were counted together due to the difficulty of distinguishing between these two types of CFUs. No significant differences were found between the numbers of CFU-GM and CFU-GEMM obtained from wild type and mutant bone marrow

(Figure 4.4 A). Based on these findings, we concluded that the increase in the number of platelets cannot be attributed to the increase in the number of common myeloid progenitors in $Rb^{N750F/N750F}$ mice.

We next compared the number of megakaryocyte precursors present in the bone marrow of wild type (n=5) and $Rb^{N750F/N750F}$ mice (n=5). Cells isolated from the bone marrow were plated in semi-solid medium supplemented with growth factors that promote outgrowth of CFU-Mk (colony forming unit – megakaryocyte). No significant differences were detected between the number of CFU-Mk present in the mutant and wild type bone marrow, indicating that the number of megakaryocyte precursors was unaffected by the Rb^{N750F} allele (Figure 4.4 B).

We also assessed the number of mature megakaryocytes present in the bone marrow. We performed FACS analysis for CD41 positive cells and discovered that there was a significant difference (p=0.012) between the number of megakaryocytes found in the bone marrow from wild type (n=11) and $Rb^{N750F/N750F}$ (n=9) mice (Figure 4.4 C). Unexpectedly, the number of mature megakaryocytes was lower in the bone marrow of $Rb^{N750F/N750F}$ mice than in the wild type mice. Based on these findings, we propose that the process of platelet formation is accelerated in $Rb^{N750F/N750F}$ mice, leading to depletion of megakaryocytes from the bone marrow and increase in the number of platelets in the peripheral blood.

Increased lymphopoiesis leads to elevated lymphocyte count in the peripheral blood of $Rb^{N750F/N750F}$ mice

Analysis of blood samples from $Rb^{N750F/N750F}$ mice also revealed an increase in the number of lymphocytes in the peripheral blood (Tables 4.3 and 4.4). This increase was more

pronounced and statistically significant (p=0.0004) in mice of 129 Sv/Ev/Tac pure background (Figure 4.5 A and B). Moreover, as with platelet count, the females were preferentially affected (p=0.0016) (Figure 4.5 C and D).

To further characterize the increase in lymphocyte number, we compared the relative distribution of B lymphocytes and T lymphocytes in the peripheral blood of the mutant mice and wild type controls. We performed FACS using anti-CD3 and anti-B220 antibodies, and discovered that the ratio of T lymphocytes to B lymphocytes was unaffected (Figure 4.6). This finding indicates that the disruption of LxCxE-binding domain of pRb results in increased production of lymphocytes either at the level of common lymphoid progenitors or pro-B and pro-T cells (see Figure 4.3).

Infiltration of megakaryocyte in the spleen of $Rb^{N750F/N750F}$ mice is increased

The existence of defects in lymphocyte proliferation prompted us to examine lymphoid organs in $Rb^{N750F/N750F}$ mice for any signs of histological abnormalities. We did not find any abnormalities in the thymus, but there was an increase in the number of megakaryocytes in the spleens of 18 out of 22 $Rb^{N750F/N750F}$ mutant mice (Figure 4.7). This phenotype was strain-specific, and was observed only in mice of 126/BL6 mixed background, but not in mice of 129 Sv/Ev/Tac pure background. No spleen defects have been previously reported in $Rb^{+/-}$ mice. A spleen-specific knockout of *Rb* has not been made, so the consequences of pRb loss in this tissue are unknown. Thus, we demonstrated for the first time that the LxCxE-binding domain of pRb regulates infiltration of megakaryocytes into the spleen in a strain-specific manner.

Female $Rb^{N750F/N750F}$ mice are infertile due to anovulation

No pregnancy was ever observed in $Rb^{N750F/N750F}$ mutant females of 129 Sv/Ev/Tac pure background. In an attempt to determine the cause of infertility, we performed histological analysis of ovarian and uterine tissues from three mutant and three wild type mice. We noticed that ovarian development during the embryonic and neonatal periods appeared to be normal in that a typical complement of oocytes, granulosa, interstitial, and connective tissue was apparent (Figure 4.8 A and B). In all mutant ovaries, the secondary interstitial (androgen producing) cells were filled with lipid droplets (likely stored cholesterol esters), and they appeared to have undergone hypertrophy and hyperplasia (Figure 4.8 C). This finding is consistent with chronic LH stimulation. The oocytes in the developing follicles of the ovaries of the mutant mice appeared to be growing and developing normally until the stage of Graafian follicles. Many of the preantral and antral (Graafian) follicles of the mutant mice contained apoptotic granulosa cells indicative of follicular atresia or demise (Figure 4.8 D). Typical healthy preovulatory follicles were not evident in the mutant ovaries. In striking contrast to wild type control ovaries, which contained multiple corpora lutea, only one corpus luteum was found in ovaries from mutant mice, suggesting that $Rb^{N750F/N750F}$ mutant mice were anovulatory (Figure 4.8 A and B). The uterus of one mutant mouse appeared to be responding to estrogen stimulation, indicating that there was sufficient FSH and LH production to cause dominant Graafian follicle development to the point where they produced estrogen. These results demonstrate that LxCxE-binding domain of pRb plays a role in oocyte maturation and ovulation, a previously unknown function of this domain.

Haploinsufficiency of Rb^{N750F} allele

We have shown that $Rb^{N750F/N750F}$ mice display defects in several processes, but the overall phenotype was fairly mild. In our attempt to uncover the role of LxCxE-binding domain of pRb we intercrossed $Rb^{+/N750F}$ and $Rb^{+/-}$ mice to generate $Rb^{N750F/-}$ mice. The latter were born at 13% frequency, which is significantly lower than the expected 25% ($p<0.0001$) (Table 4.5). We also noted that at weaning, $Rb^{N750F/-}$ males represented only 35% of $Rb^{N750F/-}$ progeny, instead of the expected 50%.

Table 4.5 Mendelian distribution of $Rb^{N750F/-}$ progeny

Genotype	$Rb^{+/+}$	$Rb^{N750F/+}$	$Rb^{N750F/-}$	$Rb^{+/-}$
# of males	79	62	24	66
# of females	85	77	44	63
Total # of mice	164	139	68	129
Percentage	33	28	13	26

The $Rb^{N750F/-}$ mice had a very characteristic hunched posture that was clearly visible at 3 weeks (Figure 4.9). Unlike $Rb^{+/N750F}$ or $Rb^{N750F/N750F}$ mice, which remained healthy and viable for 1.5 years, $Rb^{N750F/-}$ mice exhibited profound mortality starting as early as three weeks of age and did not survive beyond 8 months (Figure 4.10 A). At birth, $Rb^{N750F/-}$ mice did not differ in size from their littermates, however, by 16 weeks there was a significant decrease ($p=0.0023$) in mass of the mutant animals (Figure 4.10 B).

Both female and male $Rb^{N750F/-}$ mice were infertile. The embryonic development of the ovaries did not appear to be affected as the basic morphology and histology appeared normal. As in $Rb^{N750F/N750F}$ females, no corpora lutea were found in the ovaries of $Rb^{N750F/-}$ females (Figure 4.11). The ovaries of $Rb^{N750F/-}$ females appeared atrophic and exhibited morphology typical of that seen in a hypophysectomized animal. We observed a number of growing preantral follicles whose growth and developments became arrested at the tertiary

stage. These follicles were undergoing atresia as evidenced by apoptotic granulosa cells and degenerate eggs. Because FSH action is essential for the formation of the dominant follicles, we conclude that in $Rb^{N750F/-}$ females there is a defect somewhere in the FSH pathway leading to the development of the dominant follicle. As with $Rb^{N750F/N750F}$ females, this defect could lie either at the level of FSH production (amount and/or activity of the hormone), or at the level of the ovary (FSH receptor signal transduction in granulosa cells). However, unlike in $Rb^{N750F/N750F}$ females, the follicles of $Rb^{N750F/-}$ females were arrested at the pre-antral stage of development. This finding indicated that with a single copy of Rb^{N750F} allele the follicular development arrested earlier than with two copies of this allele. Moreover, in $Rb^{N750F/-}$ ovaries the interstitial cells appeared as undifferentiated fusiform fibroblast-like cells, demonstrating an additional defect in LH pathway.

In $Rb^{N750F/-}$ males, testis appeared to be smaller than in wild type littermates (Figure 4.12 A and B), however, abundant sperm was still observed inside the seminiferous tubules (Figure 4.12 C and D).

DISCUSSION

Knockout of the *Rb* gene in mice results in embryonic lethality at Ed 12.5(7, 17, 19). Mutant embryos display extensive ectopic cell cycle entry and elevated levels of apoptosis in the CNS, PNS and in the ocular lens. Additionally, these embryos suffer from defects in erythrocyte maturation and trophoblast differentiation(38). To overcome embryonic lethality, several tissue-specific *Rb* knockout mice were created. Careful examination of these animals

revealed that pRb also regulates development and function of myotubes, hepatocytes, keratinocytes, melanocytes, and hair cells of the inner ear (2, 16, 25, 31, 40).

Despite an extensive catalogue of defects found in various tissues and organs in the absence of pRb, little is known about the molecular mechanisms that bring about these defects. The existence of several protein-binding sites within pRb, as well as numerous proteins that have been documented to interact with pRb, makes it even harder to determine which of these proteins might be responsible for the defects observed in the absence of pRb. We attempted to narrow down the list of possible candidates by creating a pRb mutant that is defective in its ability to bind only a subset of proteins. Specifically, the N750F mutation removes the interactions between pRb and proteins that contain the LxCxE motif, which is crucial for their ability to bind pRb(5). Previous studies with the pRB-N757F mutant, a human equivalent of pRb-N750F, demonstrated that it was unable to establish irreversible growth arrest in terminally differentiated murine myotubes, suggesting that LxCxE-containing proteins are involved in regulation of this process(5). These findings were consistent with previous studies by other investigators that demonstrated a cell-autonomous requirement for pRb in muscle differentiation(28).

To further investigate the role of the LxCxE-binding domain in pRb function, we created a knockin mouse with a germ line Rb^{N750F} mutation. We did not observe embryonic lethality, erythtroid defects or muscle malformations in $Rb^{N750F/N750F}$ mice. No pituitary tumors developed in Rb^{N750F} homozygous or heterozygous mice. However, we discovered previously unknown functions of the LxCxE-binding domain of pRb in regulation of

thrombopoiesis, lymphocyte production and ovulation. We also discovered that females were preferentially affected by this mutation.

Rb^{N750F} mice are viable and free of pituitary tumors

We examined $Rb^{N750F/N750F}$ mice for the presence of pituitary tumors, erythroid defects or any histological abnormalities in the brain and liver. None of the mice developed pituitary tumors even after 20 months of observation. In contrast, $Rb^{+/-}$ mice died from pituitary tumors by the age of one year. There were no defects in erythrocyte enucleation in $Rb^{N750F/N750F}$ mice. The size and overall architecture of the brain and liver were unaffected by Rb^{N750F} allele.

These results, combined with the lack of embryonic lethality, indicate that none of the previously described phenotypes observed in the absence of pRb resulted from the disruption of interactions between pRb and LxCxE-containing proteins. However, this conclusion should be treated with caution due to the fact that two other members of pocket protein family, p130 and p107, also have the ability to bind LxCxE-containing proteins, and might be substituting for this function of pRb in Rb^{N750F} heterozygous and homozygous mice(11, 14). In order to explore this possibility, it will be necessary to study the effects of Rb^{N750F} mutation in the absence p107 or p130 by crossing $Rb^{N750F/N750F}$ mice with $p107^{-/-}$ and $p130^{-/-}$ knockout mice, which are viable and fertile.

Myogenic differentiation in $Rb^{N750F/N750F}$ mice is normal

Initial experiments with pRB-N757F in tissue culture demonstrated that this mutant was defective in establishing irreversible growth arrest in differentiated myotubes(5). We

hypothesized that, if present *in vivo*, this mutation would cause excessive proliferation of muscle tissue. This prediction was based on the phenotype seen in the CNS of embryos with telencephalon-specific knockout of *Rb*, where excessive proliferation of neurons led to a 30% increase in the size of telencephalic lobes(12). We carefully examined histological sections of skeletal and cardiac muscles from Rb^{N750F} homozygous and heterozygous mice, but were unable to find any increase in muscle size or disorganization of the muscle fibers. Also, there was no overall increase in the mass of the mutant animals.

The lack of muscle phenotype in Rb^{N750F} homozygous and heterozygous mice is consistent with my findings from the tissue culture experiments. When I subjected $Rb^{N750F/N750F}$ cells to myogenic differentiation *in vitro*, I found that myotubes derived from these cells were able to exit the cell cycle and maintain permanent growth arrest, even after being placed back into serum-rich media (see Chapter III). This discrepancy between results of tissue culture experiments and mouse phenotype might be due to the differences in experimental systems. Initially, the authors used *Rb*-null MEFs that were transduced with MyoD and pRB (either wild type or N757F)(5). The human *RB* gene was under the control of the MSCV promoter and was randomly integrated throughout the mouse genome. In contrast, $Rb^{N750F/N750F}$ MEFs express a murine pRb under the control of endogenous regulatory elements. The difference in the outcomes of muscle differentiation experiments might be explained by the fact that human pRB is only 90% identical to murine pRb and, therefore, cannot completely substitute for pRb in differentiating myotubes.

Even though I was not able to repeat the results of the original tissue culture experiments with pRB-N757F, the lack of muscle phenotype in $Rb^{N750F/N750F}$ mice was in

agreement with some recently published data. Experiments with skeletal muscle-specific knockout of *Rb* demonstrated that pRb played an essential role during early stages of myogenesis, but was dispensable for the maintenance of irreversible growth arrest in differentiated myotubes(16). Therefore, once myotubes passed a certain "point of no return" in their differentiation program, they became insensitive to mitogenic signals even in the absence of pRb. In cardiomyocytes, differentiation defects were observed only after combined loss of *p130* and *Rb*, demonstrating overlapping functions of pocket proteins in myocardium(22).

New functions of pRb

The lack of embryonic lethality in $Rb^{N750F/N750F}$ mice allowed us to study the effects of this mutation in the adult organism. We observed new phenotypes that have not been previously described, and discovered new tissues and processes that require the presence of pRb for their proper function. Moreover, because N750F mutation destroyed only one protein-binding domain of pRb, we could determine the contribution of that domain to pRb function. We report for the first time that disruption of the LxCxE-binding domain of pRb causes perturbations in the processes of thrombopoiesis, lymphocyte production and ovulation in females.

The LxCxE-binding domain of pRb regulates the rate of thrombopoiesis

Increased platelet count was observed in $Rb^{N750F/N750F}$ mice of mixed (129/BL6) and pure (129) background, with a statistically significant difference only in female mice. We attempted to determine whether this increase in the number of platelets was due to an increase in one or more types of precursor cells that eventually give rise to megakaryocytes.

No increase in the number of myeloid precursors or megakaryocyte precursors was observed, indicating that differentiation of hematopoietic stem cells along this lineage was not perturbed by Rb^{N750F} mutation. However, the number of megakaryocytes in the bone marrow was actually decreased. Because megakaryocytes are destroyed in the process of platelet production, increase in the rate of platelet production without a compensatory increase in the rate of megakaryocyte differentiation would result in depletion of megakaryocytes from the bone marrow.

Previous studies by other investigators reported that pRb plays a role in megakaryocyte differentiation and platelet production in mice. Megakaryocyte-specific expression of SV40 T antigen, which binds and inactivates pRb, led to morphological abnormalities and thrombocytopenia (low platelet count)(30). Expression of the E2F1 transgene in megakaryocytes also resulted in thrombocytopenia, caused by blocked differentiation of megakaryocytes (13). Analysis of cells from fetal livers of *Rb*-null embryos and bone marrow from lethally irradiated mice transplanted with *Rb*-null fetal livers revealed an increased number of immature megakaryocytes and decreased number of platelets (Kay Macleod, personal communication). Together, these observations suggest that pRb promotes megakaryocyte differentiation by downregulating E2f1 activity. Because pRb-N750F can still bind E2f1, the process of megakaryocyte differentiation is not disturbed in $Rb^{N750F/N750F}$ mice, as evidences by normal appearance of these cells.

Increase in the number of platelets in $Rb^{N750F/N750F}$ mice indicates that pRb also functions in differentiated megakaryocytes. Specifically, pRb regulates platelet production through its LxCxE-binding domain. This finding is supported by data from mice with tissue-

specific knockout of *Rb* in HSC. Inducible deletion of *Rb* from adult HSC resulted in progressive thromobocytosis (increased platelet count) in the peripheral blood, increased size of megakaryocytes in the bone marrow and infiltration of megakaryocytes into the spleen and liver (Carl Walkley, personal communication). In these animals the platelet count was double that of the wild type controls, while in $Rb^{N750F/N750F}$ mice the increase was only 34 % (129/B6). Taken together, these findings indicate that the LxCxE-binding domain of pRb is partially responsible for regulation of platelet number in the peripheral blood, however, the exact mechanism of it's action remains to be determined.

Increased rate of lymphopoiesis in $Rb^{N750F/N750F}$ mice

We observed increased number of lymphocytes in the peripheral blood of female $Rb^{N750F/N750F}$ mice in 129 Sv/Ev/Tac background. Previously, pRb has been shown to regulate lymphocyte proliferation in response to mitogenic stimulation(34, 39). However, complete loss of pRb in lymphocytes did not alter the number or function of *Rb*-null lymphocytes(4, 35). The discrepancy between our findings and previous studies might be due to the fact that, in the complete absence of pRb, a compensatory mechanism might have been activated resulting in normal differentiation and function of *Rb*-null lymphocytes. This hypothesis is supported by the observations of functional compensation by pocket family proteins in $p130^{-/-}$ and $p130^{-/-};p107^{-/-}$ lymphocytes(27). Moreover, *Rb*-null MEFs were reported to display only minimal alterations of the cell cycle, while removal of all three members of the pocket family resulted in a dramatic deregulation of this process(15, 32). Taken together, these studies indicate that in the complete absence of pRb other members of the pocket family can compensate for its function. In $Rb^{N750F/N750F}$ mice, such compensation

might not have occurred because pRb protein, albeit a mutant version of it, was still present. This lack of compensation resulted in increased production of lymphocytes in $Rb^{N750F/N750F}$ mice.

While we documented an increase in the number of lymphocytes in $Rb^{N750F/N750F}$ females, we did not conduct any experiments to assess lymphocyte function. pRb has been implicated in regulation of inducible gene expression during T cell activation(36). Specifically, hypophosphorylated pRb was shown to bind to Elf-1 transcription factor in resting, but not activated T lymphocytes. The binding of pRb to Elf-1 resulted in repression of transcription from GM-CSF (granulocyte-macrophage colony-stimulating factor) promoter. Elf-1 contains an LxCxE motif, which was shown to be required for its binding to pRb *in vitro*. Because pRb-N750F mutant does not bind LxCxE-containing proteins, the Elf-1 function in lymphocytes might be deregulated, leading to excessive proliferation and activation of lymphocytes. The binding of hypophosphorylated pRb to Elf-1 might serve as a mechanism of coupling proliferation and activation of T lymphocytes ensuring that these processes occur in coordinated fashion.

Regulation of ovulation by the LxCxE-binding domain of pRb

The role of pRb in reproduction has not been determined due to the embryonic lethality of $Rb^{-/-}$ mice. $Rb^{+/-}$ mice do not show any impairment in fertility. No pregnancy was ever observed in $Rb^{N750F/N750F}$ females of 129 Sv/Ev/Tac background. Examination of ovarian tissues from the mutant mice revealed lack of ovulation as evidenced by the absence of corpora lutea. The possible causes of anovulation can be divided into two broad categories: defects in hormonal regulation of the estrous cycle, or the inability of the ovarian

tissue to respond to gonadotropic hormones. Histological analysis of ovarian tissues from $Rb^{N750F/N750F}$ mice revealed that follicular development proceeded normally up to the stage of Graafian follicle. This finding indicates that enough follicle stimulating hormone (FSH) and luteinizing hormone (LH) were released by the pituitary to promote follicular development, and that ovarian tissue was responding normally to these hormones. The absence of corpora lutea suggests that either there was no LH surge to trigger ovulation, or that the follicles failed to respond to the surge.

In an attempt to determine which of the two possible mechanisms might be responsible for the lack of ovulation in $Rb^{N750F/N750F}$ females, we compared their phenotype to the phenotypes of mice with knockout of either FSH (FSH KO), or FSH receptor (FSHR KO), or LH (LH KO) or LH receptor (LHR KO)(1, 10, 18, 20, 21, 42). FSH KO mice phenocopy FSHR KO mice, while LH KO phenocopy LHR KO. Interestingly, $Rb^{N750F/N750F}$ females did not phenocopy either of these two phenotypes, indicating that pRb-N750F regulates follicular development and ovulation by a novel mechanism.

Since there is no tissue-specific knockout of pRb in the ovaries, the consequences of the loss of pRb in this organ are not known. Thus, we demonstrated for the first time that the LxCxE-binding domain of pRb regulates ovulation. Recently, promoters of several genes encoding regulators of reproductive function have been reported to contain homeobox-binding elements. Specifically, gonadotropin-releasing hormone (GnRH) promoter was shown to be repressed by homeodomain-containing protein MSX1 and activated by homeodomain-containing protein OCT1(29). Expression of GnRH during development was also regulated by homeodomain-containing proteins. Proximal region of LHβ subunit

contains a homeobox element, which was shown to be required for maximal induction of LHβ by activin(8). Gonadotropin-releasing hormone receptor gene is activated by LHX3, which is a homeodomain protein(26). Gene expression profiling experiments with MEFs revealed deregulation of several homeobox-containing genes (Chapter III). Therefore, female infertility observed in $Rb^{N750F/N750F}$ mice might be due to defects in hormonal regulation of the estrous cycle, which in turn is caused by defects in expression of homeobox-containing genes.

Haplo-insufficiency of Rb^{N750F} allele

The $Rb^{N750F/N750F}$ mice were born at the expected Mendelian ratio. Except for defects in thrombopoiesis, lymphopoiesis and ovulation, they were healthy and viable. In contrast, $Rb^{N750F/-}$ mice were born at a significantly reduced Mendelian ratio and died by eight months of age. In the ovaries of $Rb^{N750F/-}$ females the follicular development arrested earlier than in $Rb^{N750F/N750F}$ females. Moreover, the interstitial cells failed to differentiate in $Rb^{N750F/-}$ ovaries, while in $Rb^{N750F/N750F}$ ovaries they were fully developed and functional. Together these findings demonstrate haplo-insufficiency of Rb^{N750F} allele as well as inability of p107 and p130 to substitute for the LxCxE-binding function of pRb. They suggest the existence of LxCxE-containing protein(s) whose interaction with pRb are essential for survival during prenatal development and in adulthood, as well as for the development of the ovarian follicles and interstitial cells. No other *Rb* allele has been demonstrated to be haploinsufficient.

Sex-specific effects of *Rb*^{N750F} allele

The phenotypes observed in mice with *Rb*^{N750F} displayed a sex-specific bias. Increase in the number of platelets and lymphocytes reached statistical significance only in *Rb*$^{N750F/N750F}$ females, while higher mortality rate was observed in *Rb*$^{N750F/-}$ males. Sex-specific differences of pRb function have been previously reported. A caspase-resistant pRb (pRb-MI) has been shown to improve survival rates following endotoxic shock in male but not female mice(3). This sex-specific protection was also strain-dependent, as it occurred only in 129 Sv/Ev/Tac mice, but not in mice of 129/BL6 mixed background. These results indicate the presence of genes that modify the function of pRb in various tissues in strain-specific and sex-specific manner.

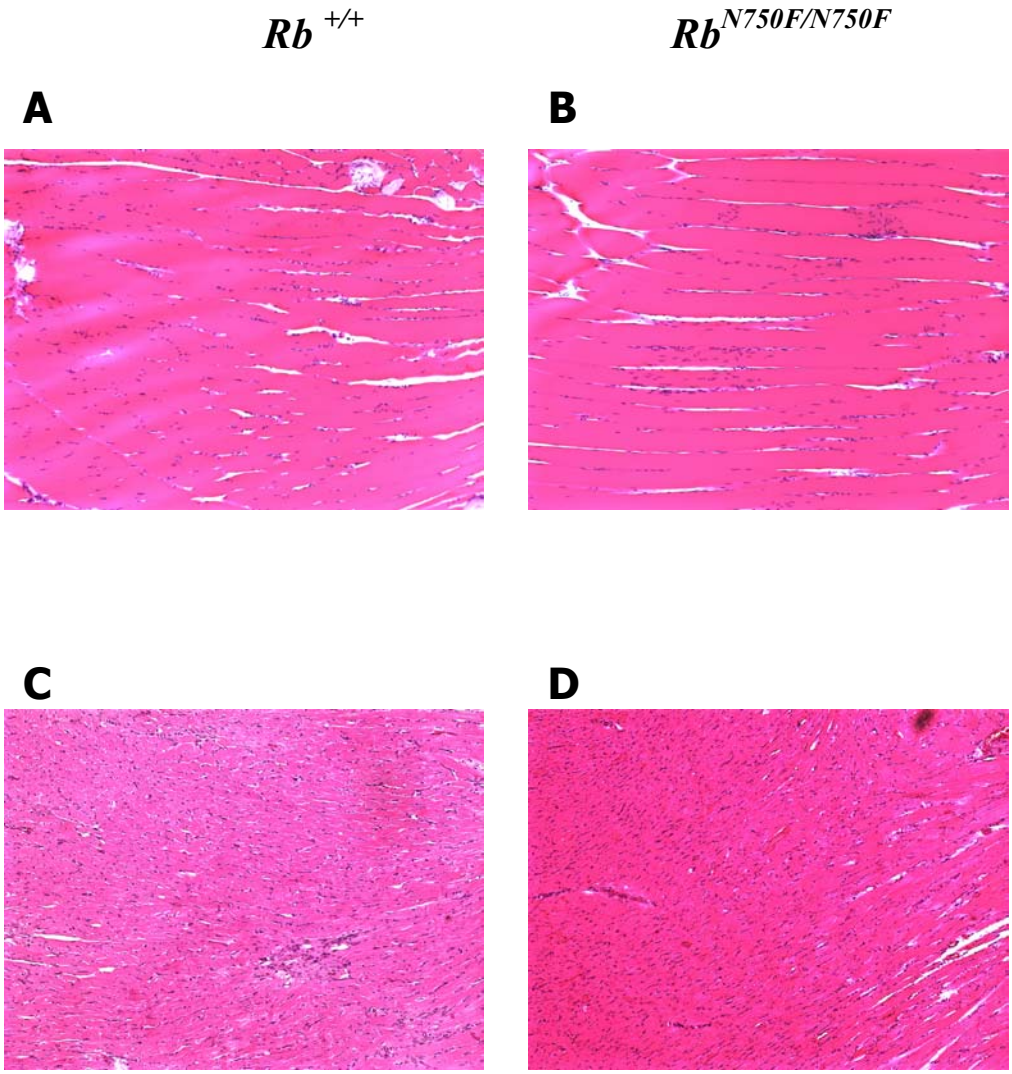

Figure 4.1 Hystological analysis of the skeletal and cardiac muscle.

H&E staining of the longitudinal section through the hind limb muscle (A and B) and myocardium (C and D) of wild type **(A and C)** and *Rb*$^{N750F/N750F}$ mutant (**B and D)** mice. Both show normal architecture of the myotubes. Original magnification is 10X.

Figure 4.2 Platelet counts in the peripheral blood.

Complete blood cell count was performed on peripheral blood samples collected from the tail vein. The number of platelets was compared using Student t test, *p* values are shown above each graph.

A. Male and female mice of 129 Sv/Ev/Tac pure background. **B**. Male and female mice of 129/B6 mixed background. **C**. Females only, 129 Sv/Ev/Tac. **D**. Females only, 129/B6 mixed. **E**. Males only, 129 Sv/Ev/Tac. **F**. Males only, 129/B6 mixed.

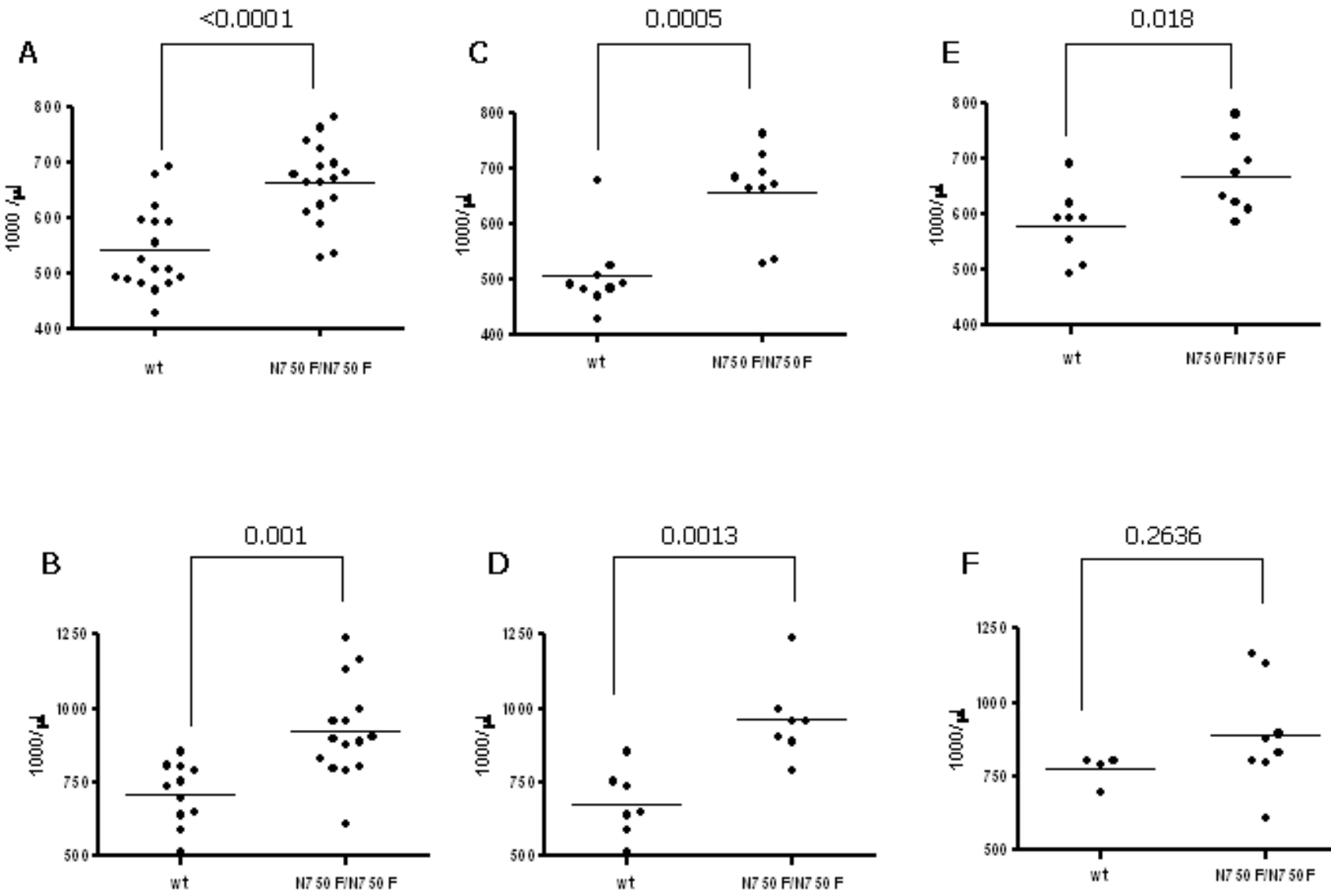
A
<0.0001
1000 /µl
800
700
600
500
400
wt
N750F/N750F
C
0.0005
1000/µl
800
700
600
500
400
wt
N750F/N750F
E
0.018
1000/µl
800
700
600
500
400
wt
N750F/N750F
B
0.001
1000/µl
1250
1000
750
500
wt
N750F/N750F
D
0.0013
1000/µl
1250
1000
750
500
wt
N750F/N750F
F
0.2636
1000/µl
1250
1000
750
500
wt
N750F/N750F

Figure 4.3 Differentiation of hematopoietic stem cells.

Hematopoietic stem cells (HSC) undergo several rounds of differentiation to produce all types of blood cells.
Abbreviations: CMP, common myeloid progenitor (CFU-GEMM); CLP, common lymphoid progenitor; MEP, megakaryocyte/erythrocyte progenitor; GMP, granulocyte/macrophage progenitor (CFU-GM).

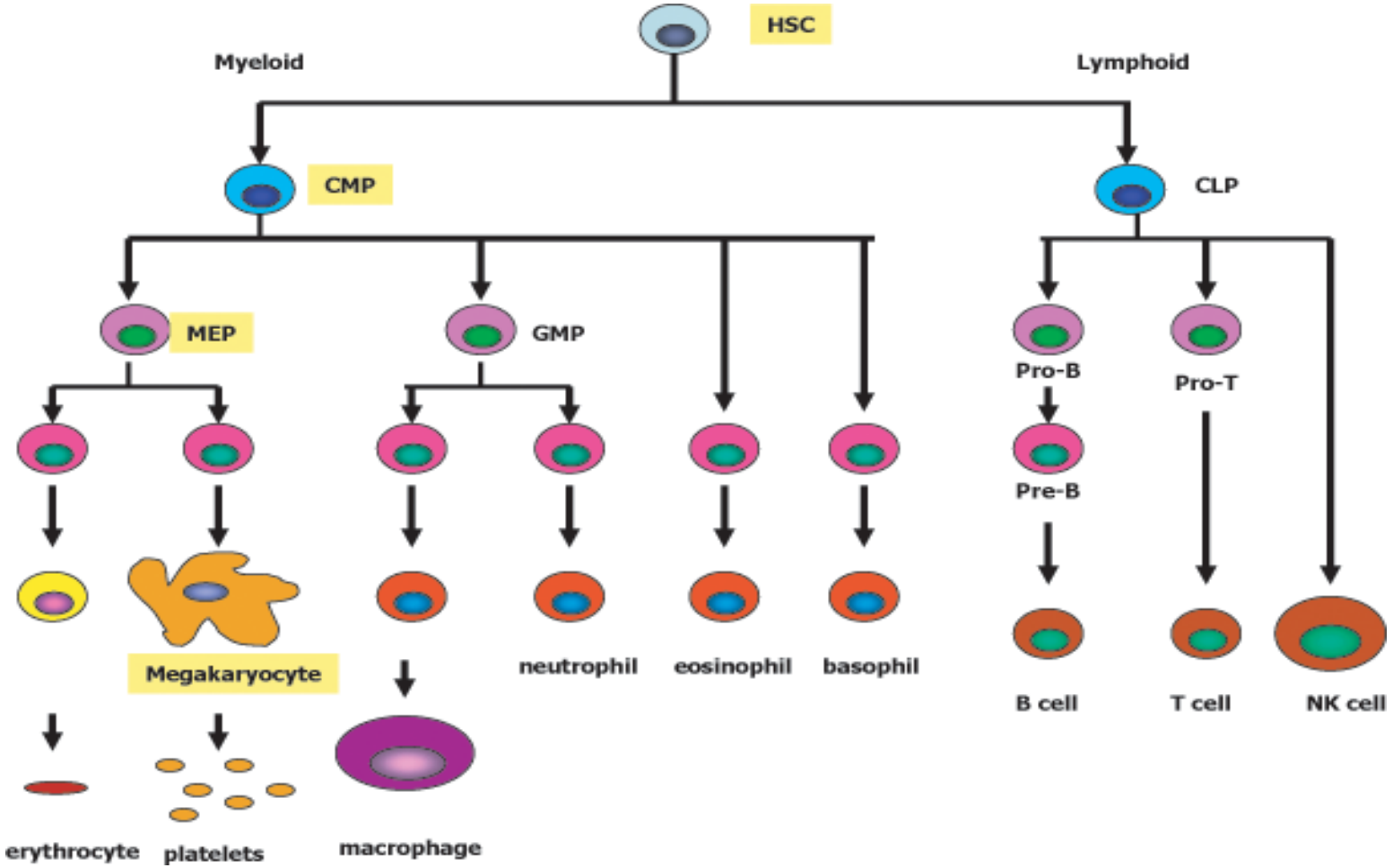
HSC
Myeloid
Lymphoid
CMP
CLP
MEP
GMP
Pro-B
Pro-T
Pre-B
Megakaryocyte
neutrophil
eosinophil
basophil
B cell
T cell
NK cell
erythrocyte
platelets
macrophage

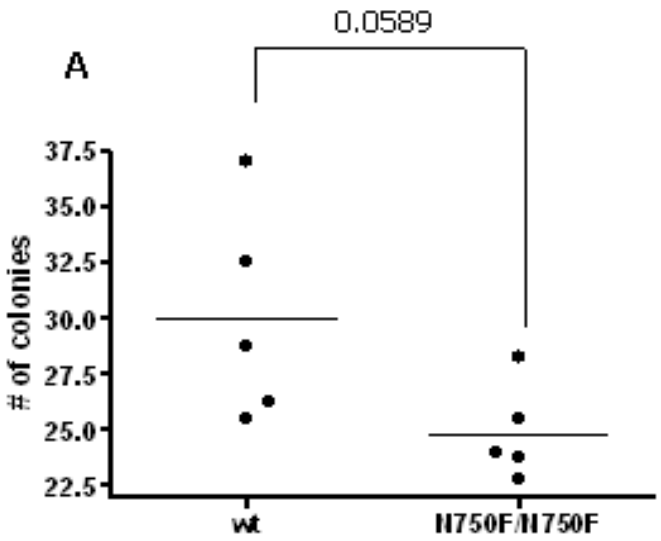

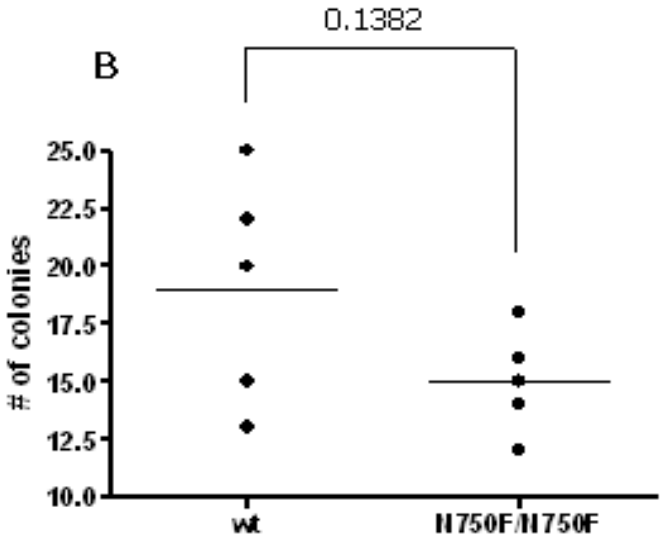

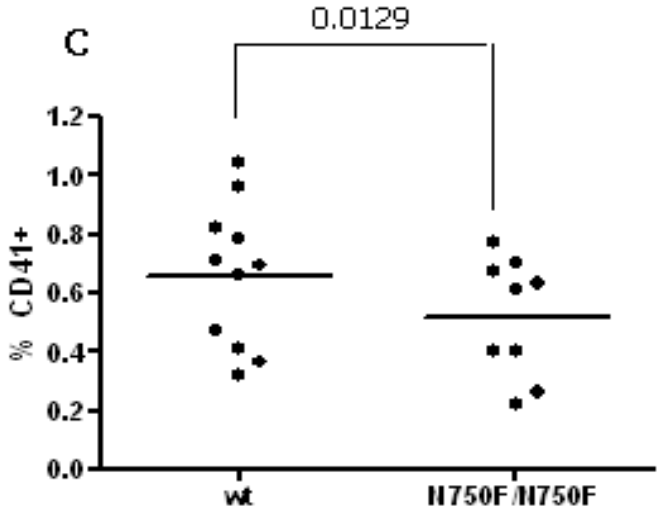

Figure 4.4 Analysis of progenitor cells in the platelet lineage.

Cells were isolated from the bone marrow and plated in the medium that promotes outgrowth of various progenitor populations (A and B), or labeled with anti-CD41 antibody and analyzed by FACS (C).

A. Colony-forming assay for CFU-GM and CFU-GEMM. B. Colony-forming assay for megakaryocyte precursors. C. FACS analysis for megakaryocytes.

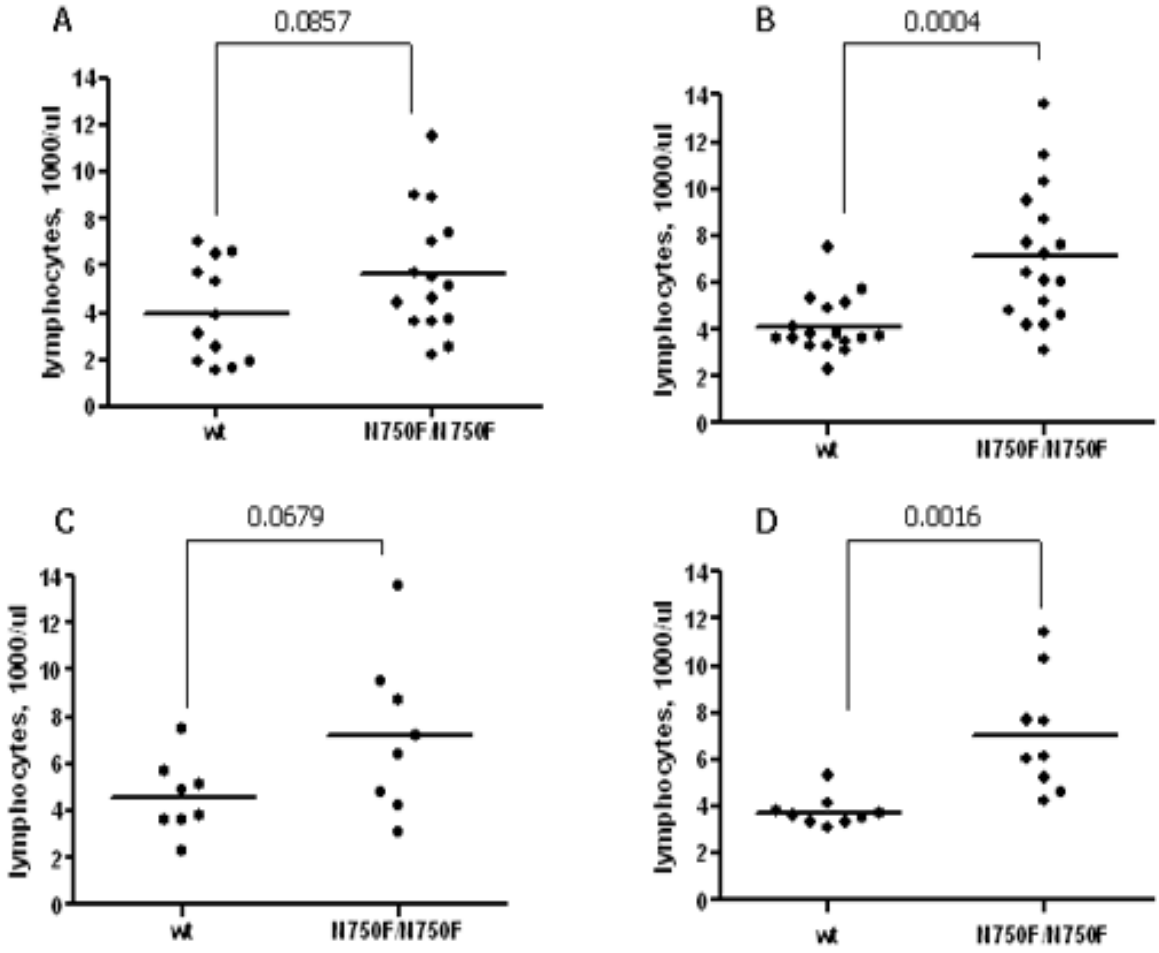

Figure 4.5 Lymphocyte counts in the peripheral blood.

Complete blood cell count was performed on peripheral blood samples collected from the tail vein. The number of lymphocytes was compared using Student t test, *p* values are shown above each graph.

A. Male and female mice of 129/B6 mixed background. **B.** Male and female mice of 129 Sv/Ev/Tac pure background. **C.** Males only, 129 Sv/Ev/Tac. **D.** Females only, 129 Sv/Ev/Tac.

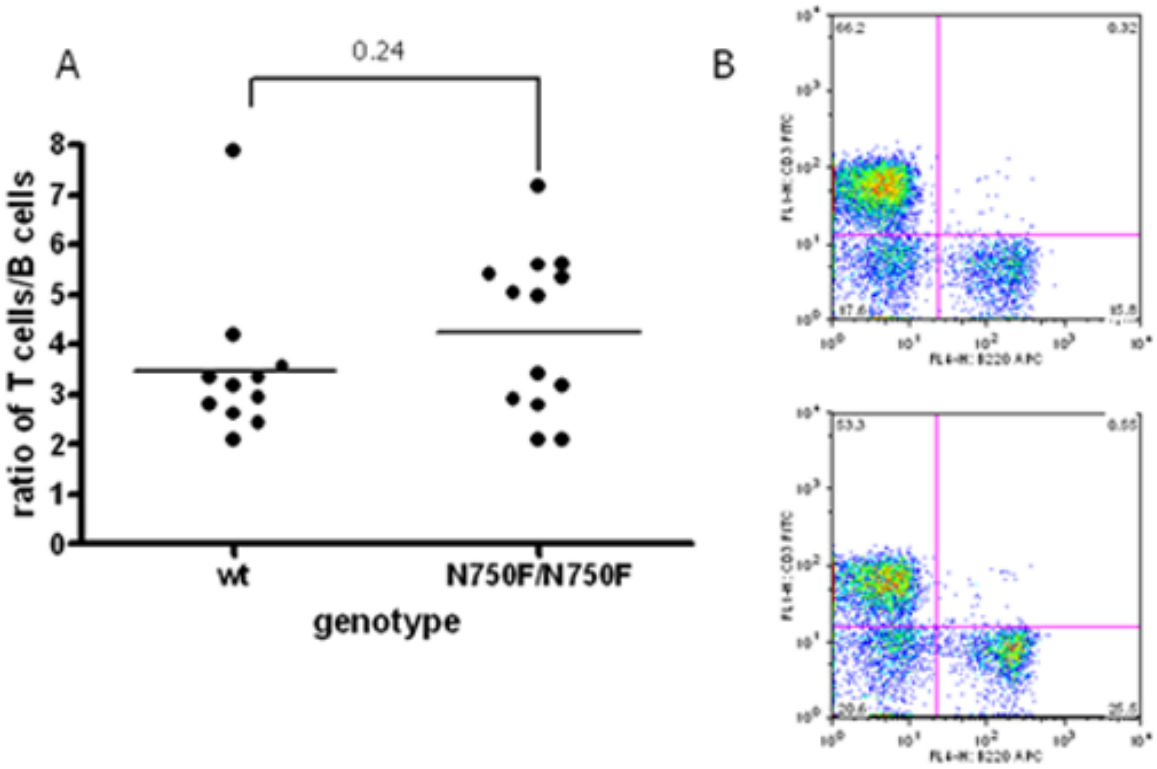

Figure 4.6 Relative ratio of T lymphocytes to B lymphocytes in the peripheral blood of *Rb*$^{N750F/N750F}$ mice.

Lymphocytes from the peripheral blood of wild type and *Rb*$^{N750F/N750F}$ mice were labeled with anti-CD3 and anti-B220 antibodies and analyzed by FACS.

A. The ratio of T lymphocytes to B lymphocytes is not altered in *Rb*$^{N750F/N750F}$ mice. **B.** FACS analysis of T and B lymphocytes in the peripheral blood of wild type (top) and in *Rb*$^{N750F/N750F}$ (bottom) mice.

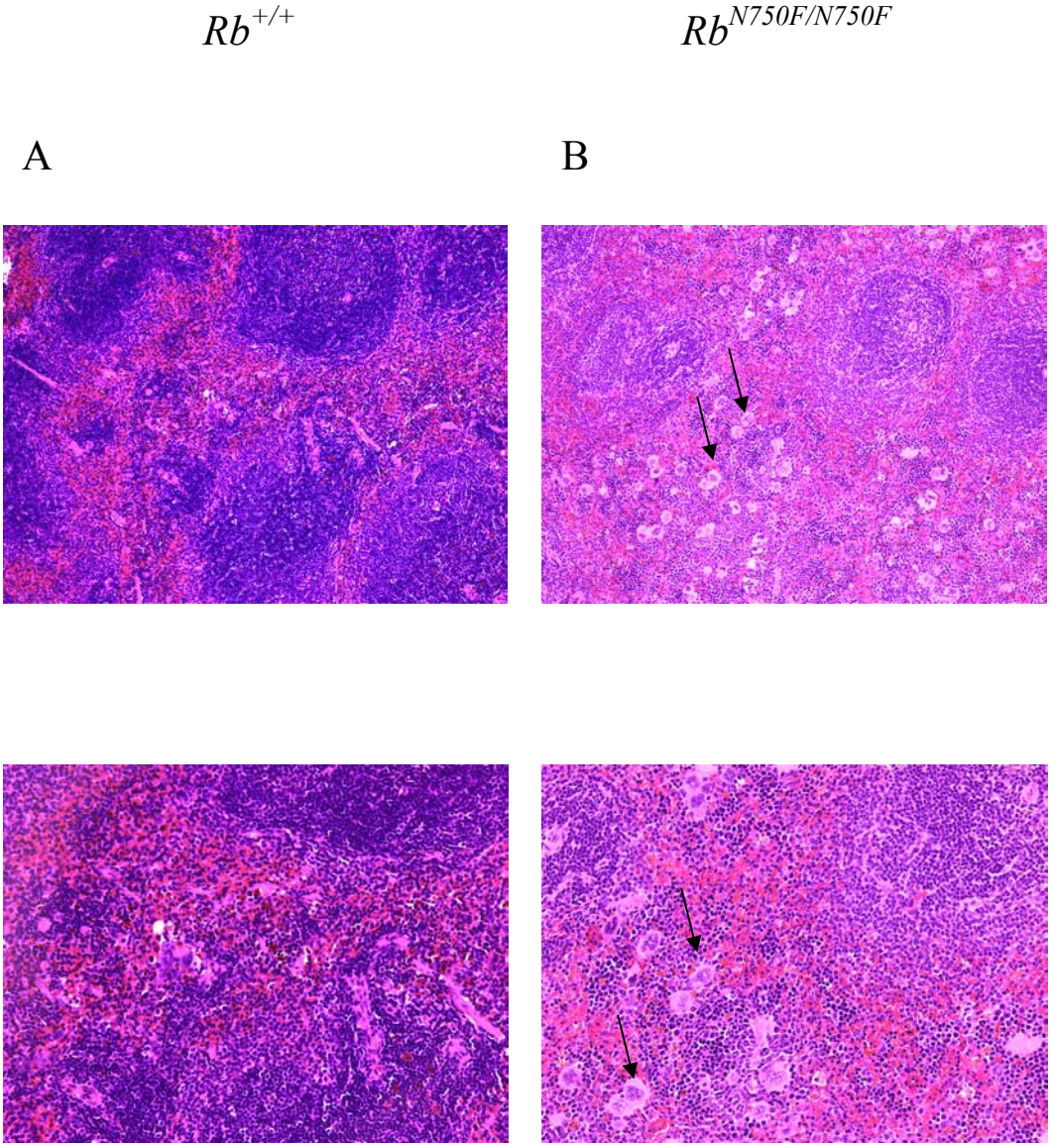

Figure 4.7 Histological analysis of the spleen.

A. Wild type mice show normal architecture of the spleen. **B.** In *RbN750F/N750F* mutant mice megakaryocytes are clearly visible in the red pulp (arrows). Original magnification is 10X (top panels) and 20X (bottom panels).

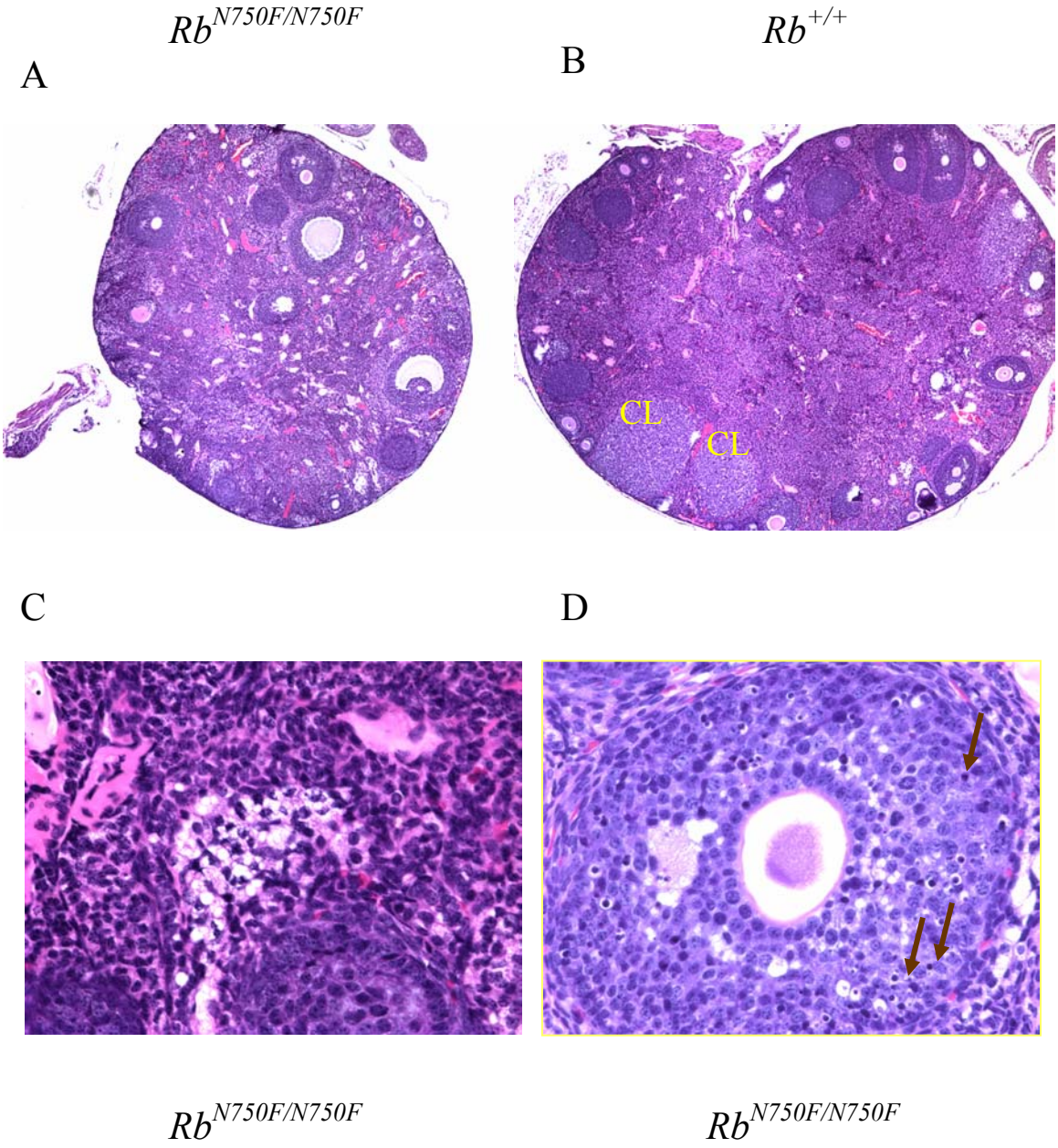

Figure 4.8 Histological analysis of the ovaries from $Rb^{N750F/N750F}$ females.

H&E staining of the ovary from $Rb^{N750F/N750F}$ (**A**) and wild type (**B**) females. No corpus luteum (CL) is found in the ovaries from the mutant mice. **C.** Secondary interstitial cells are filled with lipid droplets (arrow). **D.** Picnotic nuclei (arrows) are present in the pre-ovulatory follicle. Original magnification is 4X in A and B, 40X in C and D.

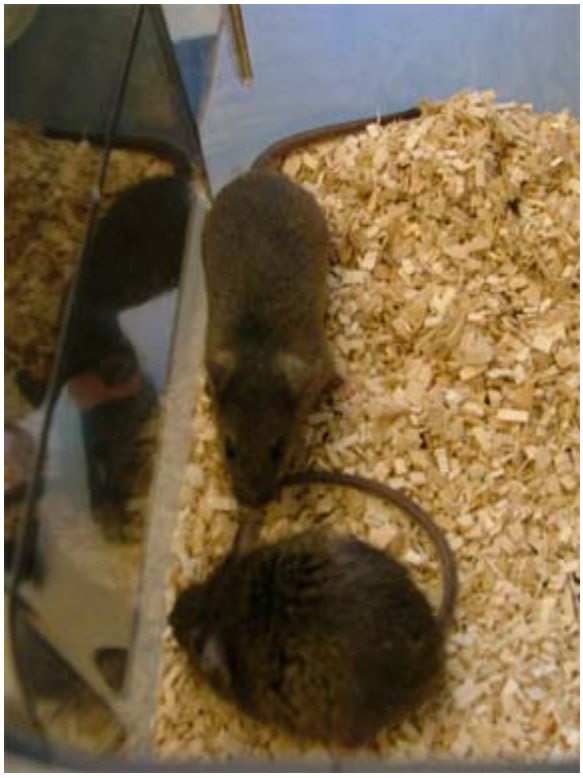

Figure 4.9 *Rb*$^{N750F/-}$ mice show a characteristic hunchback posture.

Wild type (top) and *Rb*$^{N750F/-}$ (bottom) littermates.

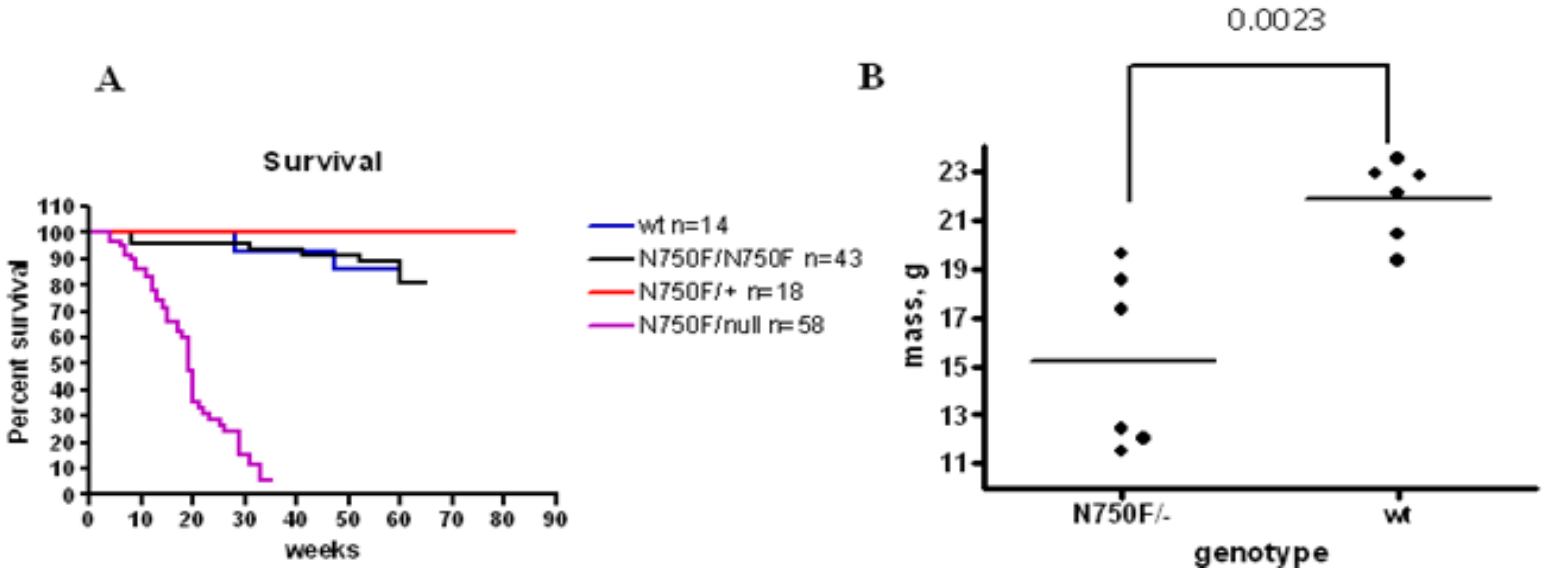

Figure 4.10 Early mortality and reduced mass of $Rb^{N750F/-}$ mice.

A. Kaplan-Meier survival curve of various Rb^{N750F} mutants and wild type control littermates. **B.** *RbN750F/-* mutant mice show reduced mass compared to their wild type littermates at 16 weeks of age.

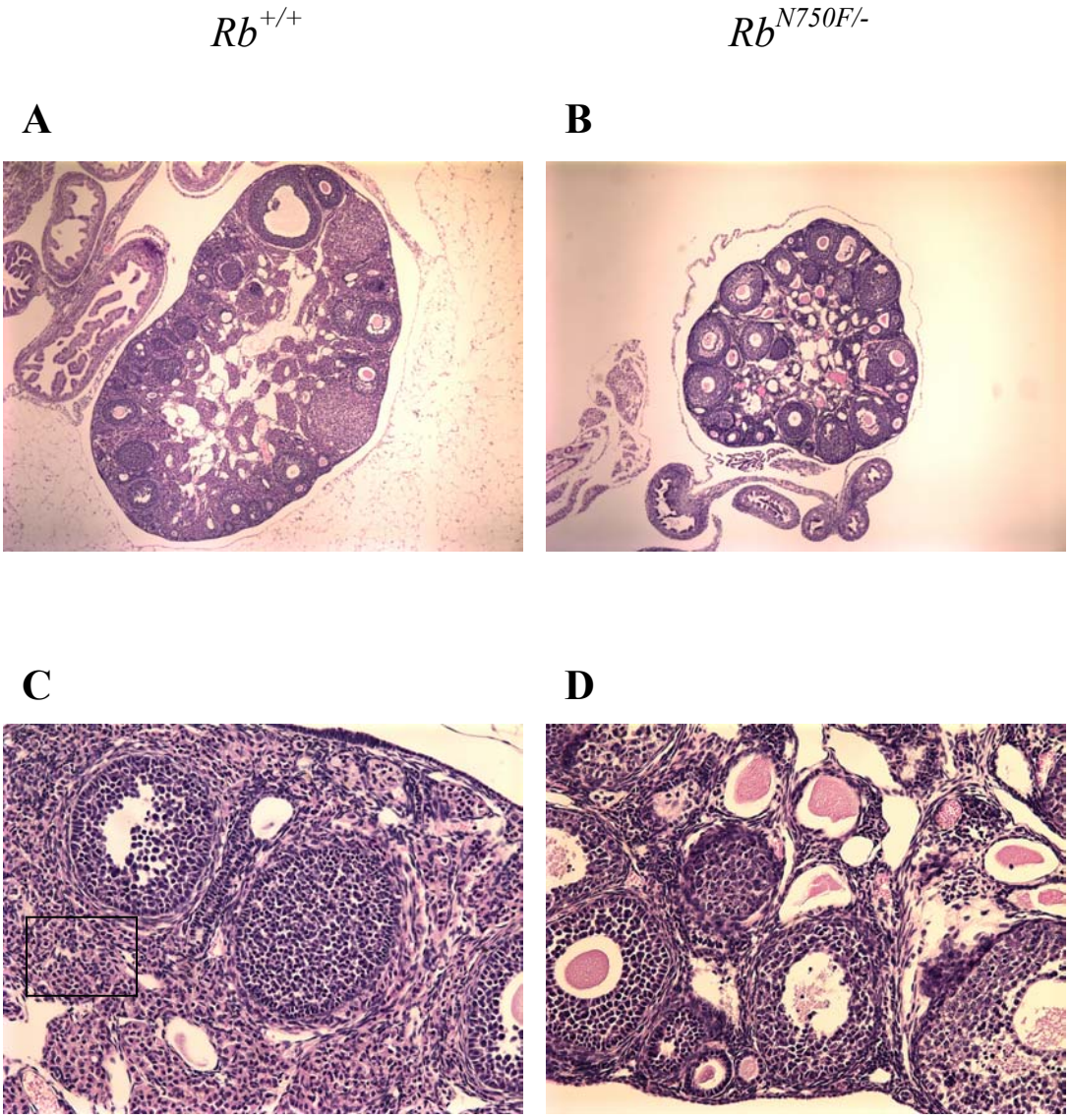

Figure 4.11 Histological analysis of ovaries from *Rb* $^{N750F/-}$ females.

H&E staining of the ovary from wild type (**A and C)** and $Rb^{N750F/-}$ **(B and D)** females. No corpus luteum (CL) is found in the ovaries from the mutant mice. Interstitial cells (boxed in C) were virtually absent from the ovaries of $Rb^{N750F/-}$ females (D). Magnification is 4X for the top panels and 20X for the bottom panels.

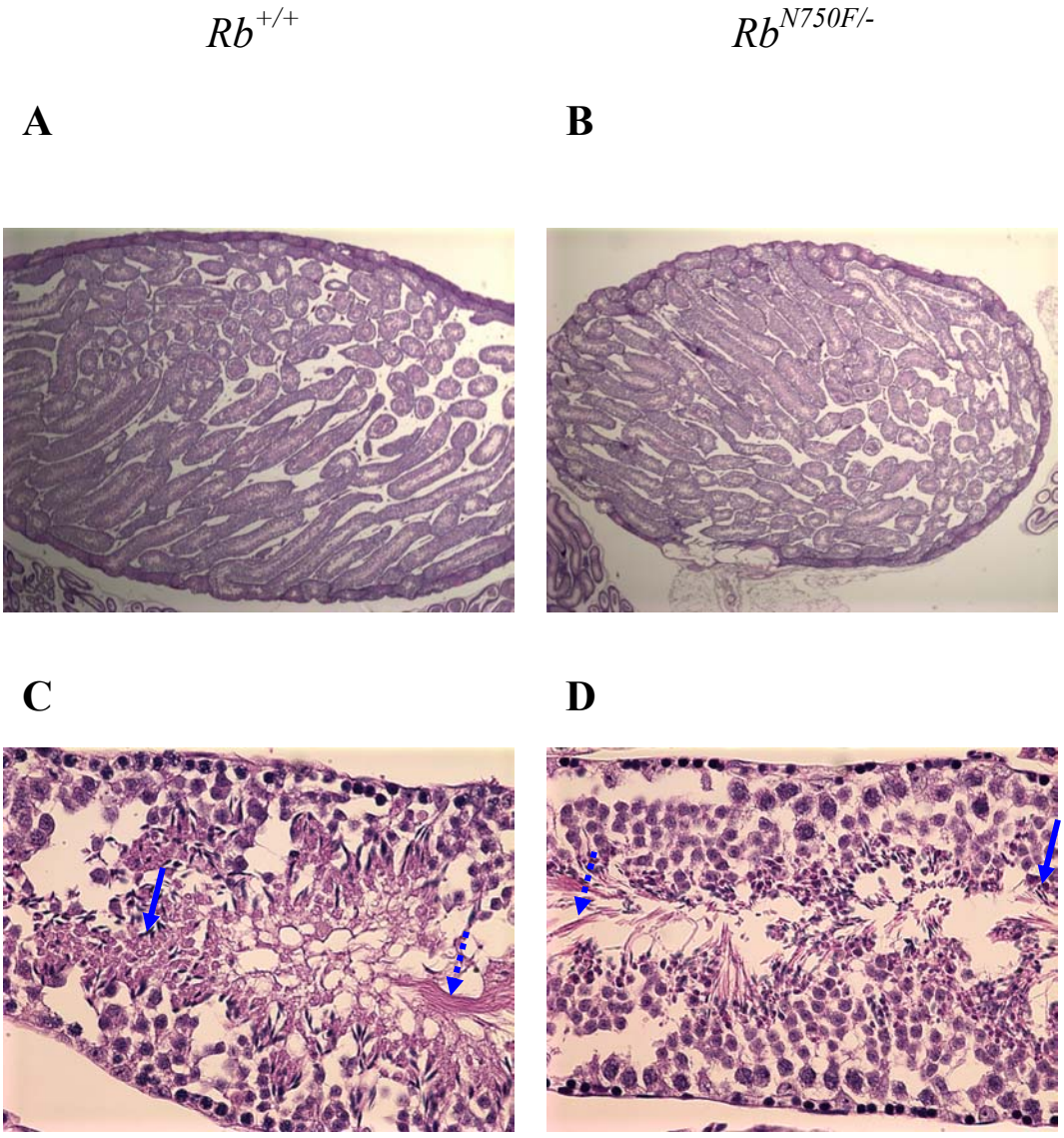

Figure 4.12 Histological analysis of the testis from $Rb^{N750F/-}$ males.

H&E staining of the testis from wild type (**A and C)** and $Rb^{N750F/-}$ **(B and D)** females. Testis from wild type males (A) appeared larger than from $Rb^{N750F/-}$ males (B). However, there was still abundant sperm present in the seminiferous tubules of both wild type (C) and $Rb^{N750F/-}$ (D) males. Original magnification is 2X in the top panels and 40X in the bottom panels. In C and D solid and broken arrows designate sperm nuclei and tail respectively.

REFERENCES

1. **Abel, M. H., A. N. Wootton, V. Wilkins, I. Huhtaniemi, P. G. Knight, and H. M. Charlton.** 2000. The effect of a null mutation in the follicle-stimulating hormone receptor gene on mouse reproduction. Endocrinology **141:**1795-803.

2. **Balsitis, S. J., J. Sage, S. Duensing, K. Munger, T. Jacks, and P. F. Lambert.** 2003. Recapitulation of the effects of the human papillomavirus type 16 E7 oncogene on mouse epithelium by somatic Rb deletion and detection of pRb-independent effects of E7 in vivo. Mol Cell Biol **23:**9094-103.

3. **Chau, B. N., H. L. Borges, T. T. Chen, A. Masselli, I. C. Hunton, and J. Y. Wang.** 2002. Signal-dependent protection from apoptosis in mice expressing caspase-resistant Rb. Nat Cell Biol **4:**757-65.

4. **Chen, J., J. R. Gorman, V. Stewart, B. Williams, T. Jacks, and F. W. Alt.** 1993. Generation of normal lymphocyte populations by Rb-deficient embryonic stem cells. Curr Biol **3:**405-13.

5. **Chen, T. T., and J. Y. Wang.** 2000. Establishment of irreversible growth arrest in myogenic differentiation requires the RB LXCXE-binding function. Mol Cell Biol **20:**5571-80.

6. **Clark, A. J., K. M. Doyle, and P. O. Humbert.** 2004. Cell-intrinsic requirement for pRb in erythropoiesis. Blood **104:**1324-6.

7. **Clarke, A. R., E. R. Maandag, M. van Roon, N. M. van der Lugt, M. van der Valk, M. L. Hooper, A. Berns, and H. te Riele.** 1992. Requirement for a functional Rb-1 gene in murine development. Nature **359:**328-30.

8. **Coss, D., V. G. Thackray, C. X. Deng, and P. L. Mellon.** 2005. Activin regulates luteinizing hormone beta-subunit gene expression through Smad-binding and homeobox elements. Mol Endocrinol **19:**2610-23.

9. **de Bruin, A., L. Wu, H. I. Saavedra, P. Wilson, Y. Yang, T. J. Rosol, M. Weinstein, M. L. Robinson, and G. Leone.** 2003. Rb function in extraembryonic lineages suppresses apoptosis in the CNS of Rb-deficient mice. Proc Natl Acad Sci U S A **100:**6546-51.

10. **Dierich, A., M. R. Sairam, L. Monaco, G. M. Fimia, A. Gansmuller, M. LeMeur, and P. Sassone-Corsi.** 1998. Impairing follicle-stimulating hormone (FSH) signaling in vivo: targeted disruption of the FSH receptor leads to aberrant gametogenesis and hormonal imbalance. Proc Natl Acad Sci U S A **95:**13612-7.

11. **Ewen, M. E., B. Faha, E. Harlow, and D. M. Livingston.** 1992. Interaction of p107 with cyclin A independent of complex formation with viral oncoproteins. Science **255:**85-7.

12. **Ferguson, K. L., J. L. Vanderluit, J. M. Hebert, W. C. McIntosh, E. Tibbo, J. G. MacLaurin, D. S. Park, V. A. Wallace, M. Vooijs, S. K. McConnell, and R. S. Slack.** 2002. Telencephalon-specific Rb knockouts reveal enhanced neurogenesis, survival and abnormal cortical development. Embo J **21:**3337-46.

13. **Guy, C. T., W. Zhou, S. Kaufman, and M. O. Robinson.** 1996. E2F-1 blocks terminal differentiation and causes proliferation in transgenic megakaryocytes. Mol Cell Biol **16:**685-93.

14. **Hannon, G. J., D. Demetrick, and D. Beach.** 1993. Isolation of the Rb-related p130 through its interaction with CDK2 and cyclins. Genes Dev **7:**2378-91.

15. **Herrera, R. E., V. P. Sah, B. O. Williams, T. P. Makela, R. A. Weinberg, and T. Jacks.** 1996. Altered cell cycle kinetics, gene expression, and G1 restriction point regulation in Rb-deficient fibroblasts. Mol Cell Biol **16:**2402-7.

16. **Huh, M. S., M. H. Parker, A. Scime, R. Parks, and M. A. Rudnicki.** 2004. Rb is required for progression through myogenic differentiation but not maintenance of terminal differentiation. J Cell Biol **166:**865-76.

17. **Jacks, T., A. Fazeli, E. M. Schmitt, R. T. Bronson, M. A. Goodell, and R. A. Weinberg.** 1992. Effects of an Rb mutation in the mouse. Nature **359:**295-300.

18. **Kumar, T. R., Y. Wang, N. Lu, and M. M. Matzuk.** 1997. Follicle stimulating hormone is required for ovarian follicle maturation but not male fertility. Nat Genet **15:**201-4.

19. **Lee, E. Y., C. Y. Chang, N. Hu, Y. C. Wang, C. C. Lai, K. Herrup, W. H. Lee, and A. Bradley.** 1992. Mice deficient for Rb are nonviable and show defects in neurogenesis and haematopoiesis. Nature **359:**288-94.

20. **Lei, Z. M., S. Mishra, W. Zou, B. Xu, M. Foltz, X. Li, and C. V. Rao.** 2001. Targeted disruption of luteinizing hormone/human chorionic gonadotropin receptor gene. Mol Endocrinol **15:**184-200.

21. **Ma, X., Y. Dong, M. M. Matzuk, and T. R. Kumar.** 2004. Targeted disruption of luteinizing hormone beta-subunit leads to hypogonadism, defects in gonadal steroidogenesis, and infertility. Proc Natl Acad Sci U S A **101:**17294-9.

22. **MacLellan, W. R., A. Garcia, H. Oh, P. Frenkel, M. C. Jordan, K. P. Roos, and M. D. Schneider.** 2005. Overlapping roles of pocket proteins in the myocardium are unmasked by germ line deletion of p130 plus heart-specific deletion of Rb. Mol Cell Biol **25:**2486-97.

23. **MacPherson, D., J. Sage, D. Crowley, A. Trumpp, R. T. Bronson, and T. Jacks.** 2003. Conditional mutation of Rb causes cell cycle defects without apoptosis in the central nervous system. Mol Cell Biol **23:**1044-53.

24. **Matsunaga, E.** 1980. Hereditary retinoblastoma: host resistance and second primary tumors. J Natl Cancer Inst **65:**47-51.

25. **Mayhew, C. N., E. E. Bosco, S. R. Fox, T. Okaya, P. Tarapore, S. J. Schwemberger, G. F. Babcock, A. B. Lentsch, K. Fukasawa, and E. S. Knudsen.** 2005. Liver-specific pRB loss results in ectopic cell cycle entry and aberrant ploidy. Cancer Res **65:**4568-77.

26. **McGillivray, S. M., J. S. Bailey, R. Ramezani, B. J. Kirkwood, and P. L. Mellon.** 2005. Mouse GnRH receptor gene expression is mediated by the LHX3 homeodomain protein. Endocrinology **146:**2180-5.

27. **Mulligan, G. J., J. Wong, and T. Jacks.** 1998. p130 is dispensable in peripheral T lymphocytes: evidence for functional compensation by p107 and pRB. Mol Cell Biol **18:**206-20.

28. **Novitch, B. G., G. J. Mulligan, T. Jacks, and A. B. Lassar.** 1996. Skeletal muscle cells lacking the retinoblastoma protein display defects in muscle gene expression and accumulate in S and G2 phases of the cell cycle. J Cell Biol **135:**441-56.

29. **Rave-Harel, N., N. L. Miller, M. L. Givens, and P. L. Mellon.** 2005. The Groucho-related gene family regulates the gonadotropin-releasing hormone gene through interaction with the homeodomain proteins MSX1 and OCT1. J Biol Chem **280:**30975-83.

30. **Robinson, M. O., W. Zhou, M. Hokom, D. M. Danilenko, R. Y. Hsu, R. E. Atherton, W. Xu, S. Mu, C. J. Saris, S. Swift, and et al.** 1994. The tsA58 simian virus 40 large tumor antigen disrupts megakaryocyte differentiation in transgenic mice. Proc Natl Acad Sci U S A **91:**12798-802.

31. **Sage, C., M. Huang, K. Karimi, G. Gutierrez, M. A. Vollrath, D. S. Zhang, J. Garcia-Anoveros, P. W. Hinds, J. T. Corwin, D. P. Corey, and Z. Y. Chen.** 2005. Proliferation of functional hair cells in vivo in the absence of the retinoblastoma protein. Science **307:**1114-8.

32. **Sage, J., G. J. Mulligan, L. D. Attardi, A. Miller, S. Chen, B. Williams, E. Theodorou, and T. Jacks.** 2000. Targeted disruption of the three Rb-related genes leads to loss of G(1) control and immortalization. Genes Dev **14:**3037-50.

33. **Spike, B. T., A. Dirlam, B. C. Dibling, J. Marvin, B. O. Williams, T. Jacks, and K. F. Macleod.** 2004. The Rb tumor suppressor is required for stress erythropoiesis. Embo J **23:**4319-29.

34. **Terada, N., J. J. Lucas, and E. W. Gelfand.** 1991. Differential regulation of the tumor suppressor molecules, retinoblastoma susceptibility gene product (Rb) and p53, during cell cycle progression of normal human T cells. J Immunol **147:**698-704.

35. **Walkley, C. R., and S. H. Orkin.** 2006. Rb is dispensable for self-renewal and multilineage differentiation of adult hematopoietic stem cells. Proc Natl Acad Sci U S A **103:**9057-62.

36. **Wang, C. Y., B. Petryniak, C. B. Thompson, W. G. Kaelin, and J. M. Leiden.** 1993. Regulation of the Ets-related transcription factor Elf-1 by binding to the retinoblastoma protein. Science **260:**1330-5.

37. **Williams, B. O., E. M. Schmitt, L. Remington, R. T. Bronson, D. M. Albert, R. A. Weinberg, and T. Jacks.** 1994. Extensive contribution of Rb-deficient

cells to adult chimeric mice with limited histopathological consequences. Embo J **13:**4251-9.

38. **Wu, L., A. de Bruin, H. I. Saavedra, M. Starovic, A. Trimboli, Y. Yang, J. Opavska, P. Wilson, J. C. Thompson, M. C. Ostrowski, T. J. Rosol, L. A. Woollett, M. Weinstein, J. C. Cross, M. L. Robinson, and G. Leone.** 2003. Extra-embryonic function of Rb is essential for embryonic development and viability. Nature **421:**942-7.

39. **Yen, A., S. Chandler, and S. Sturzenegger-Varvayanis.** 1991. Regulated expression of the RB "tumor suppressor gene" in normal lymphocyte mitogenesis: elevated expression in transformed leukocytes and role as a "status quo" gene. Exp Cell Res **192:**289-97.

40. **Yu, B. D., M. Becker-Hapak, E. L. Snyder, M. Vooijs, C. Denicourt, and S. F. Dowdy.** 2003. Distinct and nonoverlapping roles for pRB and cyclin D:cyclin-dependent kinases 4/6 activity in melanocyte survival. Proc Natl Acad Sci U S A **100:**14881-6.

41. **Zacksenhaus, E., Z. Jiang, D. Chung, J. D. Marth, R. A. Phillips, and B. L. Gallie.** 1996. pRb controls proliferation, differentiation, and death of skeletal muscle cells and other lineages during embryogenesis. Genes Dev **10:**3051-64.

42. **Zhang, F. P., M. Poutanen, J. Wilbertz, and I. Huhtaniemi.** 2001. Normal prenatal but arrested postnatal sexual development of luteinizing hormone receptor knockout (LuRKO) mice. Mol Endocrinol **15:**172-83.

CHAPTER V

GENERAL DISCUSSION

Retinoblastoma protein was first discovered as the product of a gene whose mutation or loss causes cancer of the retina in humans. Numerous cell culture studies firmly established the crucial role of pRB in regulation of cell cycle entry into S-phase(7, 10, 13). The phenotype of *Rb*-knockout mice demonstrated the importance of pRb for proper differentiation and function of numerous tissues (2, 6, 14, 15, 18-20, 23, 27-29). However, elucidation of biochemical mechanisms responsible for the wide range of pRb functions was greatly hindered by the presence of several protein-binding domains within pRb as well as multiple proteins that interact with pRb(21).

Determination of the crystal structure of pRB bound to an LxCxE-containing peptide opened the possibility to design mutations that would target only one protein-binding domain of pRB without affecting other domains or the overall structure of the protein(16). Substitution of asparagine 757 with phenylalanine resulted in disruption of interactions between pRB and LxCxE-containing proteins, but not with E2F1 transcription factor(4). Tissue culture studies revealed that the pRB-N757F mutant retained the ability to induce cell cycle arrest and flat cell phenotype in *RB*-null Saos2 cells. However, this mutant was incapable of establishing irreversible growth arrest in differentiated myotubes.

In order to fully characterize the role of LxCxE-binding domain in pRB function, we proceeded to create knockin mice with an equivalent mutation in pRb. We utilized gene targeting technology to introduce a mutation in the *Rb* locus that resulted in

substitution of asparagine (N) 750 with phenylalanine (F) in pRb. We examined $Rb^{N750F/N750F}$ and $Rb^{+/N750F}$ mice for any phenotypes that have been previously described in $Rb^{-/-}$ and $Rb^{+/-}$ mice, as well as any new phenotypes.

Rb-null embryos die at Ed 12.5 from defects in myoblasts, trophoblasts, erythrocytes, and neurons of the CNS and PNS even though they contain functional p107 and p130, demonstrating that pRb has a unique developmental function that cannot be substituted by other members of the pocket family of proteins. $Rb^{N750F/N750F}$ mice were born at the expected Mendelian ratio of 25 %, indicating that pRb-N750F retains all the functions of the wild type pRb that are essential for viability and proper differentiation of the tissues found to be affected in $Rb^{-/-}$ embryos. These findings can be interpreted in three different ways. First, the LxCxE-binding domain of pRb might not regulate enucleation of erythrocytes, permanent withdrawal from the cell cycle in neurons of the CNS, PNS, lens and myotubes, apoptosis of the neurons in PNS and lens, and differentiation of trophoblasts. Second, it is possible that N750F substitution did not disrupt interactions between all LxCxE-containing proteins, but only with the ones that rely exclusively on this motif for binding to pRb. Proteins that interact with pRb through one or more regions in addition to the LxCxE motif might not have been affected by this mutation. For example, the LxCxE-containing fragment of interferon-inducible protein p202 has been shown to bind to pRb with high affinity(5). However, another region at the N-terminus of p202 was also shown to bind pRb, although with lower affinity. Third, two other members of the pocket family of proteins – p107 and p130 – can be substituting for pRb-N750F. Functional substitution among pocket family proteins has been documented in tissue culture systems as well as in mice(8, 17, 24). Moreover, both

p107 and p130 contain highly conserved A and B regions and have been shown to bind to viral oncoproteins that contain LxCxE motif(9, 11, 12). This final possibility can be explored by crossing $p107^{-/-}$ and $p130^{-/-}$ mice to $Rb^{N750F/N750F}$ mice in order to create double mutants mice. If either p107 or p130 is able to substitute for the LxCxE-binding function of pRb, $p107^{-/-}$; $Rb^{N750F/N750F}$ or $p130^{-/-}$; $Rb^{N750F/N750F}$ double mutant mice will display defects in addition to the ones described here for $Rb^{N750F/N750F}$ mice.

The $Rb^{+/-}$ mice develop pituitary tumors with complete penetrance and die from them by the age of one year(14). Neither $Rb^{+/N750F}$ nor $Rb^{+/N750F}$ mice developed pituitary tumors after 20 months of observation, indicating that the LxCxE-binding mutant of pRb retained a tumor-suppressor function in the pituitary. This finding correlated with the data from tissue culture experiments showing that MEFs and 3T3 derived from $Rb^{+/N750F}$ and $Rb^{N750F/N750F}$ mice retained normal cell cycle distribution and sensitivity to contact inhibition. Moreover, gene expression analysis in $Rb^{N750F/N750F}$ MEFs demonstrated that there was no deregulation of genes that control cell cycle progression.

Normal development, fertility and survival of $Rb^{+/-}$ mice, except for pituitary tumors, indicate that one copy of wild type *Rb* allele is enough to insure the wellbeing of mice. In contrast, the survival of $Rb^{N750F/-}$ mice is severely compromised. These mice are born at 13% frequency, instead of the expected 25%, with still further reduction in the number of males (35% of the total $Rb^{N750F/-}$ progeny). Hunchback posture, decreased body mass and early mortality indicate that Rb^{N750F} allele is haploinsufficient, and that the LxCxE-binding domain of pRb performs essential functions during embryonic development and in adult mice which cannot be substituted for by the LxCxE-binding domains of p107 and p130.

The lack of embryonic lethality in $Rb^{N750F/N750F}$ mice allowed us to study the effects of this mutation in the adult animal. We observed new phenotypes that have not been previously described, and discovered new tissues and processes that require the presence of pRb for their proper function. Moreover, because N750F mutation destroyed only one protein-binding domain of pRb, we could determine the contribution of that domain to pRb function. We report for the first time that disruption of the LxCxE-binding domain of pRb causes perturbations in the processes of thrombopoiesis, lymphocyte production and ovulation in females.

Histological examination of tissues from $Rb^{N750F/N750F}$ mice revealed increased penetration of megakaryocytes into the spleen. Subsequent analysis of the peripheral blood uncovered a reproducible and statistically significant increase in platelet counts. In order to determine the source of the increased platelets, we assessed the number of common myeloid progenitors, megakaryocyte progenitors and megakaryocytes in the bone marrow of the $Rb^{N750F/N750F}$ mice. We did not find a statistically significant difference in the number of common myeloid progenitors and megakaryocyte progenitors in $Rb^{N750F/N750F}$ mice as compared to the wild type littermates, indicating that the increased platelet count could not be attributed to the increase in the number of these precursors. However, we detected a small reduction in the number of megakaryocytes, suggesting that in $Rb^{N750F/N750F}$ mice the rate of platelet production might be accelerated as compared to the $Rb^{+/+}$ littermates. The accelerated rate of platelet production in the absence of a compensatory increase in the number of megakaryocytes will lead to the depletion in the number of megakaryocytes. This possibility can be explored by monitoring the rate of platelet recovery following irradiation. Previous studies have

demonstrated that subjecting mice to γ radiation (250 or 500 cGy) caused a five-fold decrease in the number of circulating platelets, followed by the complete recovery by 25 days post-irradiation(26). If platelets are produced at an accelerated rate in $Rb^{N750F/N750F}$ mice, one would expect to see a speedier recovery of the normal platelet count in the mutant mice as compared to the wild type controls. Alternatively, the increased number of platelets in $Rb^{N750F/N750F}$ mice can be attributed to the prolonged survival of the platelets that are produced at a normal rate. This possibility can be investigated by labeling platelets with biotin *in vivo* and monitoring their survival by flow cytometry(3). Detection of biotinylated platelets in $Rb^{N750F/N750F}$ mice after they are no longer found in $Rb^{+/+}$ control mice (4.7 days) would support the hypothesis that the LxCxE-binding domain of pRb regulates survival of platelets.

Analysis of the peripheral blood also revealed a reproducible and statistically significant increase of lymphocyte counts in $Rb^{N750F/N750F}$ mice. To further characterize this phenotype, we compared the relative distribution of B lymphocytes and T lymphocytes in the peripheral blood of the mutant mice and wild type controls. We discovered that the ratio of T lymphocytes to B lymphocytes was unaffected, indicating that the increase in lymphocyte production in $Rb^{N750F/N750F}$ mice occurred at the level of common lymphoid progenitors. This hypothesis can be further tested by scoring the number of common lymphoid progenitors in the bone marrow of $Rb^{N750F/N750F}$ mice and comparing it to the wild type controls(22). In addition, bone marrow transplantation experiments can be performed in order to determine whether increased lymphopoiesis is due to the defects intrinsic to the HSC or to the bone marrow microenvironment. If the first possibility is correct, lethally irradiated wild type recipients that receive bone

marrow transplant from $Rb^{N750F/N750F}$ mice would also display elevated levels of lymphocytes in their peripheral blood.

No pregnancy was ever observed in $Rb^{N750F/N750F}$ females of 129 Sv/Ev/Tac pure background. Histological examination revealed that the immediate cause of infertility was anovulation. The possible causes of anovulation can be divided into two broad categories: defects in hormonal regulation of the estrous cycle, or the inability of the ovarian tissue to respond to gonadotropic hormones. Further experiments will be necessary to differentiate between these possibilities. Ovarian hyperstimulation can be achieved by injecting females with PMSG and HCG(1). If anovulation in $Rb^{N750F/N750F}$ females is caused by hormonal defects, supplying them with exogenous hormones should result in ovulation and pregnancy. However, if anovulation is caused by the inability of the ovarian tissues to respond to gonadotropic hormones, ovarian hypersitmulation would have no effect.

Histological examination of the ovaries from $Rb^{N750F/-}$ females revealed an even more sever defect in the follicular development than the one observed in $Rb^{N750F/N750F}$ females. Only primordial follicles were observed in the ovaries of $Rb^{N750F/-}$ females, indicating that no FSH-dependent follicular development occurred. Moreover, in $Rb^{N750F/-}$ ovaries the interstitial cells appeared as undifferentiated fusiform fibroblast-like cells, demonstrating an additional defect in LH pathway. Once again, ovarian hyperstimulation experiments are necessary in order to determine whether these abnormalities are due to the defects in the hormonal regulation of the estrous cycle or the ability of the ovarian tissues to respond to gonadotropins.

The work presented in this dissertation describes the *in* vivo function of the LxCxE-binding domain of pRb. The phenotype of $Rb^{N750F/N750F}$ mice demonstrates that pRb-N750F protein retains all functions of the wild type pRb that have been initially uncovered in Rb-null mice and tissues. Specifically, pRb-N750F was able to suppress pituitary tumorigenesis, support normal proliferation and differentiation of the skeletal muscles, neurons of the CNS, PNS and the lens, and placental trophoblasts. These findings indicate that the LxCxE-binding domain of pRb is not involved in regulation of these processes. However, we discovered new functions of pRb, and specifically its LxCxE-binding domain, which have not been previously described. Our work demonstrates that pRb regulates platelet and lymphocyte numbers in the peripheral blood, although the exact molecular mechanism of its action remains to be elucidated. Increase in the number of platelets in the absence of pRb in HSC has been reported before, thus, our work provides further confirmation of this finding as well as points out a specific defect that might be causing this phenotype(25). We also demonstrate a novel role for pRb in ovarian development and ovulation. Because the histological abnormalities observed in $Rb^{N750F/N750F}$ females have not been observed in mice with knockout of *Fsh*, *Fshr*, *Lh* or *Lhr* genes, our discovery points out to a new pathway whose function is crucial for the proper reproductive function in mice. However, further studies are necessary to identify pRb-interacting proteins that are responsible for failed ovarian development and ovulation in $Rb^{N750F/N750F}$ and $Rb^{N750F/-}$ females.

REFERENCES

1. **Abel, M. H., A. N. Wootton, V. Wilkins, I. Huhtaniemi, P. G. Knight, and H. M. Charlton.** 2000. The effect of a null mutation in the follicle-stimulating hormone receptor gene on mouse reproduction. Endocrinology **141:**1795-803.

2. **Balsitis, S. J., J. Sage, S. Duensing, K. Munger, T. Jacks, and P. F. Lambert.** 2003. Recapitulation of the effects of the human papillomavirus type 16 E7 oncogene on mouse epithelium by somatic Rb deletion and detection of pRb-independent effects of E7 in vivo. Mol Cell Biol **23:**9094-103.

3. **Berger, G., D. W. Hartwell, and D. D. Wagner.** 1998. P-Selectin and platelet clearance. Blood **92:**4446-52.

4. **Chen, T. T., and J. Y. Wang.** 2000. Establishment of irreversible growth arrest in myogenic differentiation requires the RB LXCXE-binding function. Mol Cell Biol **20:**5571-80.

5. **Choubey, D., and P. Lengyel.** 1995. Binding of an interferon-inducible protein (p202) to the retinoblastoma protein. J Biol Chem **270:**6134-40.

6. **Clarke, A. R., E. R. Maandag, M. van Roon, N. M. van der Lugt, M. van der Valk, M. L. Hooper, A. Berns, and H. te Riele.** 1992. Requirement for a functional Rb-1 gene in murine development. Nature **359:**328-30.

7. **Cobrinik, D.** 2005. Pocket proteins and cell cycle control. Oncogene **24:**2796-809.

8. **Cobrinik, D., M. H. Lee, G. Hannon, G. Mulligan, R. T. Bronson, N. Dyson, E. Harlow, D. Beach, R. A. Weinberg, and T. Jacks.** 1996. Shared role of the pRB-related p130 and p107 proteins in limb development. Genes Dev **10:**1633-44.

9. **DeCaprio, J. A., J. W. Ludlow, J. Figge, J. Y. Shew, C. M. Huang, W. H. Lee, E. Marsilio, E. Paucha, and D. M. Livingston.** 1988. SV40 large tumor antigen forms a specific complex with the product of the retinoblastoma susceptibility gene. Cell **54:**275-83.

10. **DiCiommo, D., B. L. Gallie, and R. Bremner.** 2000. Retinoblastoma: the disease, gene and protein provide critical leads to understand cancer. Semin Cancer Biol **10:**255-69.

11. **Dyson, N., P. M. Howley, K. Munger, and E. Harlow.** 1989. The human papilloma virus-16 E7 oncoprotein is able to bind to the retinoblastoma gene product. Science **243:**934-7.

12. **Egan, C., S. T. Bayley, and P. E. Branton.** 1989. Binding of the Rb1 protein to E1A products is required for adenovirus transformation. Oncogene **4:**383-8.

13. **Goodrich, D. W.** 2006. The retinoblastoma tumor-suppressor gene, the exception that proves the rule. Oncogene **25:**5233-43.

14. **Jacks, T., A. Fazeli, E. M. Schmitt, R. T. Bronson, M. A. Goodell, and R. A. Weinberg.** 1992. Effects of an Rb mutation in the mouse. Nature **359:**295-300.

15. **Lee, E. Y., C. Y. Chang, N. Hu, Y. C. Wang, C. C. Lai, K. Herrup, W. H. Lee, and A. Bradley.** 1992. Mice deficient for Rb are nonviable and show defects in neurogenesis and haematopoiesis. Nature **359:**288-94.

16. **Lee, J. O., A. A. Russo, and N. P. Pavletich.** 1998. Structure of the retinoblastoma tumour-suppressor pocket domain bound to a peptide from HPV E7. Nature **391:**859-65.

17. **Lee, M. H., B. O. Williams, G. Mulligan, S. Mukai, R. T. Bronson, N. Dyson, E. Harlow, and T. Jacks.** 1996. Targeted disruption of p107: functional overlap between p107 and Rb. Genes Dev **10:**1621-32.

18. **MacPherson, D., J. Sage, D. Crowley, A. Trumpp, R. T. Bronson, and T. Jacks.** 2003. Conditional mutation of Rb causes cell cycle defects without apoptosis in the central nervous system. Mol Cell Biol **23:**1044-53.

19. **MacPherson, D., J. Sage, T. Kim, D. Ho, M. E. McLaughlin, and T. Jacks.** 2004. Cell type-specific effects of Rb deletion in the murine retina. Genes Dev **18:**1681-94.

20. **Mayhew, C. N., E. E. Bosco, S. R. Fox, T. Okaya, P. Tarapore, S. J. Schwemberger, G. F. Babcock, A. B. Lentsch, K. Fukasawa, and E. S. Knudsen.** 2005. Liver-specific pRB loss results in ectopic cell cycle entry and aberrant ploidy. Cancer Res **65:**4568-77.

21. **Morris, E. J., and N. J. Dyson.** 2001. Retinoblastoma protein partners. Adv Cancer Res **82:**1-54.

22. **Perry, S. S., R. S. Welner, T. Kouro, P. W. Kincade, and X. H. Sun.** 2006. Primitive lymphoid progenitors in bone marrow with T lineage reconstituting potential. J Immunol **177:**2880-7.

23. **Sage, C., M. Huang, K. Karimi, G. Gutierrez, M. A. Vollrath, D. S. Zhang, J. Garcia-Anoveros, P. W. Hinds, J. T. Corwin, D. P. Corey, and Z. Y. Chen.** 2005. Proliferation of functional hair cells in vivo in the absence of the retinoblastoma protein. Science **307:**1114-8.

24. **Sage, J., G. J. Mulligan, L. D. Attardi, A. Miller, S. Chen, B. Williams, E. Theodorou, and T. Jacks.** 2000. Targeted disruption of the three Rb-related genes leads to loss of G(1) control and immortalization. Genes Dev **14:**3037-50.

25. **Walkley, C. R., and S. H. Orkin.** 2006. Rb is dispensable for self-renewal and multilineage differentiation of adult hematopoietic stem cells. Proc Natl Acad Sci U S A **103:**9057-62.

26. **Wallace, P. M., J. F. MacMaster, J. R. Rillema, J. Peng, S. A. Burstein, and M. Shoyab.** 1995. Thrombocytopoietic properties of oncostatin M. Blood **86:**1310-5.

27. **Wu, L., A. de Bruin, H. I. Saavedra, M. Starovic, A. Trimboli, Y. Yang, J. Opavska, P. Wilson, J. C. Thompson, M. C. Ostrowski, T. J. Rosol, L. A. Woollett, M. Weinstein, J. C. Cross, M. L. Robinson, and G. Leone.** 2003. Extra-embryonic function of Rb is essential for embryonic development and viability. Nature **421:**942-7.

28. **Yu, B. D., M. Becker-Hapak, E. L. Snyder, M. Vooijs, C. Denicourt, and S. F. Dowdy.** 2003. Distinct and nonoverlapping roles for pRB and cyclin D:cyclin-dependent kinases 4/6 activity in melanocyte survival. Proc Natl Acad Sci U S A **100:**14881-6.

29. **Zacksenhaus, E., Z. Jiang, D. Chung, J. D. Marth, R. A. Phillips, and B. L. Gallie.** 1996. pRb controls proliferation, differentiation, and death of skeletal muscle cells and other lineages during embryogenesis. Genes Dev **10:**3051-64.